Pleistocene terraces in the Hochrhein area – formation, age constraints and neotectonic implications

Inauguraldissertation
zur
Erlangung der Würde eines Doktors der Philosophie
Vorgelegt der
Philosophisch-Naturwissenschaftlichen Fakultät
Der Universität Basel

von
Stéphane Kock
aus Coppet VD

Basel 2008

Genehmigt von der Philosophisch-Naturwissenschaftlichen Fakultät auf Antrag von

Prof. Dr. Andreas Weztel
Institut für Geologie und Paläontologie, Universität Basel

PD. Dr. Frank Preusser
Institut für Geologie, Universität Bern

Basel, 24. Juni 2008

Prof. Dr. Hans-Peter Hauri
(Dekan der Philosophisch-Naturwissenschaftlichen Fakultät)

Abstract

Pleistocene fluvial gravel terraces appear to be useful to decipher neotectonic movements. To achieve this, however, chronologic and sedimentologic data on the terraces are required. Thus, this thesis represents a multidisciplinary approach. After presenting methodological aspects of U/Th (Uranium-series disequilibrium) dating, compared to OSL (Optically Stimulated Luminescence), the ages obtained are used, together with sedimentological data, to constrain the formation processes and timing of the Late Pleistocene terraces in the Hochrhein area. Finally, the geometry of these terraces is interpreted in terms of neotectonics.

Hitherto, dating coarse-grained sediment has proved often impossible due the lack of datable material, and developing new methods in this domain is thus of crucial importance. U/Th is a well established method, often used for speleothems and coral dating, and it is tested here on pedogenetic crusts growing within the Late Pleistocene gravels of the Hochrhein area. These results are compared to OSL ages from the same sampling sites. Our results show that this method has a development potential, but is highly dependant on a sufficient and stable Uranium content of the samples, which is partly controlled by bacterial activity. Comparisons with OSL ages highlight the fact that the event that is dated by mean of U/Th is the precipitation of the crust, not the deposition of the sediment.

Sedimentological and morphological data show that the Late Pleistocene gravels (Lower Terrace) were deposited as a braided river, where flood events played a major shaping role. The gravels are arranged into terrace levels, where the highest level is an accumulation level, and the lower levels are erosion level with minor re-accumulation. The flood deposits are mostly conserved on top of the different terrace levels because the general incision regime prevented them from being reworked. OSL ages show that the main gravel accumulation occurred between 27 an 11 ka in the Hochrhein area, but minor re-accumulation occurred until historical times. The accumulation level was thus formed during the Younger Dryas, and the lower levels were formed from the Youger Dryas on, until historical times. These results are confirmed by radiocarbon ages from fossil trees and U/Th ages from speleothems.

Terrace longitudinal profiles are used to assess neotectonic activity in the Hochrhein area. Four main groups of Pleistocene terrace exist in this area: the Earliest Pleistocene Higher Deckenschotter, the Early Pleistocene Lower Deckenschotter, the Middle-Late Pleistocene High Terrace and the Late Pleistocene Lower Terrace. The three older terrace groups do not show original surfaces anymore, so outcrop altitudes are used to build the longitudinal profile. This profile shows that the gradient of the terraces increases with their age, and each of the terrace groups show an increased gradient at the location where the profile crosses the eastern main border fault (MBF) of the Upper Rhine Graben (URG). The terraces converge, cross and finally continue as basin filling. This suggests a relative uplift of the headwater area and extensional activity for the MBF during Pleistocene. The Lower Terrace features still well preserved surfaces and these are analysed with a high precision Digital Terrain Model (DTM). Using a high precision DTM highlights the complex arrangement of sublevels and the irregularities of the surfaces, which are mostly caused by sedimentary and erosive processes. NW of Basel in the URG, field evidences indicate Late Pleistocene activity of NW-SE striking normal faults.

Acknowledgments

Many people have helped me in a way or another during my researches in Basel, and therefore deserve my gratitude.

In the first place, I want to thank Prof. Andreas Wetzel, my supervisor. He proposed the subject of this thesis and always trusted me, even when sometimes I didn't trust me. He showed a great availability whenever I came to him.

I learned a lot about Quaternary geology and scientific writing with Frank Preusser. Discussing with him always proved very constructive. I am further indebted to him for all those hours and days he spent in his red-light lab measuring my samples.

I also appreciated the wise comments and advice of Stefan Schmid, Peter Ziegler, and Peter Huggenberger, and I learned a lot discussing with them.

I am indebted to Jan Kramers, who accepted to measure my U/Th samples, and devoted some of his valuable time to them and to me.

The Swisstopo and Nagra are acknowledged for providing the DTM-AV dataset. Peter Jordan is thanked for his most valuable support with ArcGIS, and for his enthusiasm in discussing the results.

Philippe Rentzel was always ready to help and share his knowledge. I appreciated working with him.

Besides being my happy and lively office mates, Marielle, Friedl, Sebastian, Horst, Kamil, Pierre and Zoltan deserve my gratitude for interesting discussions and for their support.

Joëlle Glanzmann was always ready to help with administrative problems or whatever else, and I really appreciated that. She started helping even before I showed up in Basel, in my search for a flat. She contributes greatly to the friendly atmosphere of the Bernoullianum.

Verena Scheuring was of very efficient help when it came to literature searches.

I owe a lot to all my other colleagues and friends, who supported me (even without noticing it) and built a joyful frame for my life in Basel or elsewhere.

I spent a great year living with James, my flat-mate, and I would have certainly enjoyed more if the mountain hadn't decided to keep him… Thank you and farewell!

I ran into a classical PhD student's problem: money! I would like to thank the Freiwillige Akademische Gesellschaft of Basel for their financial support.

Last but not least, my family was always there and backed me in all kind of ways.

Table of content

Introduction **1**

Chapter 1 *Dating of Late Pleistocene terrace deposits of the River Rhine using uranium series and luminescence methods: potential and limitations* **9**
1. Introduction 11
2. Luminescence dating 16
3. U/Th dating of calcite crusts 23
4. Discussion 28
5. Conclusion 29
References 30

Chapter 2 *Formation and evolution of the Lower Terrace of the Rhine River in the area of Basel* **35**
1. Introduction 37
2. Materials and Methods 41
3. Results 42
4. Discussion 51
5. Conclusion 57
References 59

Chapter 3 *Neotectonic activity in the area of Basel as inferred from morphological analysis of fluvial terraces of the Rhine River* **63**
1. Introduction 65
2. Methods 72
3. Results 76
4. Discussion 79
5. Conclusion 85
References 86

Summary **93**

Introduction

Introduction

The Upper Rhine Graben (URG) is a major element of the Eurpean Cenozoic rift system (Ziegler, 1992; Dèzes et al., 2004; Fig.1), and is a densely populated and industrialised area. The Basel earthquake of 1356 (Meyer et al., 1994; Lambert et al., 2005) dramatically highlighted the fact that the area of Basel is tectonically active (Plenefisch and Bonjer, 1997; Becker et al., 2005). Assessing seismic hazards has become a key question in such a vulnerable area. Furthermore, in its project to find a suitable location for deep disposal of radioactive waste, The NAGRA (Swiss National Cooperative for the Disposal of Radioactive Waste) is especially concerned with future tectonic evolution of northern Switzerland. It is therefore essential to gain knowledge about past and present tectonic activity, and to interpret and project these into the future.

The area of Basel is tectonically complex, because different structures are present and may interact: The ENE-WSW striking Permo-Carboniferous trough system is a deep structure that is known mostly from bore holes and seismics (Schumacher, 2002), and its compressive reactivation in Cenozoic plays a key role in the folding of the Jura (Ustaszewski and Schmid, 2007; Madritsch et al., accepted). The NNE-SSW striking Upper Rhine Graben (URG) and its shoulders, the Vosges and Black Forest crystalline massifs, are the expression of a Paleogene ESE-WNW extension (Ziegler, 1992). The URG links up with the Bresse Graben through the Rhine-Bresse transfer zone (Laubscher, 1970; Contini and Théobald, 1974; Madritsch et al., accepted). Pliocene folding has been reported by Giamboni et al (2004a) in the Sungau area, and Pliocene to recent activity has been observed in the Jura fold-and-thrust belt by Ustaszewski and Schmid (2007) and by Madritsch et al. (accepted). The Dinkelberg is a down faulted block from the Black Forest, and is as such a part of the URG (Hinsken et al., 2007).

Aim of the thesis

Previous promising studies successfully used geomorpholgical tools, such as river and terrace longitudinal profiles analysis, to asses neotectonic evolution in the southern URG (Giamboni et al., 2004a; 2004b; 2005) and in the northern URG (Peters and van Balen, 2007), although the displacement rates are rather low in these areas. This work applies the same concept to the region directly upstream from the URG, the Hochrhein. This region is located at the limit between the Tabular Jura and the crystalline Black Forest massif and has a dense network of faults, most of which are inactive, but some of them may control the modern trace of the Rhine (Haldimann et al., 1984). This region also has numerous outcrops of Pleistocene fluvial deposits organized in terrace levels, and they are seen as potential recorders of neotectonic activity. However, constraining

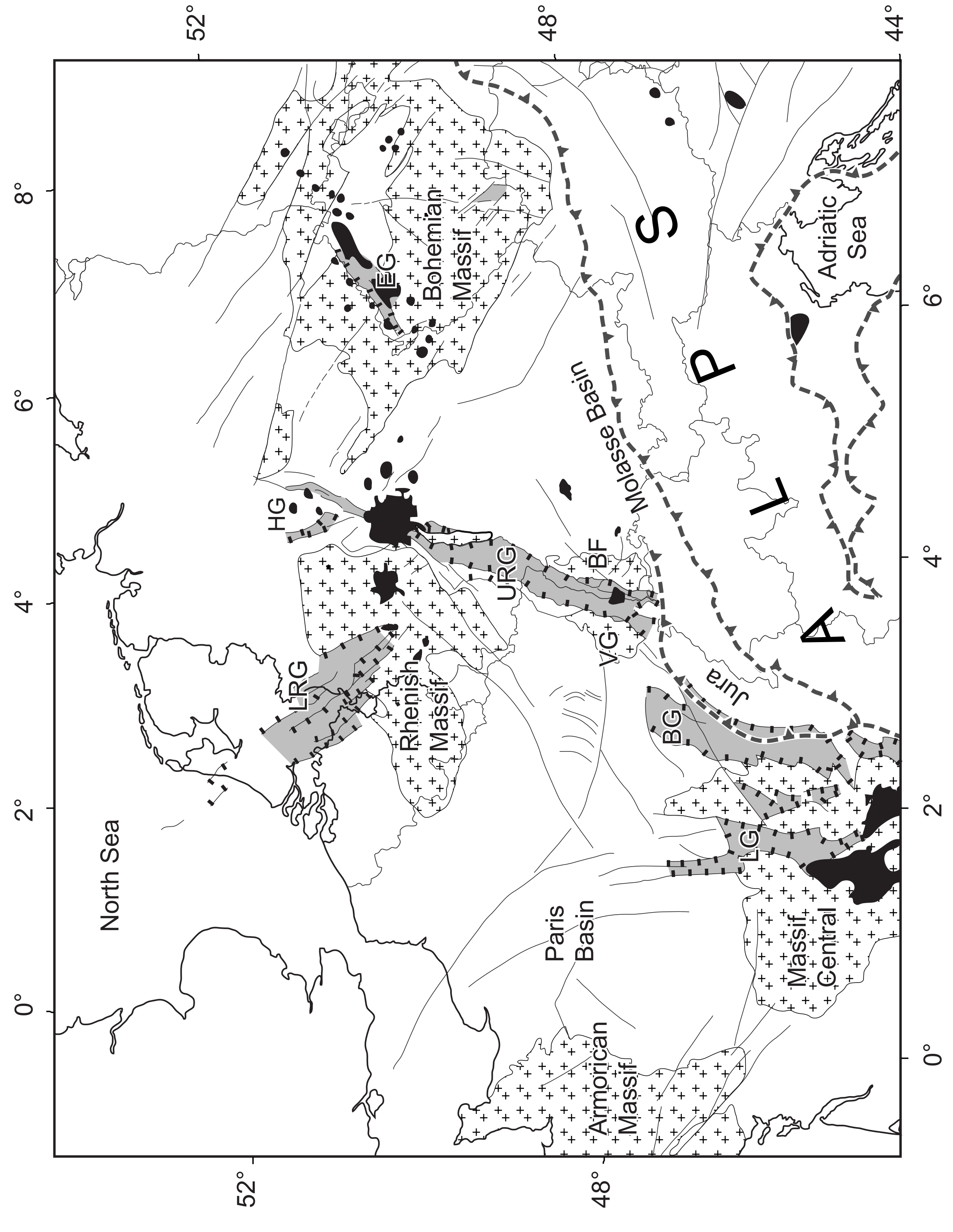

Fig. 1. Map of central Europe showing the structure of the European Cenozoic rift system (ECRIS, in grey). Cross-pattern: Variscan massifs; black pattern: Late Cretaceous to Cenozoic volcanics; BF: Black Forest; BG: Bresse Graben; EG: Eger Graben; LG: Limagne Graben; LRG: Lower Rhine Graben; URG: Upper Rhine Graben (after Ziegler et al., 2004).

neotectonic activity with fluvial deposits and landforms requires a good comprehension of the erosional and depositional processes that led to their formation. and quantitative results are only possible with age control. A part of this thesis focuses, hence, on the dating of fluvial deposits, and on the description of possible erosional and depositional processes.

Organisation of the thesis

This thesis contains three chapters that either have been published or are meant to be published in the form of scientific articles.

Chapter 1 presents an attempt to use U-series disequilibrium dating on calcite crust that formed within the Lower Terrace gravels of the Rhine. The original aim of the study was to constrain the lowering of the groundwater level within the gravel. Those data would then enable to detect potential recent vertical movements. However, this concept had to be abandoned, because 1) the outcrop are too distant from each other to attain sufficient precision, 2) age uncertainties proved to be too high, and 3) laboratory processing was a bottleneck, because only a limited amount of samples could be dated. The study was, thus, refocused on a comparison between U-Th dating and OSL (Optically Stimulated Luminescence) dating.

Chapter 2 uses the OSL data to propose a chronology of formation of the Lower Terrace. Indeed, the Lower Terrace has already been studied by a number of authors, but chronometric ages have been generally lacking due to the absence of suitable dating method. It appears that the period of accumulation is much younger as expected. Furthermore, the main sedimentary processes responsible formation of the Lower Terrace are presented.

Chapter 3 is an attempt to detect recent tectonic movements through fluvial sediments. On one hand, the four terrace formations (Lower Terrace, High Terrace, Lower Deckenschotter and higher Deckenschotter) are investigated together in their longitudinal profile, on the other hand, the Lower terrace is investigated into more details thank to a high precision digital elevation model. Furthermore, two ephemeral outcrops that appeared during the study period are documented, as they also provide evidence for neotectonic movements.

References

Becker, A., Ferry, M., Monecke, K., Schnellmann, M. & Giardini, D. 2005: Multiarchive paleoseismic record of late Pleistocene and Holocene strong earthquakes in Switzerland. Tectonophysics 400, 153-177.

Contini, D. & Theobald, N. 1974: Relations entre le Fosse rhenan et le Fosse de la Saone; tectonique des regions sous-vosgiennes et prejurassiennes. Approaches to taphrogenesis; southern extensions of the Rhinegraben. Illies, J. H. & Fuchs, K. Stuttgart: 310-321.

Dèzes, P., Schmid, S. M. & Ziegler, P. A. 2004: Evolution of the European Cenozoic Rift System:

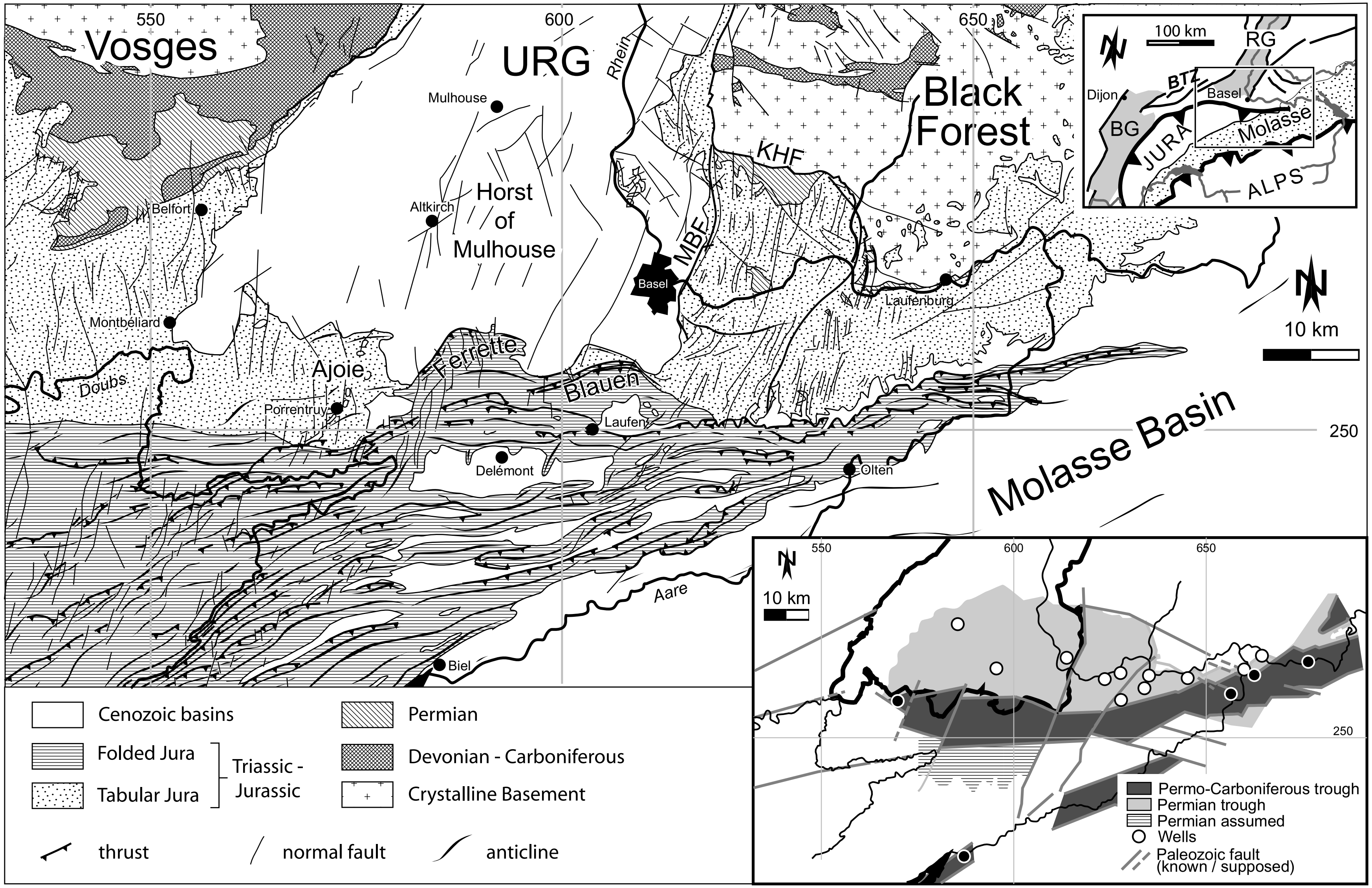

Fig. 2. Tectonic map of the southern Upper Rhine Graben. KHF: Kandern Hausen Fault; MBF: eastern Main Border Fault of the URG. The bottom rhight inset is a map of the same area showing the position of the Perm-Carboniferous trough system. The top right inset is an overview map.

interaction of the Alpine and Pyrenean orogens with their foreland lithosphere. Tectonophysics 389, 1-33.

Giamboni, M. E., Ustaszewski, K., Schmid, S. M., Schumacher, M. E. & Wetzel, A. 2004a: Plio-Pleistocene transpressional reactivation of Paleozoic and Paleogene Structures in the Rhine-Bresse transform zone (northern Switzerland and eastern France. International Journal of Earth Sciences 93, 207-223.

Giamboni, M. E., Wetzel, A., Nivière, B. & Schumacher, M. E. 2004b: Plio-Pleistocene folding in the southern Rhinegraben recorded by the evolution of the drainage network (Sundgau area; northwestern Switzerland and France). Eclogae geol. Helv. 97, 17-31.

Giamboni, M. E., Wetzel, A. & Schneider, B. 2005: Geomorphic response of alluvial rivers to active tectonics: Example from the southern Rhinegraben. Austrian Journal of Earth Sciences 97, 24-37.

Haldimann, P., Naef, H. & Schmassmann, H. 1984: Fluviatile Erosions- und Akkumulations-formen als Indizien jungpleistozäner und holozäner Bewegungen in der Nordschweiz und angrenzenden Gebieten. Nagra Technischer Bericht 84-16.

Hinsken, S., Ustaszewski, K. & Wetzel, A. 2007: Graben width controlling syn-rift sedimentation: the Palaeogene southern Upper Rhine Graben as an example. International Journal of Earth Sciences 96, 979-1002.

Lambert, J., Winter, T., Dewez, T., J., B. & Sabourault, P. 2005: New hypotheses on the maximum damage area of the 1356 Basel earthquake (Switzerland). Quaternary Science Reviews 24, 383-401.

Laubscher, H. 1970: Grundsätzliches zur Tektonik des Rheingrabens. Graben Problems. Illies, J. H. & Mueller, S. Stuttgart, Proceedings 1174 of an International Rift Symposium held in Karlsruhe 1968, International Upper Mantle Project.

Madritsch, H., Schmid, S. M. & Fabbri, O. accepted: Interactions between thin- and thick-skinned tectonics at the northwestern front of the Jura fold-and-thrust belt (Eastern France). Tectonics.

Meyer, B., Lacassin, R., Brulhet, J. & Mouroux, B. 1994: The Basel 1356 earthquake: which fault produced it? Terra Nova 6, 54-63.

Peters, G. & Van Balen, R. T. 2007: Pleistocene tectonics inferred from fluvial terraces of the northern Upper Rhine Graben, Germany. Tectonophysics 430, 41-65.

Plenefisch, T. & Bonjer, K.-P. 1997: The stress field in the Rhine Graben area inferred from earthquake focal mechanisms and estimation of frictional parameters. Tectonophysics 275, 71-97.

Schumacher, M. E. 2002: Upper Rhine Graben: Role of preexisting structures during rift evolution. Tectonics 21, 6-1 - 6-17.

Ustaszewski, K. & Schmid, S., M. 2007: Latest Pliocene to recent thick-skinned tectonics at the Upper Rhine Graben - Jura Mountains junction. Swiss j. geosci. 100, 293-312.

Ziegler, P. A. 1992: European Cenozoic rift system. Tectonophysics 208, 91-111.

Chapter 1

Chapter 1

Dating of Late Pleistocene terrace deposits of the River Rhine using uranium series and luminescence methods: potential and limitations

Stéphane Kock, Jan D. Kramers, Frank Preusser, Andreas Wetzel

Submitted to *Quaternary Geochronology*

Abstract

Uranium series dating of pedogenic carbonate crusts from fluvial gravels is tested using Optically Stimulated Luminescence (OSL) ages as reference. OSL dating yielded ages of 30-15 ka and 13-11 ka, which correlates with the cold periods of the Last Glacial Maximum and the Younger Dryas. These ages are internally coherent and consistent with the geological background and are thus regarded as reliable. Most of the U/Th results scatter widely in the $^{230}Th/^{232}Th$ vs. $^{234}U/^{232}Th$ isochron diagram. Dates obtained by regression were found to be mostly overestimated compared to the OSL ages and the geological context, and it is suggested that a heterogeneous initial ^{230}Th input, not relatable to a detrital component, is responsible for the observed discrepancies. This input may be due to bacterial activities and Th transport on organic colloids. It appears necessary to avoid samples where bacteria could have contributed to carbonate precipitation.

Key words: U series dating, optical dating, fluvial deposits, River Rhine, Pleistocene, meteoric cement

1. Introduction

Fluvial deposits are important archives reflecting the response of drainage networks to past environmental and sea-level changes (e.g., Blum and Törnqvist, 2000; Houben 2003). This is, for example, demonstrated by the change from highly depositional fluvial environments of braided river systems to more erosional dominated meandering flow patterns. Additionally, in areas of local to regional uplift the vertical difference between the surface of the present-day river and raised fluvial terraces can be used to reconstruct the uplift rate of an area (Bonnet et al., 1998; Nivière and Marquis, 2000; Houtgast et al., 2002). In both cases outlined above, the age of the investigated fluvial deposits is of crucial importance to either correlate the local findings with a global scale of climate change or for quantifying uplift rates.

Until recently, the dating of fluvial sediments has been problematic. The only way would have been radiocarbon dating of organic material found in the fluvial deposits. While this may be straightforward for many Holocene deposits, it is only rarely possible for sediments formed during glacial periods, where organic remains are only infrequently found. Furthermore, radiocarbon dating is limited to the last 50 ka due to the half-life of the ^{14}C isotope. A relatively new method that overcomes these problems is Optically Stimulated Luminescence (OSL), which allows the direct determination of sediment deposition ages (e.g., Wallinga, 2002). Most problems encountered with the method, such as the identification of incompletely bleached sediments, have been largely solved and an increasing number of studies have used OSL for establishing chronological frameworks in the past decade (e.g., Wallinga et al., 2004; Rittenour et al., 2005). However, two major problems remain with the dating of fluvial sediments. The first is related to the absence of suitable sand layers for OSL dating in some fluvial environments, especially in high fluvial energy regimes in mountainous areas and proglacial settings. The second is related to the upper dating limit of OSL. Although it should be, in principle, possible to date back to several 100 ka by OSL (e.g., Schokker et al., 2005; Rhodes et al., 2006), it is highly dependant on the radioactive dose rate in any particular setting. In sediments rich in radioactive elements, the saturation dose of the OSL signal may be reached in about 150 ka or even less. Furthermore, to confirm OSL beyond 200-300 ka, independent age control is desirable because many samples approach saturation and fitting of growth curves gets less precise: a recent study reports a systematic underestimation of quartz OSL dates in this age range (Wallinga et al., 2007). Besides OSL and the recently tested approach of burial dating using cosmogenic nuclides (Häuselmann et al., 2007), age control for fluvial sediments beyond 100 ka may be possible by U/Th methodology.

U/Th is now a commonly used method for dating speleothems and corals (e.g., Spötl et al., 2002; Spötl and Mangini, 2006; Fleitmann et al., 2007; Scholz and Hoffmann, 2008). In addition, some promising pioneer studies showed that calcrete-like carbonate precipitates that formed within the gravel or soil of a fluvial terrace can also be dated using U/Th (Ku et al., 1979; Radtke et al., 1988; Kelly et al., 2000; Candy et al., 2004, 2005). While these studies concern arid to semi arid areas, other types of sinter from temperate areas proved useful: Spötl and Mangini (2006) used flowstones precipitated in a fracture to constrain the deposition age of the host rock, a Quaternary breccia. Besides, the ages obtained by the authors were also used to constrain climatic conditions and glacier extension. Blisniuk and Sharp (2003) and Sharp et al. (2003) were able to give a chronologic frame to the formation of Pleistocene fluvial terraces from Tibet and Wyoming using carbonate crusts that formed within the gravel of those terraces. Blisniuk and Sharp (2003), for

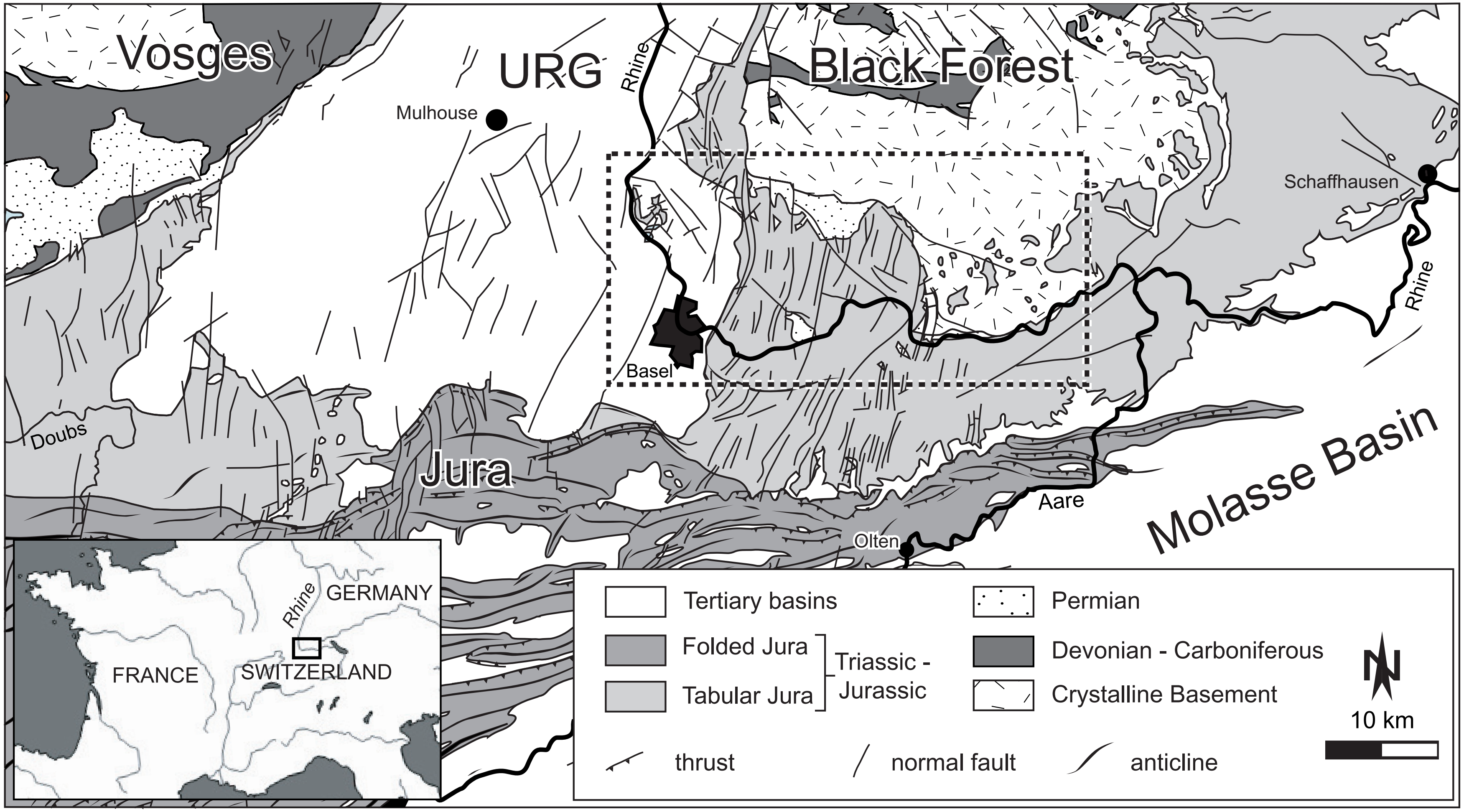

Fig. 1. Tectonic map of northern Switzerland, with the neighboring parts of France and Germany. The dashed box indicates the study area. In this area, the main geological features are the folded and tabular jura (mainly limestones), the Black Forest massive (mainly crystalline) and the Upper Rhine Graben (URG, mainly detritals). The Rhine and Aare rivers (thick black lines) represent the main drainage system of Switzerland, including all the northern Alps.

example, obtained ages between 16 and 233 ka with a fair error. Such results enabled these authors to quantify recent fault displacement.

U/Th methodology enables to measure the time elapsed since a carbonate precipitated. Thus, in the case of an investigation on the host rock of the carbonate, it only provides a minimal age, since there is usually no definite time relation between the formation of the host sediment and that of the precipitate, although in some cases it may be possible to assess this time gap (Sharp et al., 2003).

In this study, fluvial deposits of the River Rhine located on the Swiss-German border between the confluence with the River Aare and the city of Basel are investigated. This part of the river is usually referred to as the Hochrhein (i.e. Preusser, 2008). From east to west, the river follows the border between the crystalline massif of the Black Forest to the north and the sedimentary rocks of the Jura Mountains to the south. At the city of Basel, the River Rhine changes its course and follows the Cenozoic Upper Rhine Graben structure to the north (Fig. 1). The most important part of the Hochrhein's drainage area and its most important sediment source are the Cenozoic molasse midlands and the Alps of Switzerland. The terrace sediments are mainly composed of gravel, with a large proportion of sand matrix and rarely some finer, sandy material. Typical braided river sedimentary structures such as cross-stratifications, imbricated pebbles, sand lenses, open framework layers, confluence scour fills and erosive structures are frequently found (Siegenthaler and Huggenberger, 1993; Huggenberger and Regli, 2006).

In the present study we investigated sediments of the so-called Lower Terrace ("Niederterrasse"), which is usually attributed to the last glaciation of the Alps. However, the Lower Terrace does not represent a single level, but can be subdivided in several sub-levels that were most likely formed by subsequent erosion of the main terrace body (Wittmann, 1961; Kock et al., submitted). Sediments attributed to the Lower Terrace and deposited in close proximity to the former ice margin have been dated by Preusser et al. (2007) in the most eastern part of the Hochrhein area. These authors report three radiocarbon ages of 18,240 ± 130 ^{14}C yr BP, 21,510 ± 510 ^{14}C yr BP and 22,190 ± 190 ^{14}C yr BP for bone fragments found in the gravel, which reflect corrected radiocarbon ages of ca. 22-27 ka. Four single-aliquot quartz OSL ages determined for sand layers from the same gravel pit confirm the correlation of this deposition with the last glaciation of the Alpine Foreland (i.e., Preusser, 2004). However, multiple-aliquot feldspar dating of Hochrhein Lower Terrace sediments presented by Frechen et al. (2004) resulted in ages significantly higher than 30 ka. These authors speculated that no deposition of gravel took place in the Hochrhein area during the Last Glacial Maximum, which is in contrast to common assumptions and especially the findings reported by Preusser et al. (2007).

In this case study two different topics are addressed. Firstly, sediments of the Lower Terrace are dated by OSL using Single-Aliquot Regenerative Dose (SAR) methodology applied to quartz to establish a reliable chronological framework for the Lower Terrace in the area. Secondly, the potential of U/Th dating of calcite crusts that formed below pebbles within the terrace deposits

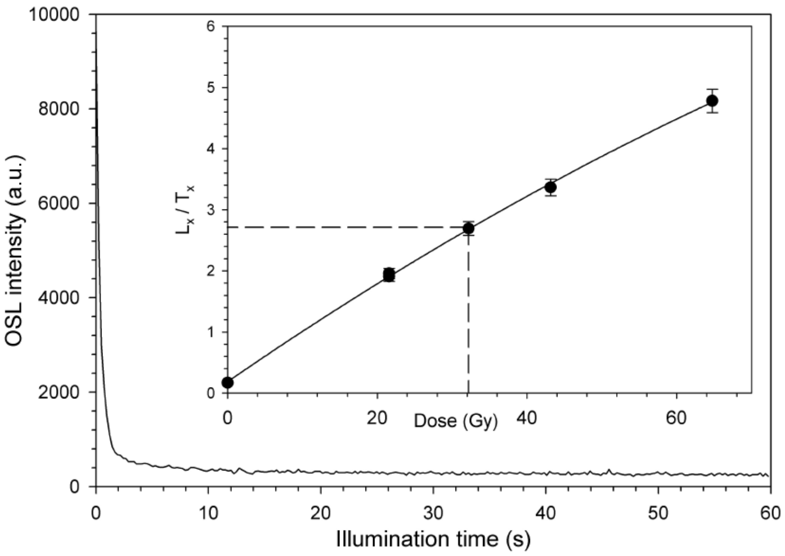

Fig. 2. Typical OSL decay curve for an aliquot of samples HRT 5. Inset: Dose response curve for the same aliquot of sample HRT 5.

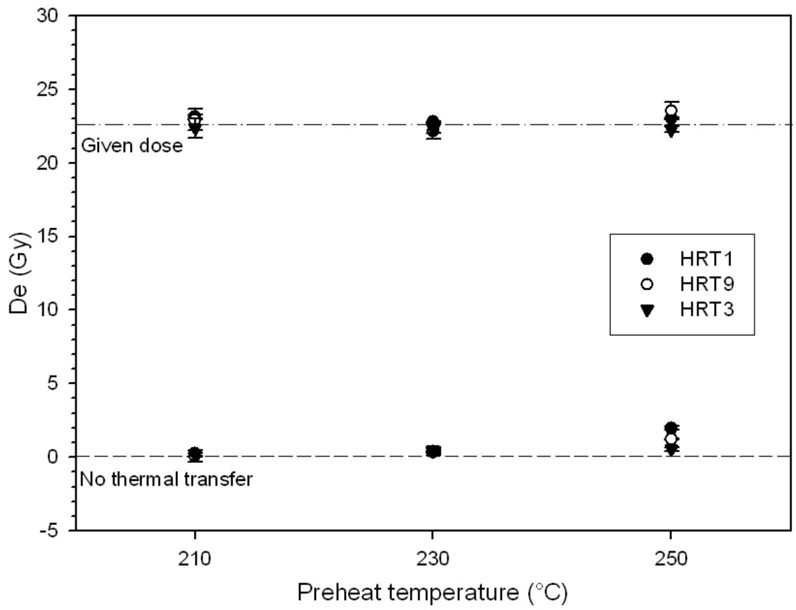

Fig. 3. Result of dose recovery (upper line) and thermal transfer tests (lower line) for three selected samples show a good performance for the choosen preheat of 230° for 10 s.

is tested. The latter is seen as a case study for dating similar but older sediments from the region, for example sediments from the High Terrace ("Hochterrasse") which is tentatively attributed to the Penultimate Glaciation (Rissian, ca. 150 ka). Further older terrace deposits known from the Hochrhein area, the "Deckenschotter" of presumably Mindelian and Günzian age, may be already beyond the limits of OSL dating and Uranium series dating may be a suitable method to get any independent age constraints on these sediments. Nevertheless, since U/Th dating of calcite crusts in mid-latitude fluvial sediments is yet only poorly established, the present contribution may be also seen as a reference for studies in other areas but with similar geological settings.

2. Luminescence dating

2.1. Sampling, preparation, measurements and calculations

Suitable sand layers are rare in the mainly coarse Lower Terrace deposits but were found in nine active gravel pits, up to 25 m deep, distributed along the Hochrhein. Samples were taken by forcing metal tubes into suitable sand lenses. The material was transported to the lab in light-proofed bags. Additional 2 kg were taken from the surrounding material for dose rate measurements. All sample preparation was carried out under subdued red-light laboratory illumination. Samples were first sieved (149-202 µm) and the material was then de-carbonised using HCl. This was followed by density separation (FastFlow© poly-tungstate) using densities of 2.70 g cm^{-3} and 2.58 cm^{-3} to isolate the quartz fraction. The latter separate was then etched by 40% HF for 1 h to remove any remaining feldspars and the outer rim of the quartz grains. The purity of the quartz samples was verified by infrared (IR) stimulation and none of the samples showed any contamination with feldspars after etching.

Determination of the Equivalent Dose (ED) was performed using the single-aliquot regeneration (SAR) protocol of Murray and Wintle (2000, 2003). We used small (2 mm) aliquots to detect

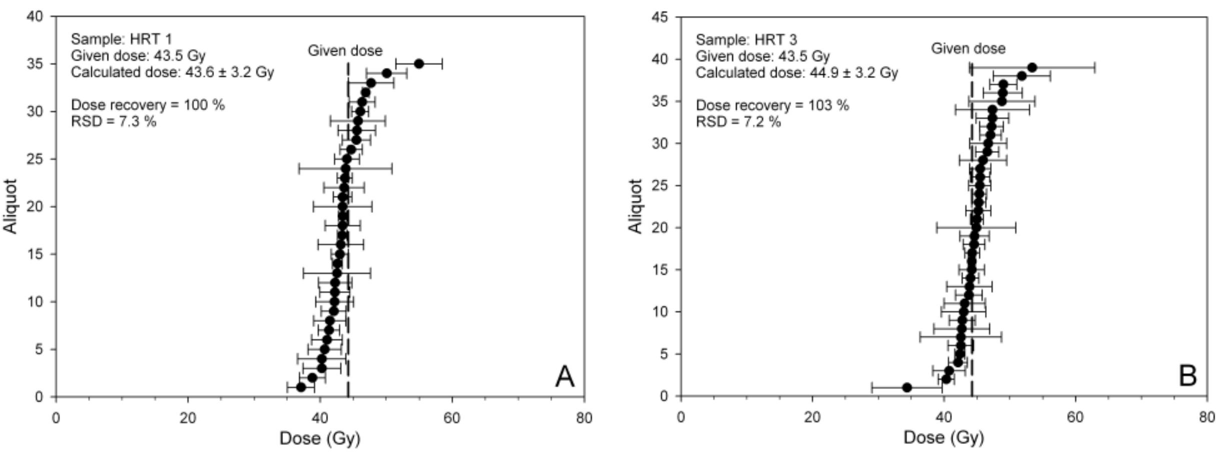

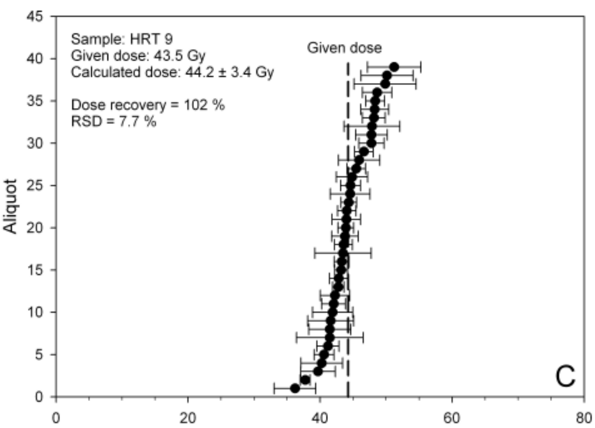

Fig. 4. Spread of individual ED values in the dose recovers tests. For all three samples, recovered dose is constituent with given does within errors and standard deviation (1σ) is similar for the different samples. The standard deviation from theses experiments is used a input data for extracting mean palaeodose out of the dose distributions.

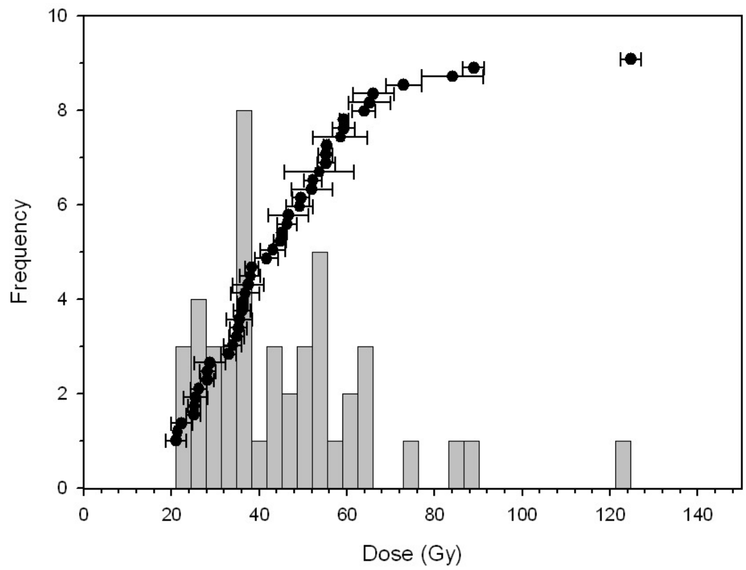

Fig. 5. Example dose distribution given for samples HRT7. The positive skewness indicates differential bleaching of the OSL singal in the different aliquots.

differential bleaching of the OSL signal in individual quartz grains. This aliquot size has been shown to suffice in previous studies on similar material (Choi et al., 2007; Fiebig and Preusser, 2007; Preusser et al., 2007). A preheat of 230°C for 10 s was used prior to all OSL measurements and the suitability of this procedure was confirmed by dose recovery and thermal transfer tests (i.e., Rhodes, 2000; Wallinga et al., 2000; Preusser et al., 2007). As in previous samples on Alpine quartz (Klasen et al., 2006, 2007; Preusser et al., 2007), we found relatively low OSL signals (Fig. 2) and negligible thermal transfer in our samples (Fig. 3). The results of dose recovery tests show no change of recovered ED with preheat temperature (Fig. 3) as well as a good to excellent recovery of given laboratory doses (Fig. 4 a-c). All this indicates that the applied SAR procedure performed well. For dating, 48 aliquots were measured for each sample and the majority of those passed through the rejection criteria of the SAR protocol (Murray and Wintle, 2000). The positively skewed dose distributions imply differential bleaching of the OSL signal prior to deposition (Fig. 5). We used two methods to extract mean ED out of the dose distributions. The first uses the Median of all individual ED values but this will mainly correct for the scatter due to microdosimetry only (e.g., Mayya et al., 2006) and may hence be seen as a maximum burial dose estimate only. The second estimate is based on the method presented by Preusser et al. (2007), which sets a certain threshold scatter up to which ED values are accepted (Model approach). In the present study, the threshold value is calculated on the basis of the observed reproducibility in dose recovery tests (7.5 %, Fig. 4 a-c) and an assumed effect of microdosimetry of 15 %, representing the mean values used in previous studies (Choi et al., 2007; Preusser et al., 2007). The later is considered as the likely mean ED estimate. For both values, standard errors were included in the age calculation.

Sample	Site	Grain size (µm)	n	K (%)	Th (ppm)	U (ppm)	W_{eff} (%)	Depth (m)	D (Gy ka^{-1})	ED_{Median} (Gy)	Age_{Median} (ka)	ED_{Modell} (Gy)	Age_{Modell} (ka)
HRT1	Chaisterfeld	149-202	41	0.97 ± 0.02	2.45 ± 0.24	0.91 ± 0.07	10 ± 5	13	1.25 ± 0.07	38.6 ± 2.9	30.8 ± 2.9	25.2 ± 0.5	20.1 ± 1.2
HRT2	Chaiste	149-202	38	1.11 ± 0.02	2.92 ± 0.23	1.08 ± 0.06	10 ± 5	9	1.45 ± 0.08	44.1 ± 3.5	30.1 ± 2.9	23.8 ± 1.0	16.2 ± 1.1
HRT3	Chleigrut	149-202	37	0.81 ± 0.02	2.78 ± 0.23	1.01 ± 0.04	10 ± 5	13	1.16 ± 0.06	41.1 ± 2.6	35.5 ± 3.0	30.9 ± 1.0	26.7 ± 1.7
HRT4	Chleigrut	149-202	38	1.16 ± 0.02	2.96 ± 0.22	1.06 ± 0.04	10 ± 5	8	1.51 ± 0.08	47.8 ± 3.2	31.6 ± 2.7	27.7 ± 0.9	18.3 ± 1.1
HRT5	Chleigrut	149-202	39	1.09 ± 0.02	2.55 ± 0.16	0.97 ± 0.03	10 ± 5	4	1.45 ± 0.07	45.6 ± 3.0	31.4 ± 2.6	33.1 ± 0.8	22.8 ± 1.3
HRT6	Markhof	149-202	42	1.02 ± 0.02	2.51 ± 0.21	0.93 ± 0.06	10 ± 5	6	1.35 ± 0.07	30.2 ± 1.8	22.3 ± 1.8	22.8 ± 0.5	16.8 ± 1.0
HRT7	Haltingen	149-202	45	0.89 ± 0.02	3.26 ± 0.19	1.22 ± 0.09	10 ± 5	15	1.30 ± 0.08	43.1 ± 3.0	33.2 ± 3.0	27.2 ± 0.7	20.9 ± 1.2
HRT8	Haltingen	149-202	38	0.78 ± 0.02	2.93 ± 0.18	1.04 ± 0.04	10 ± 5	12	1.15 ± 0.06	34.5 ± 3.8	29.9 ± 3.7	19.0 ± 0.5	16.5 ± 1.0
HRT9	Haltingen	149-202	39	1.32 ± 0.03	4.35 ± 0.27	1.39 ± 0.06	10 ± 5	5	1.85 ± 0.10	40.4 ± 2.5	21.8 ± 1.8	21.2 ± 0.5	11.4 ± 0.7
HRT10	Muttenz	149-202	39	0.76 ± 0.02	3.49 ± 0.18	1.17 ± 0.05	10 ± 5	18	1.18 ± 0.07	43.4 ± 2.3	36.7 ± 2.9	25.0 ± 0.9	21.1 ± 1.4
HRT11	Muttenz	149-202	40	1.02 ± 0.02	3.10 ± 0.21	1.16 ± 0.05	10 ± 5	7	1.43 ± 0.08	32.3 ± 1.5	22.5 ± 1.6	17.8 ± 0.7	12.4 ± 0.8
HRT12	Wallbach	149-202	37	1.09 ± 0.02	2.88 ± 0.31	1.11 ± 0.05	10 ± 5	7	1.47 ± 0.08	47.6 ± 2.2	32.4 ± 2.3	40.4 ± 1.1	27.5 ± 1.7
HRT17	Habsheim	150-200	40	1.16 ± 0.04	4.43 ± 0.11	1.58 ± 0.10	10 ± 5	0.6	1.84 ± 0.13	33.0 ± 2.3	18.0 ± 1.8	24.3 ± 0.6	13.2 ± 1.0

Age Model assumes 7.5 % scatter from lab reproducibility and 15 % scatter from microdosimetry (= 16.8 % total scatter).

Tab. 1. Results of dosimetry and luminescence measurement, and calculated median and model OSL ages.

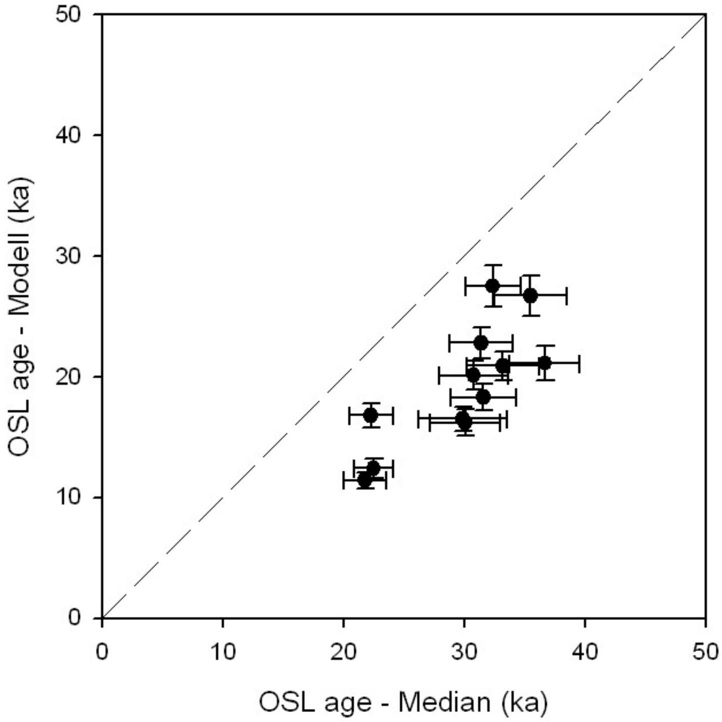

Fig. 6. Plot of OSL ages calculated using either the Median or Model approach. Using Median for age calculation systematically overestimates the ages compared to Model.

Determination of dose rate relevant elements (K, Th, U) was carried out by high-resolution gamma spectrometry (Preusser and Kasper, 2001). We found no evidence for radioactive disequilibrium in the Uranium decay chain in the sand layers. The concentration of dose relevant elements was transformed into dose rates using the conversion factors by Adamiec and Aitken (1998). For all samples, mean moisture content during burial of 5-15 % was assumed. This value is justified by typical water contents of 5 % observed in several dozens of sampled sand layers from Late Pleistocene braided river deposits, which likely give the minimum water content during burial (Preusser, unpublished data). The upper limit is set recognizing that incision of the present river bed into the Lower Terrace gravel deposits occurred most likely soon after deposition (e.g., Choi et al., 2007) and samples were water saturated for only a relatively short period of time. The contribution of cosmic dose to the total dose rate was calculated using present day depth following Prescott and Hutton (1994).

2.2 Results and discussion of OSL dating

It is important to recognize that there is a systematic difference between the two different age estimates calculated for each sample (Tab. 1). It is clearly shown that using the Median gives significantly higher age estimates than using the Model-approach (Fig. 6). We are here favoring the second approach for the following reasons: The dose distributions are clearly skewed which implies the presence of incompletely bleached aliquots. Using Median will hence most likely include some ED values that do not represent the dose absorbed during burial but also inherited

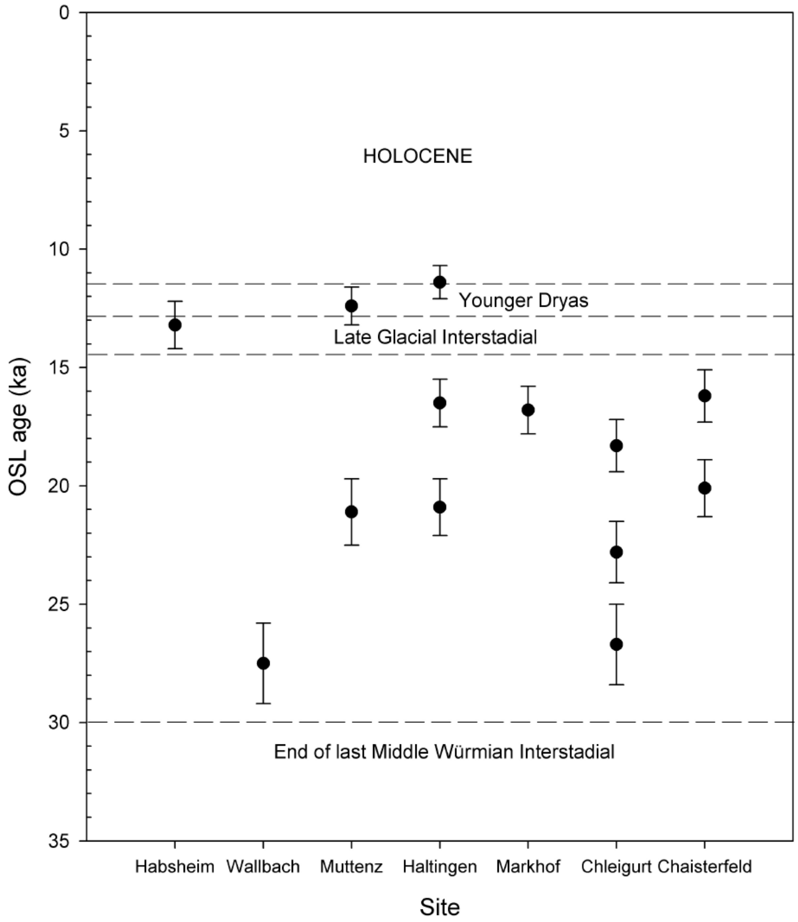

Fig. 7. Plot of OSL ages for the different sites investigated. OSL ages fall into two cluster correlation with the Last Glacial Maximum and the Younger Dryas, respectively.

dose and therefore overestimate the true deposition age of the samples. This observation is supported by evidence of dating Lower Terrace deposits of known age both in the Swiss lowlands (Preusser et al., 2007) as well as in the Middle Rhine Valley (Choi et al., 2007). The latter is located in a similar morphological setting (valley incised in midlands with expected high slope sediment input). In both these studies, ages calculated using Median (or even Mean) gave ages significantly overestimated, whereas the Model-approach resulted in ages in fair to good agreement compared to independent age control. In the following, we will hence purely concentrate on the ages calculated using the latter approach.

An overview of the calculated ages (Fig. 7) shows that eleven results fall within the period 30-15 ka, thus in the period considered to represent full glacial conditions in the Swiss lowlands (Preusser, 2004). The lower limit of this period is given by the end of the last Middle Würmian Interstadial that ended about 30 ka ago and was followed soon afterwards by the advance of Alpine glaciers into the lowlands (e.g., Preusser et al., 2003, 2007). The upper limit is the beginning of the Late Glacial Interstadial, which according to Litt et al. (2003) started about 14.5 ka ago. In response to the change in environmental conditions, many rivers switched from a braided to a meandering

Fig. 8. The concretions that are investigated here form on the lower face of pebbles in open-framework condition, and build meniscuses at contact points with other pebbles. Thickness varies from 0.5 to 1.5 mm, up to 7 mm on the meniscuses.

Fig. 9. Thin section of a crystalline pebble from the Markhof outcrop. The crust shows macroporosity. Scale is 1 mm.

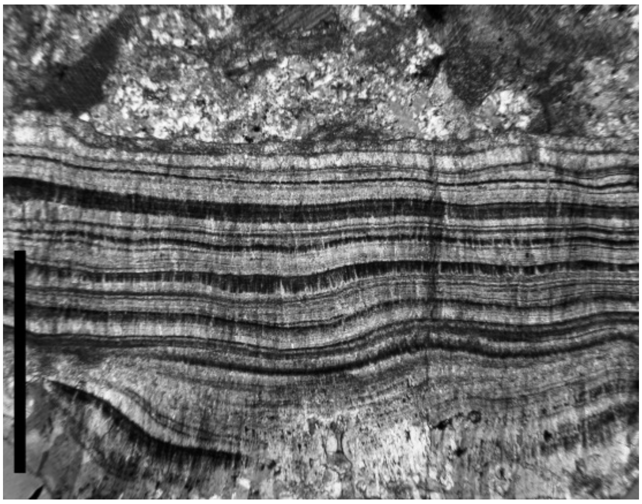

Fig. 10. Thin section of a limestone pebble from the Muttenz outcrop. Several drak laminae are visible. Scale is 1 mm.

flow pattern and started to incise into their own sediments (e.g., Törnqvist, 1998). This change in dynamics also affected the River Rhine downstream (Choi et al., 2007) and it presumably occurred in the study area as well. With the cooling during the Younger Dryas Chron, many rivers, including the Rhine, shifted for a short time back to a braided system (Törnqvist, 1998; Andres et al., 2001) and actually three OSL dates of 11.4 ± 0.7 ka (HRT9), 12.4 ± 0.8 ka (HRT11) and 13.2 ± 1.0 ka (HRT17) imply deposition during this last cold period prior to the Holocene warming. Those samples have been taken several meters below the present surface, which implies that the

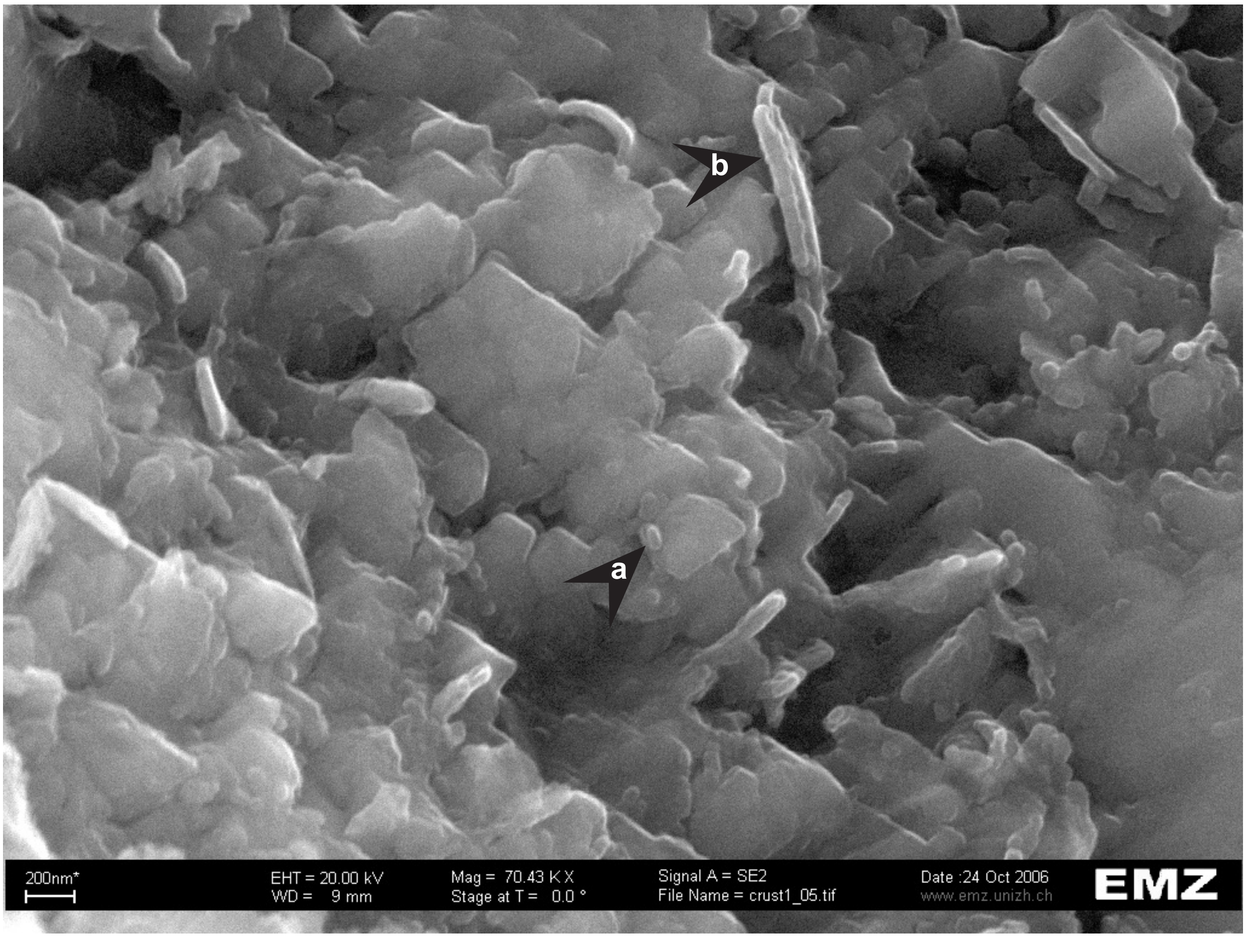

Fig. 11. SEM picture of the surface of a crust. The arrows show two probable bacteria: a) nanoglobolus shaped, and b) vibrio shaped. Bactereia possibly played an important role in carbonate precipitation.

Sample	δ13C VPDB	δ18O SMOW
MUMS1 l-a	-10	-6.9
MUMS1 l-b	-10.4	-6.7
MUMS1 l-c	-10.2	-6.7
MUMS1 l-d	-10.5	-7.7
WYKG2 h-a	-10.8	-8
WYKG2 h-b	-10.9	-7
WYKG2 h-c	-11.1	-7.2
WYKG2 h-d	-10.8	-7.8
WYKG2 h-d2	-10.8	-8.1

Tab. 2. Oxygen and carbon isotopes measured on pebbles from two different outcrops.

aggradation phase during the Younger Dryas was significant. This is in good agreement with OSL-dated evidence from the Middle Rhine Valley, which even indicates the formation of an individual terrace level during this time (Choi et al., 2007).

3. U/Th dating of calcite crusts

3.1 Description and origin of the crusts

Different types of carbonate cements can be observed in the gravels of the Lower Terrace. Here we focus on well developed stalactitic calcite cement that occurs commonly in open framework gravels in the study area, and which was used for U/Th dating. The crusts typically cover a wide

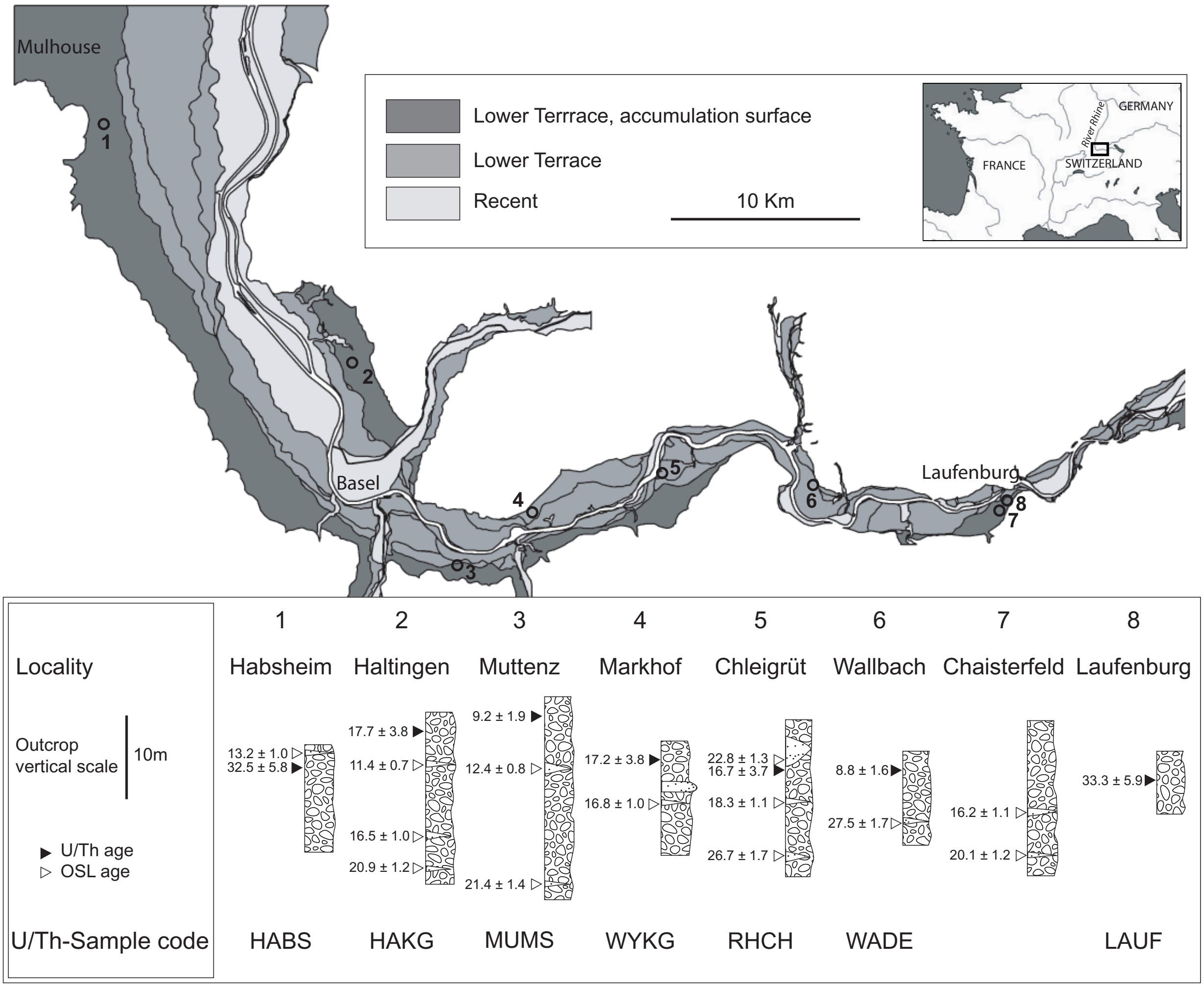

Fig. 12. Map showing the location of the outcrops in relation with the OSL (empty triangles) and U/Th ages (plain triangles). At locations 1 to 6, samples for both OSL and U/Th investigation were available from the same outcrop. Location 7 was devoid of encrusted pebble, whereas location 8 lacked suitable sand deposit for OSL.

part of the lower side of pebbles (Fig. 8), with a thickness between 0.5 and 1.5 mm, and form meniscuses at contact points with other pebbles, where the thickness can reach 7 mm. X-ray diffractometry detected calcite only. Colours range from brownish-yellowish to almost colourless. At those locations, the crust can be very irregular and can feature “mushroom-like” shapes, which can be responsible for macroporosity (Fig. 9). It is usually possible to macroscopically distinguish different strata within the thickest crusts.
Observations in thin sections under an optical microscope reveal several dark laminae within calcite crystals (Fig. 10). A closer look suggests that these dark laminae are formed by an accumulation of organic matter, where bacteria-like forms can be recognized, which could have contributed to calcite precipitation (Riding, 2000; Krumbein et al., 2003). SEM pictures of a crust surface also suggest the presence of bacteria comparable to those described by Aloisi et al. (2006) (Fig. 11 a) and van Lith et al. (2003) (Fig. 11 b). These are, however, only morphological evidences, complementary work is needed to state that these structures are fossil microorganisms.
Stable isotopes analysis were performed on a Thermo Finnigan DELTAplus XP Continuous Flow Isotope Ratios Mass Spectrometer (GasBench II) on some samples and yielded $\delta\ ^{13}C$ values between -10.0 and -11.1 ‰, with $\delta\ ^{18}O$ values between -6.7 and -8 ‰. (Tab. 2: Stable isotopes). The $\delta\ ^{13}C$ values cannot be explained by the sole dissolution of limestone pebbles within the terrace or from the nearby limestone substratum, since these have values close to 0 (marine carbonates). It is thus reasonable to assume a contribution by organic matter from soil, which has typical values of ca. -27 in Europe (Hemming et al., 2005). This implies a significant presence of soil during the formation of the calcite crust and hence temperate climatic conditions. Such conditions are also suggested by the heavy oxygen isotope ratio (modern rainwater mean $\delta\ ^{18}O$ values in Basel: -8.5; unpublished measurements of the Swiss Federal Office for the Environment).

3.2 U/Th methodology

Pebbles covered with crusts were collected in seven gravel pits (Fig. 12). Whenever possible, the pebbles were collected out of matrix-free zones (open framework), in order to get the best developed crusts and to avoid the risk of limestone-sand being incorporated in the crust. Crusts from 41 pebbles were analyzed for Uranium-series ages. 0.1–0.2 g of sample were mechanically separated from the pebble, spiked with a mixed ^{229}Th–^{236}U spike, dissolved in HCl, taken to dryness and then converted to the nitrate form. Organic material, if present, was attacked with 0.5 ml of H_2O_2+HNO_3 (conc.). U and Th were separated on anion columns using 0.5 ml Eichrom U-TEVA ® resin. Matrix was removed with 7 M HNO_3; Th was eluted with 5 N HCl and finally U with 0.5 NHCl. After evaporation, U and Th fractions were treated in oxygen plasma to destroy organic remnants from the resin. U and Th mass spectrometry was done as described by Fleitmann et al. (2007), using a Nu Instruments® multicollector ICP–MS equipped with an ESI Apex® desolvating system without membrane and using a self-aspirating nebulizer. With an uptake rate of ca 50

Sample	c(U)		c(Th)		(234U/238U)		(238U/232Th)		(234U/232Th)		(230Th/232Th)		(230Th/238U)		(230Th/234U)		Age		Pebble
	(ppb)	±	(ppb)	±		±		±		±		±		±		±	(ka)	±	
HABS a	403.4	0.7	145.798	0.850	1.0896	0.0010	8.3504	0.0506	9.0986	0.0557	3.9908	0.0301	0.4779	0.0024	0.4386	0.0023			sandstone
HABS b	383.0	0.6	90.253	0.523	1.0644	0.0013	12.8073	0.0772	13.6332	0.0839	3.6213	0.0261	0.2828	0.0013	0.2656	0.0013			quartzite
HABS f	677.4	1.1	3792.093	21.607	0.9672	0.0009	0.5391	0.0032	0.5214	0.0031	0.4124	0.0033	0.7650	0.0044	0.7910	0.0046	32.498	5.671	crystalline
HABS g	323.9	0.5	202.550	1.155	1.0775	0.0009	4.8257	0.0287	5.1996	0.0312	1.9235	0.0147	0.3986	0.0021	0.3699	0.0020			quartzite
HABS i	352.2	0.6	135.130	0.766	1.0746	0.0016	7.8670	0.0465	8.4538	0.0516	1.9225	0.0148	0.2444	0.0013	0.2274	0.0013			quartzite
HAKG a	329.2	0.4	820.900	5.700	1.1290	0.0011	1.2103	0.0086	1.3665	0.0098	0.9956	0.0091	0.8226	0.0050	0.7286	0.0044			quartzite
HAKG b	403.6	0.7	123.161	0.677	1.0739	0.0013	9.8905	0.0568	10.6213	0.0623	2.7975	0.0225	0.2829	0.0017	0.2634	0.0016			crystalline
HAKG b	389.4	0.5	265.900	1.700	1.0730	0.0012	4.4195	0.0293	4.7423	0.0320	2.5611	0.0207	0.5795	0.0029	0.5401	0.0028			crystalline
HAKG c	393.6	0.5	265.400	1.800	1.1043	0.0020	4.4758	0.0318	4.9429	0.0362	2.4619	0.0262	0.5501	0.0045	0.4981	0.0042	17.726	3.785	chert
HAKG d	299.5	0.5	69.485	0.392	1.0725	0.0011	13.0104	0.0764	13.9544	0.0831	3.3356	0.0266	0.2564	0.0015	0.2390	0.0014			limestone
HAKG e	209.5	0.4	52.985	0.297	1.0705	0.0014	11.9320	0.0699	12.7734	0.0766	2.7381	0.0236	0.2295	0.0015	0.2144	0.0015			limestone
HAKG f	206.0	0.4	179.957	1.033	1.0873	0.0020	3.4540	0.0207	3.7556	0.0235	1.1321	0.0120	0.3278	0.0030	0.3015	0.0028			sandstone
LAUF b	433.3	0.7	313.028	1.827	1.0653	0.0009	4.1779	0.0253	4.4510	0.0272	2.1178	0.0164	0.5069	0.0027	0.4758	0.0026			quartzite
LAUF c	384.8	0.6	58.369	0.350	1.0666	0.0013	19.8991	0.1239	21.2257	0.1349	10.8327	0.0931	0.5444	0.0035	0.5104	0.0033			sandstone
LAUF c	454.3	0.6	84.500	0.600	1.1205	0.0013	16.2169	0.1142	18.1715	0.1298	6.8306	0.0676	0.4212	0.0030	0.3759	0.0028	33.299	5.888	sandstone
LAUF d	448.9	0.7	64.061	0.348	1.0769	0.0012	21.1461	0.1201	22.7736	0.1317	2.9512	0.0235	0.1396	0.0008	0.1296	0.0008			sandstone
LAUF d	592.9	0.8	1023.700	7.100	1.0991	0.0015	1.7478	0.0123	1.9211	0.0138	1.5480	0.0131	0.8857	0.0045	0.8058	0.0042			sandstone
MUMS1 c	569.4	1.0	187.871	1.151	1.1349	0.0018	9.1469	0.0583	10.3811	0.0683	2.6928	0.0358	0.2944	0.0035	0.2594	0.0031			volcanic sandstone
MUMS1 c	572.2	1.0	201.531	1.342	1.1138	0.0018	8.5686	0.0591	9.5444	0.0675	2.5635	0.0436	0.2992	0.0047	0.2686	0.0043			volcanic sandstone
MUMS1 c	535.9	1.0	224.019	1.541	1.0827	0.0014	5.3166	0.0263	5.7565	0.0294	1.7713	0.0168	0.3332	0.0028	0.3077	0.0026			volcanic sandstone
MUMS1 c	720.2	1.3	408.806	1.887	1.0921	0.0015	7.2189	0.0513	7.8842	0.0570	1.8822	0.0240	0.2607	0.0028	0.2387	0.0026			volcanic sandstone
MUMS1 e	397.2	0.7	209.050	1.465	1.0775	0.0019	5.7338	0.0415	6.1782	0.0460	2.3267	0.0368	0.4058	0.0058	0.3766	0.0054	9.249	1.898	quartzite
MUMS1 f	417.6	0.7	364.313	2.643	1.0919	0.0027	3.4592	0.0258	3.7773	0.0297	2.0877	0.0380	0.6035	0.0101	0.5527	0.0094			limestone
MUMS1 f	332.5	0.6	129.172	0.536	1.0697	0.0017	7.7685	0.0351	8.3104	0.0399	1.8468	0.0251	0.2377	0.0031	0.2222	0.0029			limestone
MUMS1 h	414.0	0.7	142.501	0.629	1.0796	0.0015	8.7683	0.0417	9.4662	0.0470	2.1383	0.0275	0.2439	0.0030	0.2259	0.0028			radiolarite
MUMS1 j	532.0	0.9	202.019	0.924	1.1213	0.0015	7.9483	0.0390	8.9130	0.0453	2.4519	0.0221	0.3085	0.0025	0.2751	0.0022			sandstone
RHCH a	338.1	0.6	213.472	1.171	1.1714	0.0019	4.7801	0.0276	5.5998	0.0336	2.8457	0.0213	0.5953	0.0032	0.5082	0.0029			limestone
RHCH b	494.3	0.7	653.257	4.673	1.1547	0.0017	2.2838	0.0166	2.6372	0.0196	1.7217	0.0160	0.7539	0.0046	0.6529	0.0041			quartzite
RHCH c	306.2	0.6	222.702	1.416	1.1210	0.0026	4.1488	0.0274	4.6508	0.0325	1.4978	0.0143	0.3610	0.0026	0.3221	0.0025	16.747	3.7070	limestone
RHCH d	459.5	0.8	387.862	2.827	1.0746	0.0013	3.5751	0.0267	3.8419	0.0291	2.1024	0.0203	0.5881	0.0039	0.5472	0.0037			quartzite
RHCH d	581.3	0.8	239.640	1.681	1.0789	0.0015	7.3203	0.0524	7.8982	0.0575	2.3421	0.0288	0.3200	0.0033	0.2966	0.0030			quartzite
WADE c	221.7	0.3	23.177	0.218	1.0817	0.0014	28.8653	0.2742	31.2242	0.2992	5.1321	0.0811	0.1778	0.0023	0.1644	0.0021			quartzite
WADE d	250.3	0.3	15.452	0.106	1.1206	0.0014	48.8846	0.3418	54.7813	0.3887	5.9460	0.1083	0.1216	0.0021	0.1085	0.0018	8.804	1.633	sandstone
WADE e	269.6	0.4	117.136	0.842	1.1062	0.0013	6.9472	0.0509	7.6855	0.0570	2.4902	0.0312	0.3585	0.0037	0.3240	0.0034			limestone
WADE f	346.4	0.6	73.439	0.402	1.1224	0.0028	14.2355	0.0816	15.9791	0.1000	2.9501	0.0230	0.2072	0.0012	0.1846	0.0012			sandstone
WYKG 2 f	322.9	0.5	134.437	0.744	1.0864	0.0017	7.2495	0.0419	7.8760	0.0472	2.0571	0.0178	0.2838	0.0019	0.2612	0.0018			crystalline
WYKG 2 g	324.0	0.5	146.193	0.847	1.1494	0.0015	6.6891	0.0402	7.6889	0.0473	2.1391	0.0176	0.3198	0.0019	0.2782	0.0017			quartzite
WYKG2 b	436.7	0.8	364.222	2.225	1.0921	0.0015	3.6186	0.0230	3.9520	0.0257	1.2166	0.0283	0.3362	0.0076	0.3078	0.0069	17.220	3.793	crystalline
WYKG2 e	743.2	1.0	2154.767	15.408	1.1353	0.0011	1.0409	0.0076	1.1818	0.0087	1.3041	0.0121	1.2529	0.0076	1.1035	0.0068			crystalline
WYKG2 j	437.4	0.8	124.035	0.484	1.1521	0.0015	10.6416	0.0456	12.2606	0.0548	2.7660	0.0265	0.2599	0.0023	0.2256	0.0020			sandstone

Tab. 3. Results of U and Th analysis, and calculated U/Th ages.

ml/min the ion yield for U and Th was about 70 V/ppm. U measurements were done from 0.5N HNO_3 solutions in static mode, whereby masses 236 and 234 were measured in parallel electron multipliers and 235 and 238 in Faraday cups. Baselines were taken on either side of peaks and interpolated. The electron multiplier yield was calibrated every 5 samples by running a NIST U050 solution. The $^{238}U/^{235}U$ ratio was used for instrumental fractionation correction if the ^{238}U signal was greater than 1V (10^{-11} A); if smaller, the fractionation factor was input from bracketing standards. Normal washout time for U between samples was 5 min with 0.5N HNO_3 (< 1‰ memory); longer washout times were used where significant isotope differences between samples were expected. Runs on the NIST U960 standard yielded $\delta(^{234}U/^{238}U)$ -37.2 ± 2.1‰ (1SD, n = 35), where the equilibrium ratio is after Cheng et al. (2000). Th measurements were made from 3N HCl solutions in a two-cycle multicollector dynamic mode, whereby one electron multiplier, equipped with a WARP filter, alternatingly measured masses 229 and 230. U standard was added to Th run solutions for two reasons, first, to enable correction for instrumental mass fractionation, and second, to provide a reference isotope (238) to eliminate the effects of plasma flicker in obtaining the $^{229}Th/^{230}Th$ ratios. Variations of U and Th signals during the run are fully correlated if no organic matter is present. Baselines were measured at 229.5 and 230.5 for samples and standards with significant (>10^{-12} A) ^{232}Th. Washout time was 5 min to 1‰ of the Th signal, if the capillary and nebulizer were free of organics. Because of the low U concentration (Tab. 3), all data from each outcrop were used to calculate a single age.

3.3 Results of U/Th dating

U/Th results are shown in Table 3. The ($^{234}U/^{238}U$) vs. ($^{230}Th/^{238}U$) plot (Fig. 13) qualitatively shows the samples to lie within the "accumulation" quadrant typical of the precipitation of solutions derived from weathering (Osmond and Ivanovich, 1991), with fairly uniform ($^{234}U/^{238}U$) ratios but a rather large range of $^{230}Th/^{238}U$ ratios. Age indications from regression of the *prima facie* ($^{230}Th/^{232}Th$) vs. ($^{234}U/^{232}Th$) data (naturally with large errors) in most cases appear too old relative

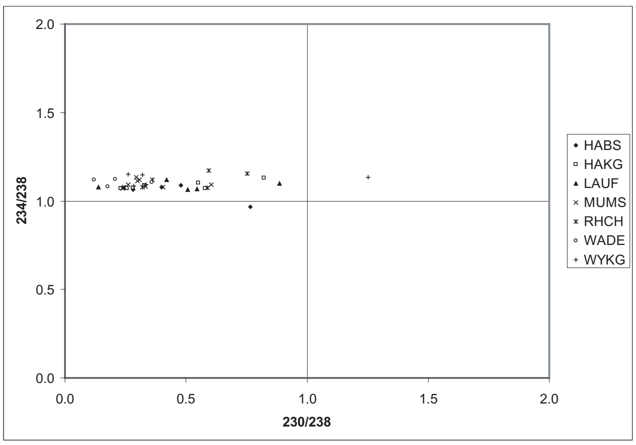

Fig. 13. ($^{234}U/^{238}U$) vs. ($^{230}Th/^{238}U$) graph where all samples plot in the "rapid accumulation" zone of Osmond and Ivanovich (1991).

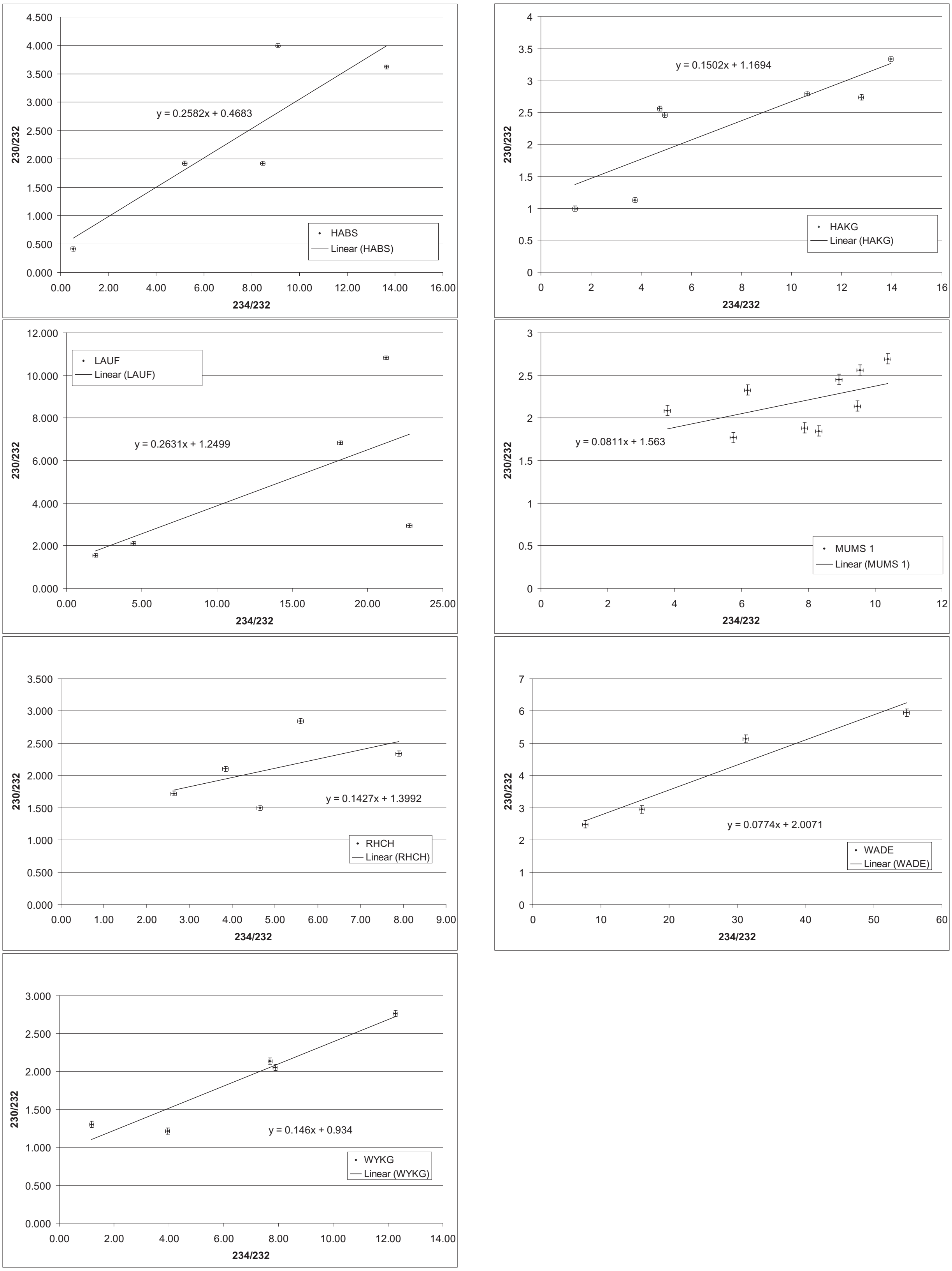

Fig. 14. (^{230}U/^{232}U) vs. (^{234}Th/^{232}U) graphs for each location. The oblique line is the regression and its formula is given next to it. In these equations, the x-factor is the slope of the line, which is used in the age calculation as ^{230}U/^{234}Th activity ratio. Error bars are 2 sigma.

to other constraints (such as OSL and geomorphology).

In the case of a detrital component contaminating the crust material, reasonably linear arrays would be expected in the ($^{230}Th/^{232}Th$) vs. ($^{234}U/^{232}Th$) plots (Fig. 14), offset by the initial $^{230}Th/^{232}Th$ ratios, a function of the source material's U/Th ratio, and with slopes giving the $^{230}Th/^{234}U$ age. However, most of our sample series show great scatter in these plots, indicating either highly variable U/Th ratios in the detrital component, or a fractionation between ^{230}Th and ^{232}Th in the environment from which the crust-forming solutions were derived. Naturally, the low U concentrations of the samples analysed increase the relative uncertainty in dates caused by the scatter.

A purely detrital contamination could carry initial $^{230}Th/^{232}Th$ ratios in the range from 0.8 (for a typical crustal igneous rock source) to about 4 (for a marine limestone source) and this would have been expected to be reasonably homogeneous within one locality, so that good isochron-type correlations should still result. In our sample suites, the scatter is thus mostly much larger than expected from a purely detrital Th input. This is best illustrated by the suite from Habsheim, where pebbles are predominantly crystalline or sandstones ("Buntsandstein"), i.e. not calcareous. Here a reasobably homogeneous initial ($^{230}Th/^{232}Th$) of c. 0.8 could be expected from a detrital contaminant, but the data show a huge scatter, and for any Holocene age, the initial ($^{230}Th/^{232}Th$) values could range up to 3.5, which is fully unexpected in a crystalline terrain. A possible solution to this problem is discussed below.

4. Discussion

The OSL data are consistent with what could be expected from geomorphic observations and their correlations with dated localities (Choi et al., 2007; Preusser et al., 2007) and consistent with each other since they become younger as depth decreases. We notice that our data are in contradiction with previous luminescence dating attempts in this area, which produced much older ages (Frechen et al. 2004). However, these ages were obtained using the Multiple Aliquot Additive Dose (MAAD) protocol, with which detection of partially bleached material is not possible. This seems to be the cause of the age discrepancy, since our measurements using the SAR protocol highlighted the occurrence of partially bleached quartz grains in the samples (Fig. 4).

The U/Th ages cannot be directly compared with OSL ages since the crusts formed some time after deposition of the terrace material, under vadose conditions. Although older terraces are being eroded in the area, and many pebbles have been reworked from these terraces, it can be excluded that the crusts themselves have been reworked. Firstly, all the crusts are exclusively on the underside of the pebbles, secondly, pre-existing crusts would have been abraded in the high energy process of deposition. The crusts were thus formed *in situ* and postdate the deposition of the gravels.

As the stable isotopic data indicated temperate conditions and with respect to the OSL ages, a Late Glacial (Bølling/Allerød Interstadial) or Holocene age from the U/Th experiments can be expected. However, this was the case only for two locations (Muttenz and Wallbach) out of the six for which OSL age control is available.

Ideally, the crusts should have been sampled within one layer, as described in Blisniuk and Sharp (2003) and Sharp et al. (2003), to avoid mixed ages from several layers and to refine the precipitation chronology. Unfortunately, the U concentrations of our samples were an order of magnitude too low. The quantity of sample material needed for the analysis therefore did not allow such precise sampling. However, this cannot be the reason for the discrepancies between our U/Th and OSL ages, since it would imply that the ages of the oldest parts of the crusts are even older, which would still be incompatible with the OSL data.

We suggest that the U/Th ages that appear overestimated most probably result from excess of initial ^{230}Th that is not connected to ^{232}Th in a detrital component, but is related to long-term weathering and pedogenesis in the source area of the crust-forming solutions. U/Th dating is based on the initial assumption that Th is not soluble, and is thus not incorporated in a solid precipitated from a liquid. However, it has been shown that Th can be transported by organic colloids (Kim, 1991; Meier et al., 2003; Schafer et al., 2004), thus enabling it to be incorporated into carbonate crusts. In the weathering environment hexavalent ^{234}U is mobile, but its daughter ^{230}Th tends to be adsorbed immediately onto iron oxide coatings or organic substances. Bacterial activity in pedogenesis can destroy iron oxide coatings, after which the ^{230}Th would bind to organic matter which could be transported as a colloid. Thus there is a decoupling of mobile ^{234}U, detrital ^{232}Th and colloid-mobile ^{230}Th, which could cause great variations in the initial (^{230}Th/^{232}Th) and (^{230}Th/^{234}U) ratios in any downstream precipitates. This would increase with the duration of pedogenesis prior to crust formation.

Organic-rich layers were indeed seen in the crusts analysed (Fig. 3.3) and organics were noted in dissolution. If bacterial desorption and colloid transport of ^{230}Th occurred, it could only have increased, not decreased the initial (^{230}Th/^{232}Th) and (^{230}Th/^{234}U) ratios. Following this logic, a regression through the data scatter of the (^{230}Th/^{232}Th) vs. (^{234}U/^{232}Th) plots would in fact be senseless. Rather, the lower envelope of a data set in these plots should give a maximum age for crust formation. Applying this principle to the Haltingen and Laufenburg samples would thus give ages of 6.4 ka and 7.6 ka, respectively, which would fit in the general context, but the Chleigrüt and Markhof samples would then give ages older than if calculated from the regression. This problem could be at least partly solved by analysing more samples and thus improving the statistical reliability. Another message from this study, relating to possible future efforts in dating sinters using U/Th, is that units or layers completely devoid of organic matter should be targeted.

5. Conclusion

Two different topics were addressed by this study: First, it provides a reliable time frame for the deposition of the Lower Terrace in the area of Basel. Two accumulation phases related with cold periods are recognized: The Last Glacial Maximum and the Younger Dryas (30-15 and 13-11 ka). Second, it shows that U/Th dating potential of calcite crust, while basically possible, can be limited by low U concentration, Th mobility and bacterial activity. U/Th is nevertheless a promising method that deserves attention, especially for geomorphology and neotectonics.

Acknowledgments

The authors are grateful to the companies for giving access to their gravel pits, sometimes even giving a hand with their excavator. Gamma spectrometry for the luminescence dating was carried out by J. Lomax at Geographisches Institut, Universität zu Köln. We thank C. Vasconcelos and E. Verrecchia for their help and comments regarding bacterial activity. The rain water $\delta\ ^{18}O$ values come from the national ground water observation NAQUA, module ISOT of the Swiss Federal Office for the Environment, in cooperation with the Physical Institute of the University of Bern.

References

Adamiec, G., Aitken, M.J., 1998. Dose-rate conversion factors: update. Ancient TL 16, 37-50.

Aloisi, G., Gloter, A., Krüger, M., Wallmann, K., Guyot, F., Zuddas, P., 2006. Nucleation of calcium carbonate on bacterial nanoglobules. Geology 34, 1017-1020.

Andres, W., Bos, J.A.A., Houben, P., Kalis, A.J., Nolte, S., Rittweger, H., Wunderlich, J., 2001. Environmental change and fluvial activity during the Younger Dryas in central Germany. Quaternary International 79, 89-100.

Blisniuk, P.M., Sharp, W.D., 2003. Rates of late Quaternary normal faulting in central Tibet from U-series dating of pedogenic carbonate in displaced fluvial gravel deposits. Earth and Planetary Science Letters 215, 169-186.

Blum, M.D., Törnqvist, T.E., 2000. Fluvial responses to climate and sea-level change: a review and look forward. Sedimentology 47, 2-48.

Bonnet, S., Guillocheau, F., Brun, J.-P., 1998. Relative uplift measured using river incisions: the case of the armorican basement (France). Comptes Rendus de l'Academie des Sciences Série II Fascicule A-Sciences de la Terre et des Planètes 327 245-251.

Candy, I., Black, S., Sellwood, B.W., 2004. Quantifying time scale of pedogenic calcrete formation using U-series disequilibria. Sedimentary Geology 170, 177-187.

Candy, I., Black, S., Sellwood, B.W., 2005. U-series isochron dating of immature and mature calcretes as a basis for constructing Quaternary landform chronologies for the Sorbas basin, southeast Spain. Quaternary Research 64, 100-111.

Cheng, H., Edwards, R.L., Hoff, J., Gallup, C.D., Richards, D.A., Asmerom, Y., 2000. The half-lives of uranium-234 and thorium-230. Chemical Geology 169, 17-33.

Choi, S.-W., Preusser, F., Radtke, U., 2007. Dating of lower terrace sediments from the Middle Rhine area, Germany. Quaternary Geochronology 2, 137-142.

Fiebig, M., Preusser, F., 2003. Das Alter fluvialer Ablagerungen aus der Region Ingolstadt (Bayern) und ihre Bedeutung für die Eiszeitenchronologie des Alpenvorlandes. Zeitschrift für Geomorphologie 47, 449-467.

Fleitmann, D., Burns, S.J., Mangini, A., Mudelsee, M., Kramers, J.D., Villa, I., Neff, U., Al-Subbary, A.A., Buettner, A., Hippler, D., Matter, A., 2007. Holocene ITCZ and Indian monsoon dynamics recorded in stalagmites from Oman and Yemen (Socotra). Quaternary Science Reviews 26, 170-188.

Frechen, M., Ellwanger, D., Hinderer, M., Lämmermann, J., Neeb, I., 2004. Late Pleistocene fluvial dynamics in the Upper Rhine Graben and the Hochrhein area – chronological frame. Abstracts DEUQUA meeting Nijmegen, p. 34.

Häuselmann, P., Fiebig, M., Kubik, P.W., Adrian, H., 2007. A first attempt to date the original "Deckenschotter" of Penck and Brückner with cosmogenic nuclides. Quaternary International 164-165, 33-42.

Hemming, D., Yakir, D., Ambus, P., Aurela, M., Besson, C., Black, K., Buchmann, N., Burlett, R., Cescatti, A., Clement, R., Gross, P., Granier, A., Grünwald, T., Havrankova, K., Janous, D., Janssens, I.A., Knohl, A., Östner, B.K., Kowalski, A., Laurila, T., Mata, C., Marcolla, B., Matteucci, G., Moncrieff, J., Moors, E.J., Osborne, B., Santos Pereira, J., Pihlatie, M., Pilegaard, K., Ponti, F., Rosanova, Z., Rossi, F., Scartazza, A., Vesala, T., 2005. Pan-European δ13C values of air and organic matter from forest ecosystems. Global Change Biology 11, 1065-1093.

Houben, P., 2003. Spatio-temporally variable response of fluvial systems to Late Pleistocene climate change: a case study from central Germany. Quaternary Science Reviews 22, 2125-2140.

Houtgast, R.F., Van Balen, R.T., Bouwer, L.M., Brand, G.B.M., Brijker, J.M., 2002. Late Quaternary activity of the Feldbiss Fault Zone, Roer Valley Rift System, the Netherlands, based on displaced fluvial terrace fragments. Tectonophysics 352, 295-315.

Huggenberger, P., Regli, C., (2006). A sedimentological model to characterize braided river deposits for hydrogeological application. In: Braided Rivers, Sambrook Smith, G.H., Best, J.L., Bristow, C.S., Petts, G.E. (Eds), International Association of Sedimentologists Special Publication 36, 51-74.

Kelly, M., Black, S., Rowan, J.S., 2000. A calcrete-based U/Th chronology for landform evolution in the Sorbas basin, southeast Spain. Quaternary Science Reviews 19, 995-1010.

Kim, J.I., 1991. Actinide colloid generation in groundwater. Radiochimica Acta 52, 71-81.

Klasen, N., Fiebig, M., Preusser, F., Radtke, U., 2006. Luminescence properties of glaciofluvial sediments from the Bavarian Alpine Foreland. Radiation Measurements 41, 866-870.

Klasen, N., Fiebig, M., Preusser, F., Reitner, J.M., Radtke, U., 2007. Luminescence dating of proglacial sediments from the Eastern Alps. Quaternary International 164-165, 21-32.

Kock, S., Huggenberger, P., Preusser, F., Wetzel, A., submitted. Formation and evolution of the Lower Terrace of the Rhine River in the area of Basel. Swiss Journal of Geosciences.

Krumbein, W.E., Paterson, D.W., Zavarzin, G.A., (Eds.), 2003. Fossil and recent biofilms: A natural history of life on Earth. Dordrecht, Kluwer Academic Press Publishers.

Ku, T.L., Bull, W.B., Freeman, S.T., Knauss, K.G., 1979. 230Th-234U dating of pedogenic carbonates in gravelly desert soils of Vidal Valley, southern California. Geological Society of America Bulletin 90, 1063-1073.

Litt, T., Schmincke, H.-U., Kromer, B., 2003. Environmental response to climatic and volcanic events in central Europe during the Weichselian Lateglacial. Quaternary Science Reviews 22, 7-32.

Mayya, Y.S., Morthekai, P., Murari, M.K., Singhvi, A.K., 2006. Towards quantifying beta microdosimetric effects in single-grain quartz dose distribution. Radiation Measurements 41, 1032-1039.

Meier, H., Zimmerhackl, E., Zeitler, G., 2003. Modeling of colloid-associated radionuclide transport in porous groundwater aquifers at the Gorleben site, Germany. Geochemical Journal 37, 325-350.

Murray, A.S., Wintle, A.G., 2000. Luminescence dating of quartz using an improved single-aliquot regenerative-dose protocol. Radiation Measurements 32, 57-73.

Murray, A.S., Wintle, A.G., 2003. The single aliquot regenerative dose protocol: potential for improvements in reliability. Radiation Measurements 37, 377-381.

Nivière, B., Marquis, G., 2000. Evolution of terrace risers along the upper Rhine graben inferred from morphologic dating methods: evidence of climatic and tectonic forcing. Geophysical Journal International 141, 577-594.

Osmond, J.K., Ivanovich, M., 1991. Uranium-series mobilization and surface hydrology. In: Uranium-series Disequilibrium, Ivanovich, M., Harmon, R.S (Eds.) Oxford Science Publications. 259-289.

Prescott, J.R., Hutton, J.T., 1994. Cosmic ray contributions to dose rates for luminescence and ESR dating: Large depths and long-term time variations. Radiation Measurements 23, 497-500.

Preusser, F., 2004. Towards a chronology of the Late Pleistocene in the northern Alpine Foreland. Boreas 33, 195-210.

Preusser, F., Blei, A., Graf, H.R., Schlüchter, C., 2007. Luminescence dating of Würmian (Weichselian) proglacial sediments from Switzerland: methodological aspects and stratigraphical conclusions. Boreas 36, 1-13.

Preusser, F., Degering, D., Fuchs, M., Hilgers, A., Kadereit, A., Klasen, N., Krbetschek, M., Richter, D.,Spencer, J., 2008,. Luminescence dating: Basics, methods and applications. Quaternary Science Journal (Eiszeitalter & Gegenwart). (in press)

Preusser, F., Geyh, M.A., Schlüchter, C., 2003. Timing of Late Pleistocene climate change in lowland Switzerland. Quaternary Science Reviews 22, 1435-1445.

Preusser, F., Kasper, H.U., 2001. Comparison of dose rate determination using high-resolution gamma spectrometry and inductively coupled plasma - mass spectrometry. Ancient TL 19, 19-23.

Radtke, U., Brückner, H., Mangini, A., Hausmann, R., 1988. Problems encountered with absolute dating (U-series, ESR) of Spanish calcretes. Quaternary Science Reviews 7, 439-445.

Rhodes, E.J., 2000. Observations of thermal transfer OSL signals in glacigenic quartz. Radiation Measurements 32, 595-602.

Rhodes, E.J., Singarayer, J.S., Raynal, J.-P., Westaway, K.E., Sbihi-Alaoui, F.Z., 2006. New age estimates for the Palaeolithic assemblages and Pleistocene succession of Casablanca, Morocco. Quaternary Science Reviews 25, 2569-2585.

Riding, R., 2000. Microbial carbonates: The geological record of calcified bacterial-algal mats and biofilms. Sedimentology 47, 179-214.

Rittenour, T.M., Goble, R.J., Blum, M.D. 2005. Development of an OSL chronology for Late Pleistocene channel belts in the lower Mississippi valley, USA. Quaternary Science Reviews 24, 2539-2554.

Schafer, T., Geckeis, H., Bouby, M., Fanghanel, T., 2004. U, Th, Eu and colloid mobility in a granite fracture under near-natural flow conditions. Radiochimica Acta 92, 731-737.

Schokker, J., Cleveringa, P., Murray, A.S., Wallinga, J., Westerhoff, W.E. 2005. An OSL dated Middle and Late Quaternary sedimentary record in the Roer Valley Graben (southeastern Netherlands). Quaternary Science Reviews 24, 2243-2264.

Scholz, D., Hoffmann, D., 2008. ^{230}Th/U dating of secondary carbonates. Quaternary Science Journal (Eiszeitalter & Gegenwart). (in press)

Sharp, W.D., Ludwig, K.R., Chadwick, O.A., Amundson, R., Glaser, L.L. 2003. Dating fluvial terraces by 230Th/U on pedogenic carbonate, Wind River Basin, Wyoming. Quaternary Research 59, 139-150.

Siegenthaler, C., Huggenberger, P., 1993. Pleistocene Rhine gravel: deposits of a braided river system with dominant pool preservation. In: Braided Rivers, Best, J. L.,Bristow, C. S. (Eds.) Geological Society. 147-162.

Spötl, C., Mangini, A., 2006. U/Th age constraints on the absence of ice in the central Inn Valley (eastern Alps, Austria) during Marine Isotope Stages 5c to 5a. Quaternary Research 66, 167-175.

Spötl, C., Mangini, A., Frank, N., Eichstädter, R., Burns, S.J., 2002. Start of the last interglacial period at 135 ka: Evidence from a high Alpine speleothem. Geology 30, 815-818.

Törnqvist, T.E., 1998. Longitudinal profile evolution of the Rhine-Meuse system during the last deglaciation: interplay of climate change and glacio-eustasy? Terra Nova 10, 11-15.

van Lith, Y., Warthmann, R., Vasconcelos, C., McKenzie, J.A., 2003. Microbial fossilization in carbonate in carbonate sediments: A result of the bacterial surface involvment in carbonate precipitation. Sedimentology 50, 237-245.

Wallinga, J., 2002. Optically stimulated luminescence dating of fluvial deposits: a review. Boreas 31, 303-322.

Wallinga, J., Bos, A.J.J., Dorenbos, P., Murray, A.S.,Schokker, J. 2007. A test case for anomalous fading correction in IRSL dating. Quaternary Geochronology 2, 216-221.

Wallinga, J., Murray, A., Wintle, A., 2000. The single-aliquot regenerative-dose (SAR) protocol applied to coarse-grain feldspar. Radiation Measurements, 32: 529-533.

Wallinga, J., Törnqvist, T.E., Busschers, F.S., Weerts, H.J.T., 2004. Allogenic forcing of the late quaternary Rhine-Meuse fluvial record: the interplay of sea-level change, climate change and crustal movements. Basin Research 16, 535-547.

Wittmann, O., 1961. Die Niederterrassenfelder im Umkreis von Basel und ihre kartographische Darstellung. Basler Beiträge zur Geographie und Ethnologie 3, 46.

Chapter 2

Chapter 2

Formation and evolution of the Lower Terrace of the Rhine River in the area of Basel

Stéphane Kock, Peter Huggenberger, Frank Preusser & Andreas Wetzel

To be submitted to *Swiss Journal of Geoscience*

Abstract: The response of fluvial systems to tectonic activity and climate change during the Late Pleistocene influenced sedimentary processes and hence the conditions of river terraces formation. The Lower Terrace system of Rhine River consists of braided river sediments that have been deposited in a periglacial environment during and after the last glaciation. Sediment accumulated during normal flow conditions, as documented by the combination of scour fills and thin gravel sheets, as well as exceptional events, as documented by massive gravel sheets. Luminescence ages indicate that the sediments of the Lower Terrace were deposited during two periods (30-15 ka and 13-11 ka), which correlate with two cold climatic phases, the Last Glacial Maximum and the Younger Dryas. These ages underline that main incision of the Lower Terrace braidplain in the area of Basel is restricted to post Younger Dryas times, as sediments of that age (13-11 ka) are found atop the highest levels. From then on, a flight of cut-terraces were formed with minor re-accumulation due to flood events. U/Th ages of speleothems from a cave, seen as proxy for water table position and directly related to the formation of the Lower Terrace, support this interpretation.

1. Introduction

The River Rhine is a major element of the central European drainage system and originates in one of the highest area of Europe, the central and eastern Swiss Alps (cf. Preusser, 2008). This area, together with large parts of the adjacent Swiss Midlands, was repeatedly glaciated during the Pleistocene. The glaciations generated manifold sediments, including glacifluvial gravels that were deposited in the Hochrhein area. Many aspects of those deposits have been studied in the past and provide substantial data about the environmental evolution of this period. However, despite the use of radiocarbon dating, constrains on the absolute ages of the deposits is rather limited, preventing most quantitative approaches. The recent evolution and progresses in luminescence dating (Wallinga et al., 2001; Wallinga, 2002; Preusser et al., 2007) provides a new tool to control the timing of accumulation and erosion processes of fluvial deposits.

The study area is located in the Rhine valley between the Aare River to the East and the city of Mulhouse to the West, and is located on the territories of Switzerland, Germany and France (Fig.1). It is characterised by several major morphological terrace levels attributed to the Upper Deckenschotter, the Lower Deckenschotter, the Upper Terrace and the Lower Terrace (Fig. 2). Each of these units shows different sublevels that may either reflect accumulation or cut terraces.

The main geological features of the area are the Jura Mountains (mainly limestones and marls) to the South, the Black Forest (mainly crystalline and detritals) to the North and the southern Upper Rhine Graben (URG) to the West (detritals and limestones). These structures lay on an ENE-WSW trending Permo-Carboniferous trough system that has been proven to be tectonically active (Schumacher, 2002; Giamboni et al., 2004a,b; Ustaszewski and Schmid, 2007). In this context, the Lower Terrace has been interpreted as a potential indicator of recent tectonic movement (e.g., Haldimann et al., 1984).

The Lower Terrace, which is the focus of this study, is commonly accepted to have been formed during the last glaciation as a periglacial braidplain. It lies partly on an older and deeper Pleistocene channel, partly on bedrock. The sediments originate from the modern drainage area of the Rhine, i.e. the northern Swiss Alps, the Swiss Molasse Basin, the Jura Mountains and the Black Forest. The closest terminal moraine ridge of the Last Glaciation is located about 25 km upstream from the eastern boundary of the study area (Fig. 1).

The Lower Terrace is a geomorphologic feature that is known from many rivers in central Europe. It was first attributed to the "Würm" ice-age by Penck and Brückner (1909) in the Danube catchment and this correlation has been later confirmed by dating for the Rhine and other rivers in Germany (Houben, 2003; Choi et al., 2007) as well as in Switzerland (Bitterli et al., 2000; Preusser et al., 2007). The main sedimentological processes responsible for the build up of the Lower Terrace gravels have been described in Siegenthaler and Huggenberger (1993) and Huggenberger and Regli (2006). Major flood events in historical times have been reported or documented from Alsace (Criqui, 1981; Ollive et al., 2006) and the Schaffhausen area (Huggenberger et al., 1997). In parts of the study area, the Lower Terrace was mapped in detail by Wittmann (1961), who also proposed a classification of seven sublevels: A1, A2, A3, B1, B2, B3 and C, where A1 is the highest and oldest terrace, recognised as an accumulation level, and C is the lowest and youngest level (Fig. 2). Wittmann (1961) tentatively attributed ages to those levels based on early radiocarbon datings (Gross, 1958): 50-40 ka for the A group, 30-26 ka for the B group and about 3 ka for the C level.

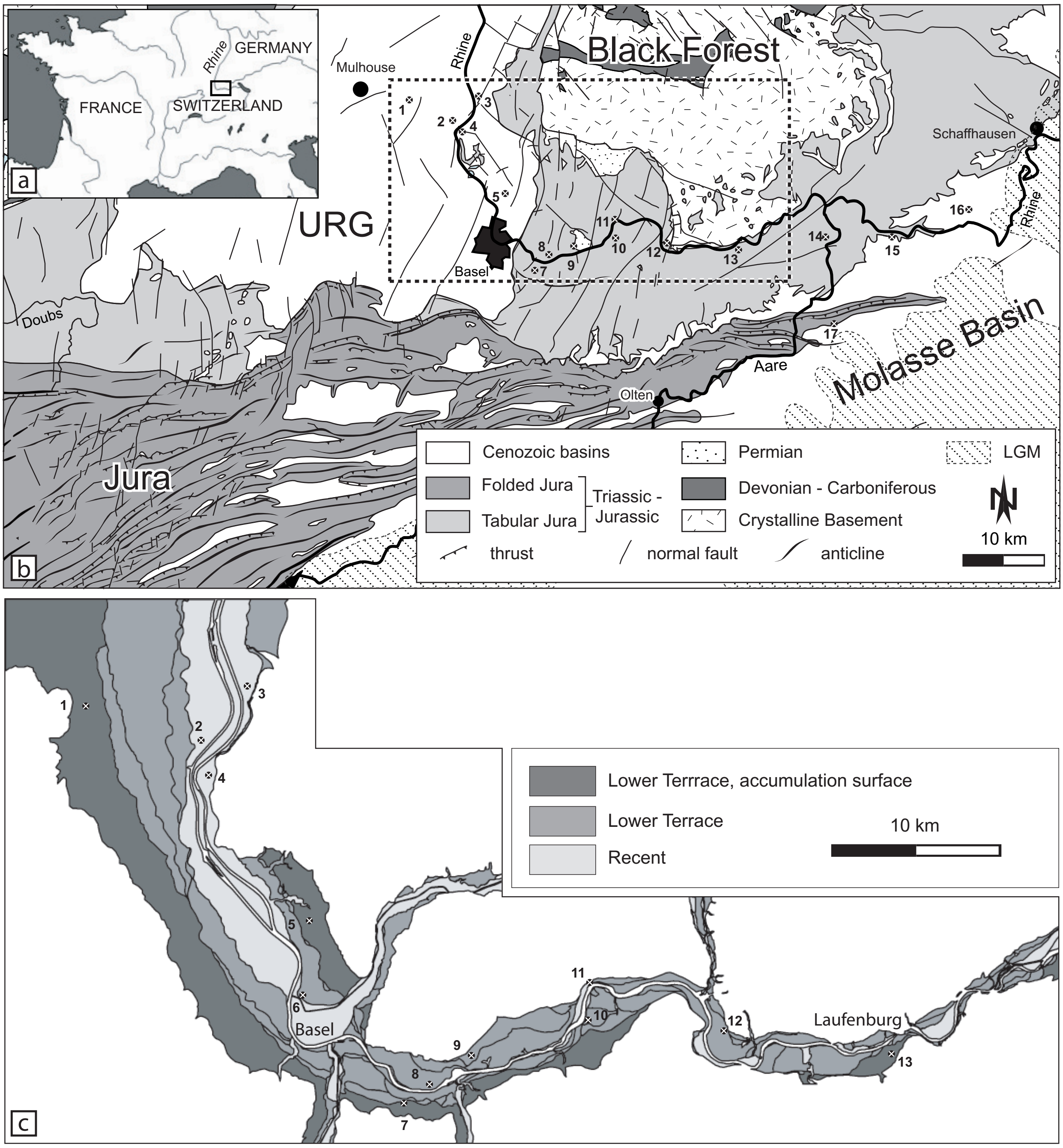

Fig. 1: Geographic and geologic situation. (a) Position of the study area in Western Europe. (b) Tectonic map of the study area. URG: Upper Rhine Graben; LGM: extent of ice-covered area during the Last Glacial Maximum. Locations cited in the text: (1) Habsheim; (2) Petit-Landau; (3) Bellingen; (4) Rheinweiler; (5) Haltingen; (6) Basel; (7) Muttenz; (8) Wyhlen; (9) Markhof; (10) Chleigrüt; (11) Tschamberhöhle; (12) Wallbach; (13) Chaisterfeld; (14) Böttstein; (15) Mellikon; (16) Hüntwangen; (17) Birmenstorf. (c) Map of the Lower and recent terrace of the river Rhine, same location code.

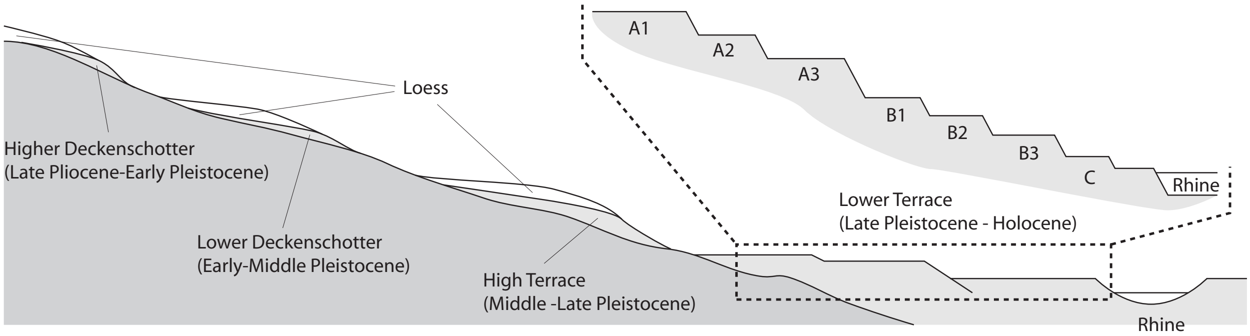

Fig. 2: Schematic situation without scale of Pleistocene fluvial deposits between the Aare inlet and Mulhouse. The original terrace surfaces of the Lower Terrace are generally conserved, being only covered by soil, contrary to the older terraces, which are covered by a thick loess layer. The enlargement shows the sub-levels classification of Wittmann (1961).

In the Hochrhein area, the age of formation of the Lower Terrace has been dated by mammoth tusks and bones, found in gravel at the locations of Böttstein and Mellikon, to 19,850 ± 150 ^{14}C yr BP (23840 ± 470 cal. yr BP) and 20,550 ± 250 ^{14}C yr BP (MBN AG 1998; Bitterli et al., 2000). Further upstream from the study area, at Hüntwangen (Fig. 1), optically stimulated luminescence (OSL) dating yielded ages between ca. 30 and 25 ka, in a location very close to Last Glacial Maximum (LGM) glacier position (Preusser et al., 2007). These OSL ages are confirmed by radiocarbon ages from the same site. Downstream, in the Middle Rhine Area within the up-lifting Rhenish Massif, the Lower Terrace is divided into two sublevels called older and younger Lower Terrace. The age of the two sublevels is well constrained by the presence of Laacher See Tephra on top of the older sublevel, while it is found reworked in the younger sublevel. Choi et al. (2007) reported OSL ages of about 20 ka for the older Lower Terrace and could confirm that the younger Lower Terrace formed during the Younger Dryas.

Some deposits pre- and postdating the deposition of the gravel have also been dated: a mammoth tooth dated 32,350 ± 280 ^{14}C yr BP (age beyond recent calibration) was found in a palaeosol underlying the Lower Terrace at Birmestorf, in the Aare catchment area (MBN AG, 1998). Overbank deposits and soils deposited on the terraces were dated at some locations by radiocarbon and palynology: different wood and organic fragments yielded ages between 2470 ± 100 ^{14}C yr BP (2600 ± 200 cal. Yr BP, Hauber, 1971) and 6160 ± 50 ^{14}C yr BP (7120 ± 160 cal. Yr BP, Rentzel, unpubl.) for some B or C levels of the Lower Terrace, and a Dryas III pollen spectrum on top of a A3 level (Rentzel, 1994).

In this study, we present remote sensing and sedimentological data as well as some new OSL and radiocarbon ages. Based on this data, we constrain the processes and timing that led to the formation of the different levels of the Lower Terrace, and make some general observations about the age of terrace surfaces.

2. Materials and Methods

2.1 DEM and picture analysis

In addition to field observations, high resolution Digital Elevation Model (DEM) images, aerial and satellite photographs, historic pictures, maps and paintings have been used, to better constrain the evolution of the river regime. The DEM used here is the DTM-AV of Swisstopo (Swiss Federal Office of Topography), with a resolution of 2 m, and it covers the Swiss and parts of the German but not the French riverside. Different aerial and satellite photographs have been collected from open internet sources. Two historic maps, the German "Rheingränz-Carte" of 1828 and the Swiss "Dufour" map of 1860, and a painting of Peter Birmann ("Blick vom Isteiner Klotz, rheinaufwärts gegen Basel", about 1820) have also been taken into account.

2.2 Geochronology

For part of the data set presented here, a detailed description of the applied methodology and experimental backup has been presented in a previous publication in the context of assessing the applicability of Uranium series methodology to date carbonate crusts with gravel (Kock et al., in review). The relevant data is included for completeness but we only briefly summarise methodology here.

2.2.1 Optically Stimulated Luminescence (OSL)

Suitable sand layers are rare in the mainly coarse Lower Terrace deposits but were found in nine active gravel pits, up to 25 m deep, distributed along the Hochrhein (see Fig. 1 for sites names and location).

Determination of the Equivalent Dose (ED) was performed on quartz separates (100-150 µm) using the SAR protocol of Murray and Wintle (2000, 2003). We used small (2 mm) aliquots to detect differential bleaching of the OSL signal. A preheat of 230°C for 10 s was used prior to all OSL measurements and the suitability of this procedure was confirmed by dose recovery and thermal transfer tests (cf., Kock et al., in review). For dating, 48 aliquots were measured for each sample and the majority of those passed through the rejection criteria of the SAR protocol (Murray and Wintle, 2000). The positively skewed dose distributions imply differential bleaching of the OSL signal prior to deposition and the method of Preusser et al. (2007) was used to extract mean dose accumulated during burial using.

Determination of dose rate relevant elements (K, Th, U) was carried out by high-resolution gamma spectrometry (Preusser and Kasper, 2001) and no evidence for radioactive disequilibrium in the Uranium decay chain has been found. For all samples, mean moisture content during burial of 5-15 % was assumed and cosmic dose rate was calculated using present day depth following Prescott and Hutton (1994).

2.2.2 Radiocarbon and U/Th dating

Several wood pieces or whole trunks or stems were found in Holocene sediments from the gravel pit at Rheinweiler, featuring gravel beds covered by overbank fine sand layer containing wood debris. Preparation and measurements for radiocarbon followed the procedure described by Hajdas et al. (2004).

A sample of stalactite and of stalagmitic floor were taken, and material for U/Th measurements was collected from the assumed oldest layers, i.e. the centre, respectively the bottom of the samples. The analytical process for U/Th is described in Kock et al. (in review).

3. Results

3.1 Morphological analysis

The shaded display of the DEM turned out to be of high interest, since braided river bed topography is often well preserved on forested land, where human influence (ploughing) was negligible. Braided patterns with drainage gullies and spring brooks could be recognised in Muttenz, Möhlin and Sisseln (Fig. 3).

Of all the aerial photographs that were inspected, only the French IGN set proved useful. On this set, a network of channels was identified along the Rhine, north of the village of Petit-Landau (location 2 on Fig. 1). Interestingly, both meandering and braided pattern are visible on those pictures (Fig. 4), the meandering pattern being on the lowest (recent) level, and the braided pattern being on a higher (older) level.

Historic maps (Fig. 5) and the painting from Birmann show that most of the Rhine in the Rhine Graben (downstream from Basel) was braided until the end of the XIXth Century, when the river started to be corrected by man.

3.2 Sedimentological analysis

The visited outcrops are described from West to East, and their relative position in the classification of Wittmann (1961) is indicated. In the several gravel pits that were visited, three different lithofacies were identified: normal braided river deposits, flood deposits and overbank deposits. The OSL ages are given for each outcrop, and are listed in Tab. 1 and displayed on Fig. 6. Radiocarbon ages are listed in Tab. 2.

The Habsheim outcrop (location 1 on Fig.1) is correlated with the A1 level (accumulation level) of the Lower Terrace. The gravel pit is under water extraction, which results in limited access to outcrops. The gravel features low density bedload sheet and pool structures. A sand lens is located less than a metre below the surface of the terrace (with soil cover removed). A sample from this sand lens (HRT 17) yielded an age of 13.2 ± 1.0 ka.

The Bellingen outcrop (Fig. 7, location 3 on Fig.1) is correlated with the C level of the Lower

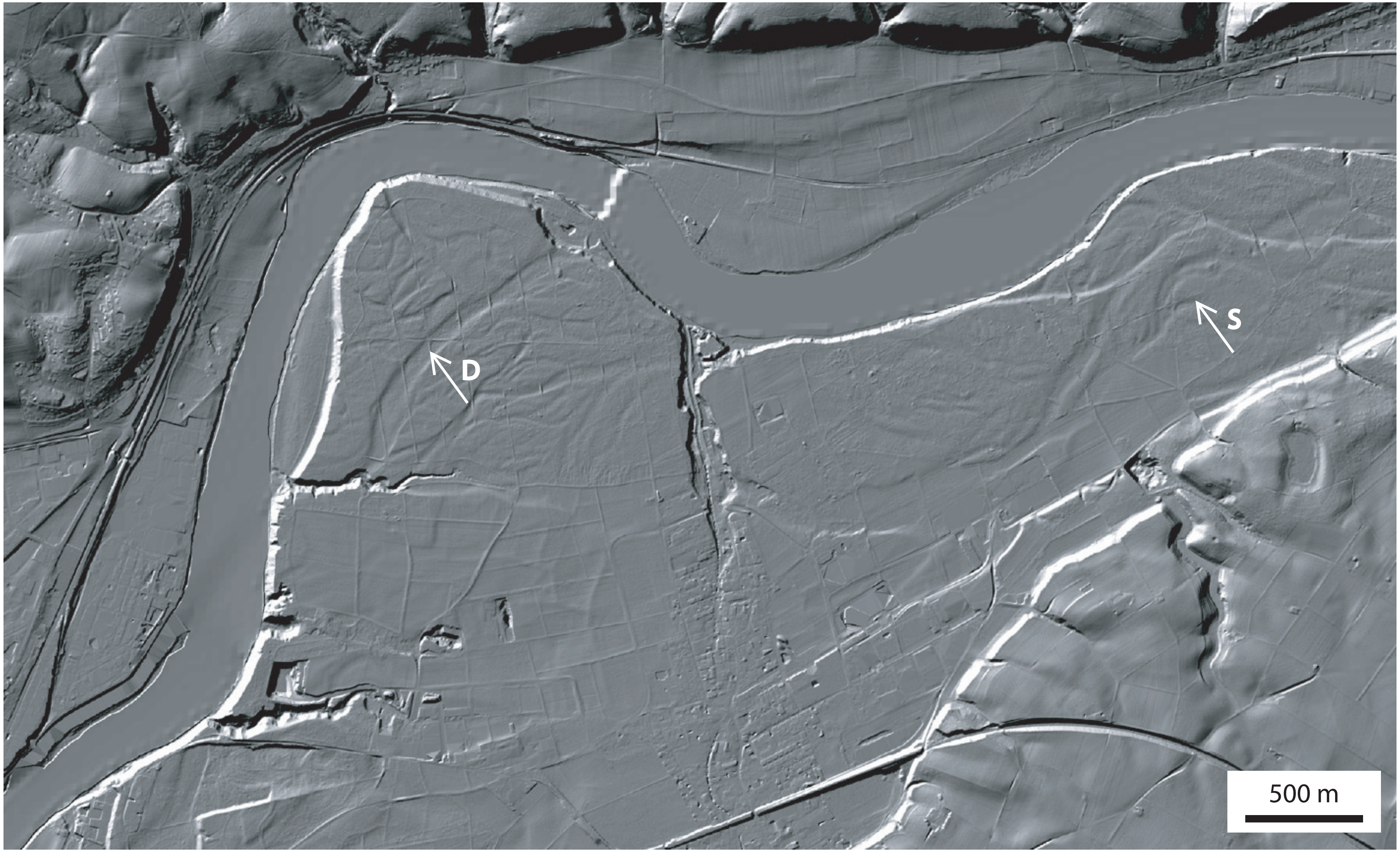

Fig. 3: shaded display of the DTM-AV in the area of Rheinfelden (between locations 10 and 11). The braided river topography is well conserved in the forested area. (D) drainage gully; (S) spring brook, formed by backwards erosion due to exfiltering of groundwater. North is to the top. Reproduced by permission of Swisstopo (BA081589).

Fig. 4: Aerial picture of the area between the villages of Petit Landau (to the South) and Hombourg (to the North). On the first third from the left, braided pattern (B) is visible, whereas further to the right, meanders (M) are visible. The arrow and the dashed line show the terrace scarp that separates the two features. North is to the top, the Grand Canal d'Alsace (C) and the Rhine river (R) are visible in the top right-hand corner. Location is shown on Fig.1. Source: IGN.

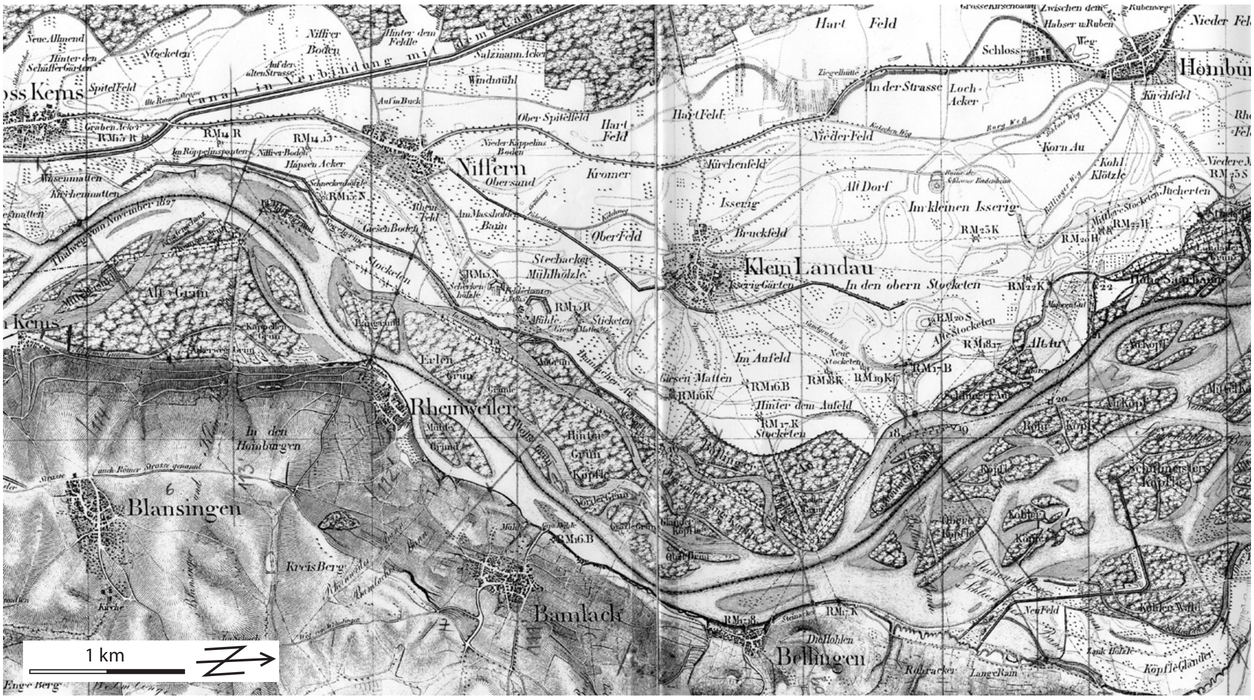

Fig. 5: Part of the historic German "Rheingränz-Carte" of 1828, showing the area of Petit-Landau (named Klein Landau on the map). Braided river morphology can be clearly seen. The terrace scarp and the abandoned meanders shown on Fig. 4 Petit Landau are also mapped here.

Terrace, located just a few metres above modern Rhine level. The bottom part of the 6 m high outcrop shows sand lenses and oblique stratifications. One of the sand lenses has an age of 27.8 ± 2.2 ka (HRT 13). Above the erosional surface is a 2 m thick massive gravel sheet (or high density bedload sheet; Todd, 1989) featuring normal grain sorting. The top of the outcrop has been removed. (Fig. 7).

The Rheinweiler outcrop (Fig. 8, location 4 on Fig.1) was a provisory outcrop in spring 2007, and is correlated with the C level of the Lower Terrace. Here, the gravel yielded a tree trunk of good size and features cross stratifications and sand lenses. It is covered by overbank deposits. OSL and radiocarbon dating gaves historical ages: a sand lens within the gravel yielded an age of 0.43 ± 0.04 ka (HRT 16), and the overbank layer gave an age of 0.26 ± 0.02 ka (HRT 15). Radiocarbon dating of the trunk gave an age of 255 ± 40 ^{14}C yr (410 ± 100 cal. Yr BP, ETH-34581), while an age of 260 ± 50 ^{14}C yr (420 ± 100 cal. yr BP, ETH-34366) was obtained from organic matter within the same sand lens where OSL sample HRT 16 comes from. Organic matter from the over bank deposit has been dated to 870 ± 60 ^{14}C yr (850 ± 110 cal. yr BP, ETH-34367).

Furthermore, a tree stem found in an adjacent gravel pit was dated to 310 ± 40 ^{14}C yr (440 ± 100 cal. yr BP, ETH-34582). In another adjacent, abandoned gravel pit, the overbank layer gave an age of 0.23 ± 0.02 ka (HRT 14).

The Haltingen outcrop (Fig. 9, location 5 on Fig.1) is located on the A1 level (accumulation level)

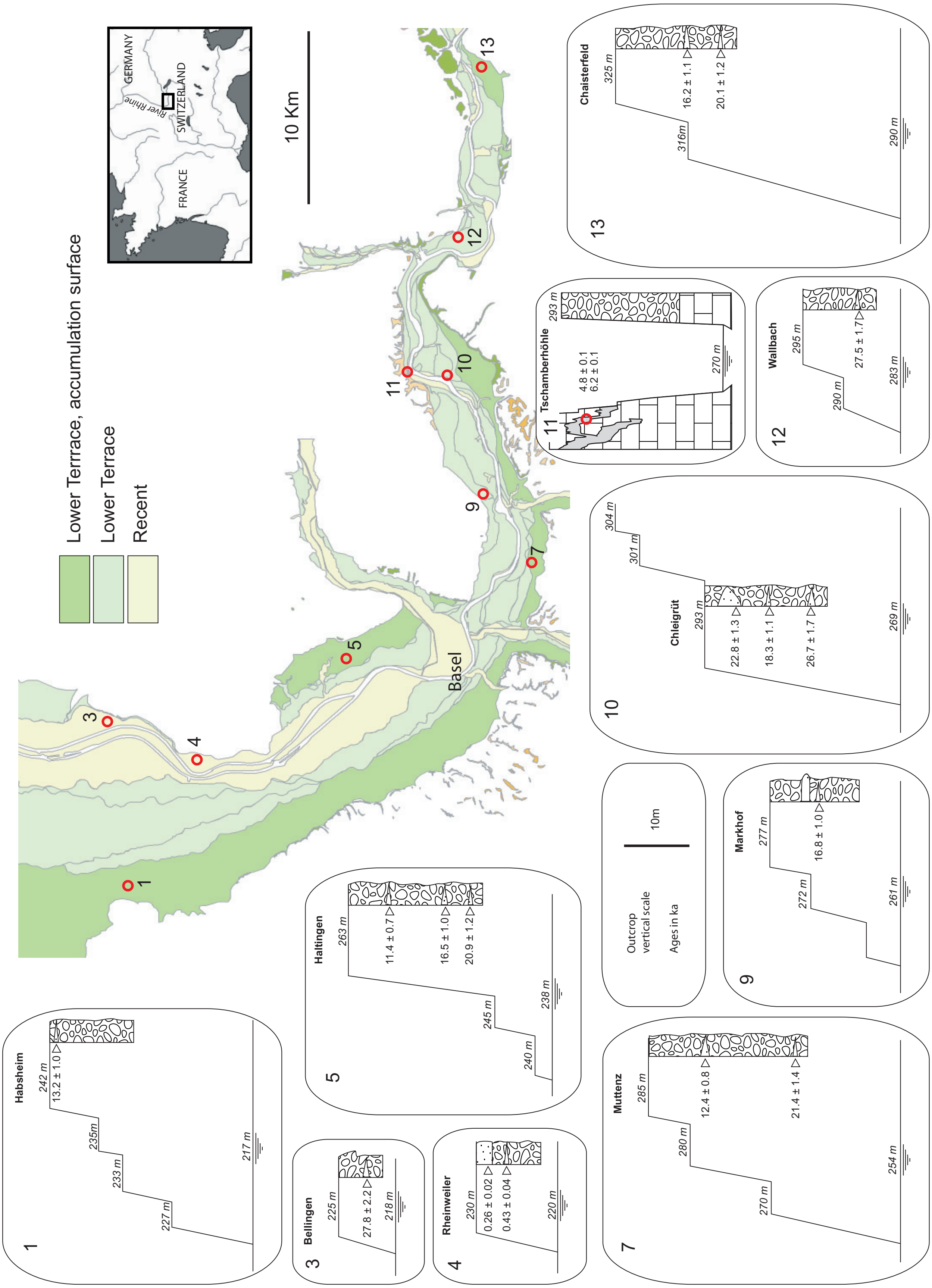
Lower Terrace, accumulation surface
Lower Terrace
Recent
10 Km
GERMANY
FRANCE
SWITZERLAND
River Rhine
Basel
1 Habsheim
242 m
235m
233 m
227 m
217 m
13.2 ± 1.0
3 Bellingen
225 m
218 m
27.8 ± 2.2
4 Rheinweiler
230 m
220 m
0.26 ± 0.02
0.43 ± 0.04
5 Haltingen
263 m
245 m
240 m
238 m
11.4 ± 0.7
16.5 ± 1.0
20.9 ± 1.2
7 Muttenz
285 m
280 m
270 m
254 m
12.4 ± 0.8
21.4 ± 1.4
Outcrop
vertical scale
Ages in ka
10m
9 Markhof
277 m
272 m
261 m
16.8 ± 1.0
10 Chleigrüt
304 m
301 m
293 m
269 m
22.8 ± 1.3
18.3 ± 1.1
26.7 ± 1.7
11 Tschamberhöhle
293 m
270 m
4.8 ± 0.1
6.2 ± 0.1
12 Wallbach
295 m
290 m
283 m
27.5 ± 1.7
13 Chaisterfeld
325 m
316m
290 m
16.2 ± 1.1
20.1 ± 1.2

Fig. 6 (*opposite*): Synthetic map showing the distribution of outcrops, and the vertical distribution within each outcrop of samples with their age. Locations 1-7, 9 and 10 show OSL ages from sand lenses or layer, and their height above modern Rhine level. The stratigraphic log represents the available outcrop (depth of the gravel pit), and the stepped plain line represents the different terrace levels in the area of the outcrop. Location 11 is a cave. U/Th ages of speleothems are shown on a cross-section across the Rhine, as well as the position of the samples with respect to the closest Terrace (Lower Terrace) and the modern Rhine level (more details in Fig. 16 Tschamberhöhle). Altitudes are given in metre a.m.s.l.

Fig. 7: Bellingen outcrop showing normal braided river deposits covered by a high density bedload sheet with normal grain sorting. The hole in the sand lens is the sampling site of HRT 13 (scale bar is 2 m).

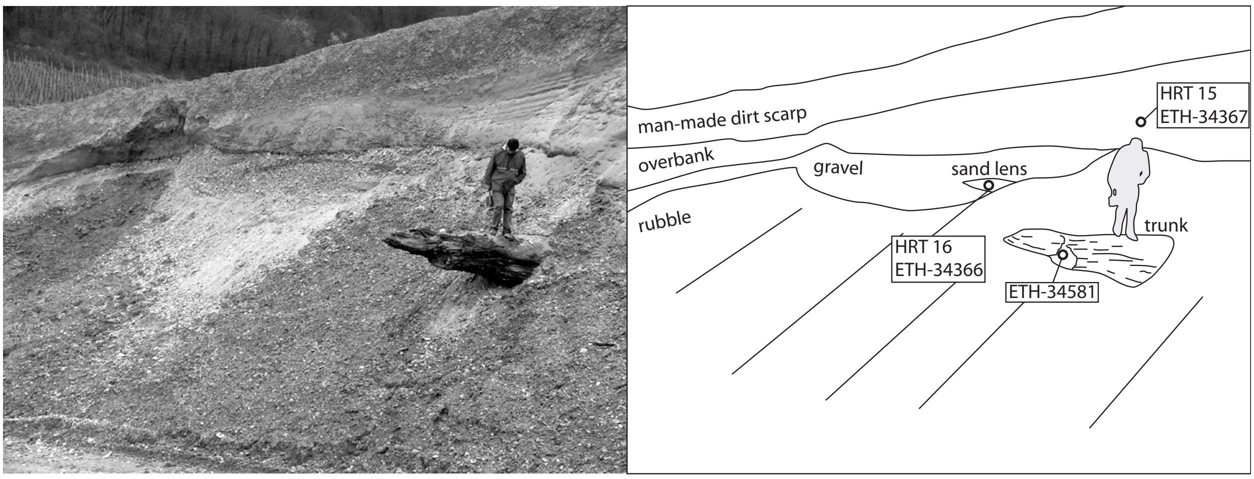

Fig. 8: Rheinweiler outcrop: the normal braided river deposits contain a tree trunk, and are capped by overbank deposits. Sampling locations for OSL and ^{14}C are shown.

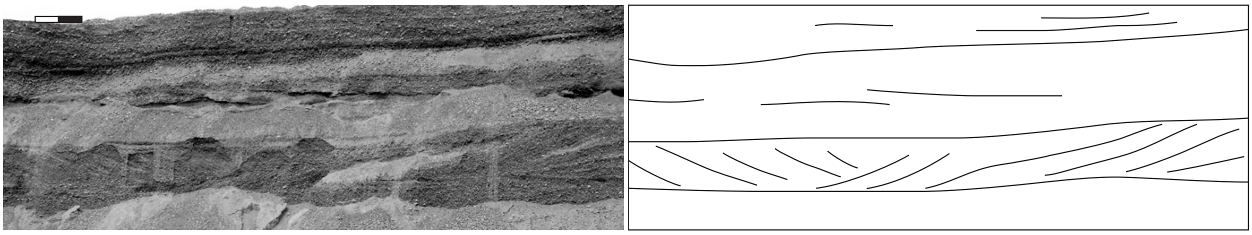

Fig. 9: Haltingen outcrop showing cross-stratifications and low density bedload sheets (scale bar is 2 m).

of the Lower Terrace. The 17 m deep gravel pit mostly features cross-stratifications and pool structures in the lower 12 metres, and gravel sheets are dominant in the upper 5 metres. Several sand lenses are present at different levels, three of which were dated to 20.9 ± 1.2 ka (HRT 7, 15 m below terrace surface), 16.5 ± 1.0 ka (HRT 8, 12 m below terrace surface) and 11.4 ± 0.7 ka (HRT 9, 5 m below terrace surface).

The almost 6 m high Basel outcrop (Fig. 10, location 6 on Fig.1) is a low level of the Lower Terrace (B3 or C). It features a 1.5 to 2 m thick Rhine gravel layer containing several oaks trunks of good size, which is covered by a 2.5 m gravel layer belonging to the Wiese river sediments, a tributary of the Rhine that originates in the Black Forest. These are topped by overbank deposits. Ground Penetrating Radar (GPR) sections clearly show pool structures below the outcrop level. The tree accumulation may have been caused by lateral erosion of long established islands.

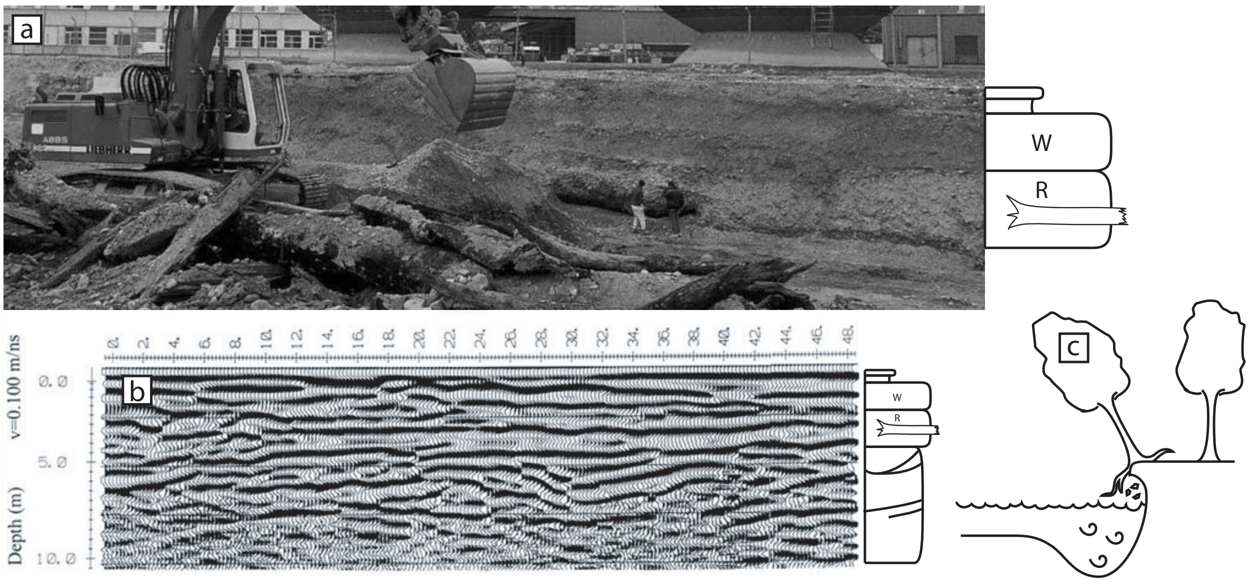

Fig. 10: (a) The Basel outcrop features a Rhine gravel layer (R) containing an accumulation of tree stems. They are covered by deposits from the Wiese river, a local tributary of the Rhine (W), and then by overbank deposits. (b) normal braided river deposits can be recognised below the outcrop level on a GPR profile. (c) An accumulation of trees of such importance can be formed when an forested island is laterally eroded. (georadar data: PulseEkko 100, 100 MHz antennae, 0,25m steps)

The Muttenz outcrop (location 7 on Fig.1) is a 20 m deep gravel pit in the A1 terrace. It mostly features pool structures in the lower 16 m, and gravel sheets are dominant in the upper 4 m. Several sand lenses are present at different levels, two of which were dated to 21.4 ± 1.4 ka (HRT 10, 18 m below terrace surface) and 12.4 ± 0.8 ka (HRT 11, 7 m below terrace surface).

The Wyhlen outcrop (Fig. 11, location 8 on Fig.1) is a C level of the Lower Terrace. The 4 m high outcrop features, as in Bellingen, different layers of normal braided river sediments with foresets and sand lenses at the bottom, covered by a 2 m thick high density bedload sheet containing cobbles up to 50 cm long. However, the texture of the high density bedload sheet contrasts with that of Bellingen as it has no grain sorting but imbricated pebbles. The top of the outcrop has been removed.

The Markhof outcrop (Fig. 12, location 9 on Fig.1) is an 11 m deep gravel pit in the B1 level. The lower 8 m show pool structures with extensive, sometimes well cemented sand lenses, and the upper 3 m is constituted of a massive gravel sheet. A clear erosive surface separates the two parts. An OSL sample (HRT 6) taken 6 m below terrace surface yielded an age of 16.8 ± 1.0 ka.

The Chleigrüt outcrop (Fig. 13, location 10 on Fig.1) is a 14 m deep gravel pit in the A3 terrace. It mostly features pool structures in the lower 11 m, and gravel sheets are dominant in the upper 3 m. Several sand lenses are present at different levels, three of which were dated to 26.7 ± 1.7 ka (HRT 3, 13 m below terrace surface), 18.3 ± 1.1 ka (HRT 4, 8 m below terrace surface) and 22.8 ± 1.3 ka (HRT 5, 4 m below terrace surface).

The Wallbach outcrop (Fig. 14, location 12 on Fig.1) is an 8 m deep gravel pit correlated with the B3 level. It features poll structures in the lower 7 m, with sand lenses. Above an erosion surface, the upper metre is a massive gravel sheet with normal grain sorting and with coarse pebbles at the base (up to 40 cm). A sand lens gave an age of 27.5 ± 1.7 ka (HRT 12, 7 m below terrace surface).

The 15 m high Chaisterfeld outcrop (Fig. 15, location 13 on Fig.1) is correlated with the A1 level of the Lower Terrace. It features mostly normal braided river sediments, with pools structures and sand lenses, but some thin layers of coarser pebbles are relicts of High density bedload sheets that have been subsequently reworked. Two OSL samples were taken here and yielded ages of 20.1 ± 1.2 ka (HRT 1, 13 m below terrace surface) and 16.2 ± 1.1 ka (HRT 2, 9 m below terrace surface).

To better constrain the incision phase, two samples of speleothems were taken for U/Th dating from a cave (the Tschamberhöhle, location 11 on Fig.1) that is located at a similar altitude as the Lower Terrace and clearly connected to the Rhine river (Fig. 16). The cave develops in the Middle Triassic "Muschelkalk" limestone and consists of a single tube branching downstream into a higher tube and a siphon. It follows a low gradient, and the section of the tube indicates formation during a phreatic phase (elliptic section) and a subsequent vadose phase ("canyon" at the base of the elliptic section). The main tube is still occupied by a stream that prevents speleothem growth.

Fig. 11: Picture of the Wyhlen outcrop. Normal braided river deposits are visible at the base, with sand lenses and cross-stratifications. These are covered by a high density bedload sheet with imbricated pebbles and occurrence of boulders. The top of the outcrop has been removed (scale bar is 2 m).

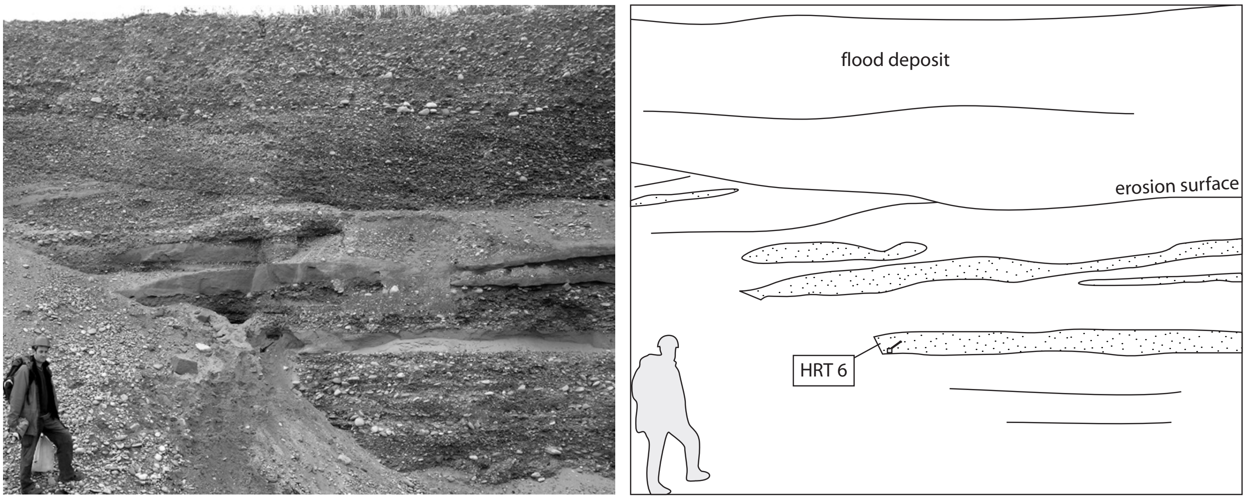

Fig. 12: Markhof outcrop. Normal braided river sediments (below) are eroded by a complex flood deposit (above). OSL sampling site is indicated.

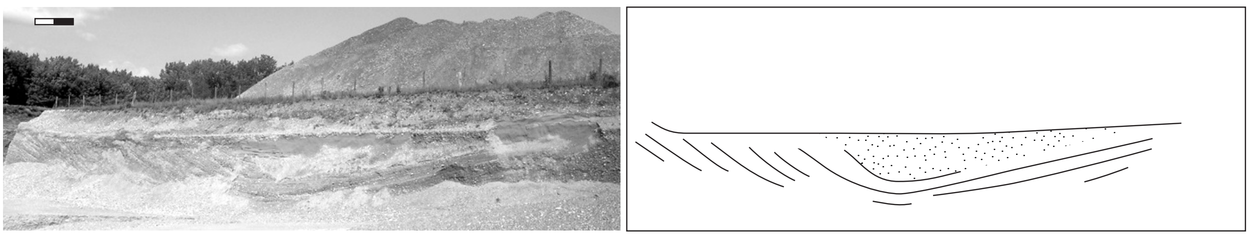

Fig. 13: Part of the Chleigrüt outcrop showing a pool structure filled with sand (scale bar is 2 m).

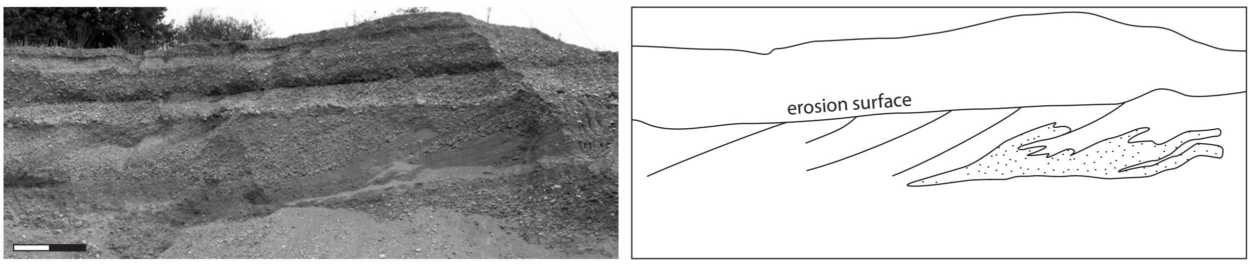

Fig. 14: Wallbach outcrop showing pool structure (below) and flood deposit above. The dark horizon in the flood deposit is manganese precipitation (scale bar is 2 m).

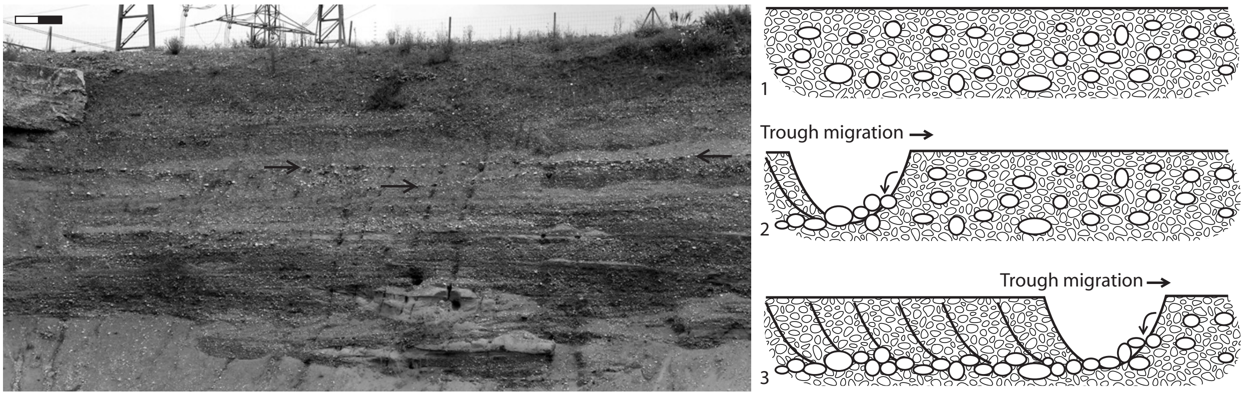

Fig. 15: Chaisterfeld outcrop showing low density gravel sheets, pool structures and relicts of flood deposits (indicated by arrows, scale bar is 2 m). The scheme shows how the relicts are interpreted.

However, the higher tube, from which the stream was shortcut by the siphon, has become dry and several kinds of speleothem are present. The U/Th ages obtained are 4.8 ± 0.1 ka and 6.2 ± 0.1 ka.

4. Discussion

4.1 Formation of terraces

Field data and morphological observations give a good impression of the terrace forming processes in the areas. Different sedimentary structures, such as pools (Fig 13) and low density bedload sheets were formed during periods of normal water discharge, and high density bedload sheets (massive gravel sheets) formed during flood events. However, the low and high density bedload sheets tend to be reworked during later pool formation and are thus much less frequently preserved than pool structures (Huggenberger and Regli, 2006). The occurrence of an eroded high density bedload sheets can nevertheless be indicated by a concentration of coarse pebbles (Fig. 15).

A morphological terrace is formed when a part of a flood plain is abandoned by active channels in an erosional context (base level fall). The base level, which controls erosion, is controlled for each river portion by the altitude of the downstream bedrock threshold, and therefore each portion can have a different erosional history, some even accommodating sediment while other become eroded.

Due to base level fall, the higher surfaces become inactive, except during extreme flood events, when the water level rises high enough to cover it again, and possibly bring more sediment (flood deposits) on top of it. Towards the end of a flood event, hydraulic conditions become progressively normal as water discharges and water level decreases, and the top of the flood deposit is reworked into normal braided river deposits. However, this reworking is short lived, because the normal level of the river is then lower than these deposits, and they are quickly abandoned. During this

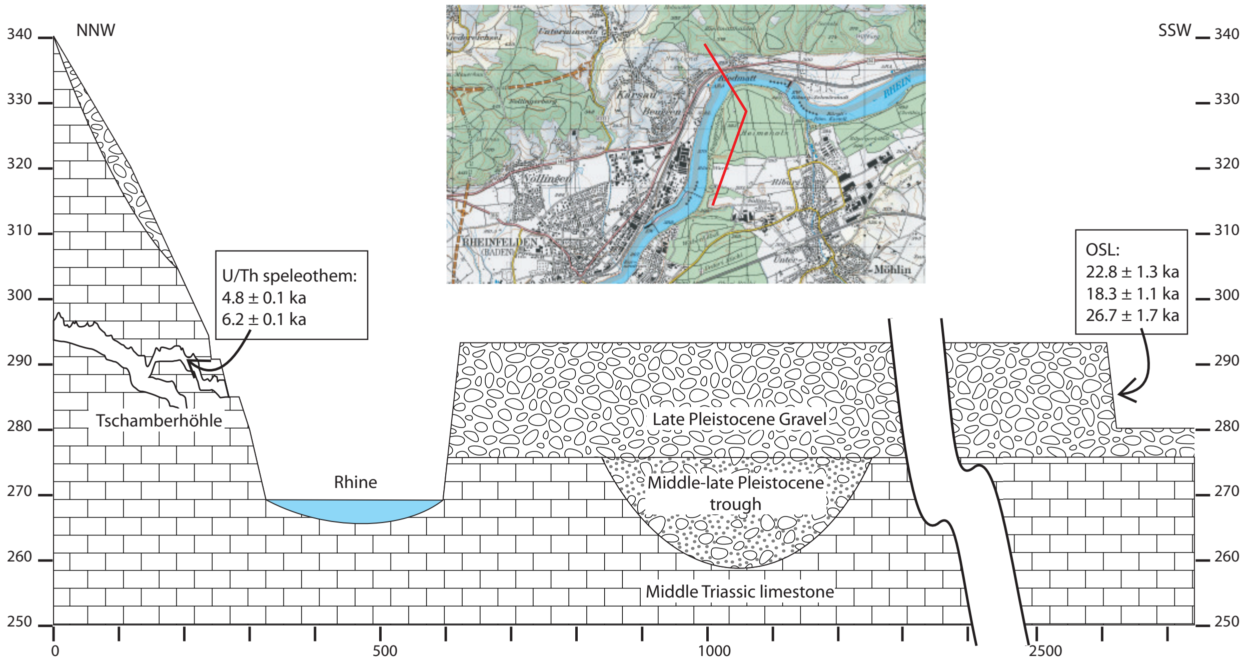

Fig. 16: Cross-section showing the position of the Tschamberhöhle (cave) relative to the Lower Terrace. Location is shown on Fig.1. The OSL ages indicated are those of Chleigrüt (location 10).

phase, drainage gullies and spring brooks are formed by the evacuation of groundwater (Fig. 3). These are the shapes that are most likely to be conserved on the surface of the terrace. An annual or seasonal flood event is then able to shape the riser of the terrace by lateral erosion. Lateral erosion can be enhanced by high groundwater discharge or by the presence of a tributary.

4.2 Geochronology

A summary of the results of OSL dating are listed in Table 1 and displayed on the map (Fig. 6). Ages decrease upward within particular outcrops, as to be expected from a typical aggradation setting, but there is no correlation between the OSL age of the sediment body and the assumed age of the terrace surfaces, which decrease downward with elevation. An overview of the calculated ages (Fig. 17) shows that eleven ages (HRT 1-8, 10, 12 and 13) fall within the period 30-15 ka, thus in the time considered to represent full glacial conditions in the Swiss lowlands (Preusser, 2004). The lower limit of this period is given by the end of the last Middle Würmian Interstadial that ended at about 30 ka ago and was followed soon after by the advance of Alpine glaciers into the lowlands (e.g. Preusser et al., 2003, 2007). The upper limit is the beginning of the Late Glacial Interstadial (Bølling-Allerød), which according to Litt et al. (2003) started at about 14.5 ka ago. Three other samples (HRT 9, 11 and17) fall in the Younger Dryas chronozone, the last cold period prior to the Holocene warming, and finally, three OSL samples (HRT 14-16) fall into historical times. The radiocarbon ages from Rheinweiler all gave historic ages, which are consistent with OSL ages from the same locality, and with the fact that this area was still an active river bed in the

Sample	Site	Grain size (µm)	n	K (%)	Th (ppm)	U (ppm)	W_{eff} (%)	Depth (m)	D (Gy ka^{-1})	ED_{Median} (Gy)	Age_{Median} (ka)	ED_{Modell} (Gy)	Age_{Modell} (ka)
HRT1	Chaisterfeld	149-202	41	0.97 ± 0.02	2.45 ± 0.24	0.91 ± 0.07	10 ± 5	13	1.25 ± 0.07	38.6 ± 2.9	30.8 ± 2.9	25.2 ± 0.5	20.1 ± 1.2
HRT2	Chaisterfeld	149-202	38	1.11 ± 0.02	2.92 ± 0.23	1.08 ± 0.06	10 ± 5	9	1.45 ± 0.08	44.1 ± 3.5	30.1 ± 2.9	23.8 ± 1.0	16.2 ± 1.1
HRT3	Chleigrut	149-202	37	0.81 ± 0.02	2.78 ± 0.23	1.01 ± 0.04	10 ± 5	13	1.16 ± 0.06	41.1 ± 2.6	35.5 ± 3.0	30.9 ± 1.0	26.7 ± 1.7
HRT4	Chleigrut	149-202	38	1.16 ± 0.02	2.96 ± 0.22	1.06 ± 0.04	10 ± 5	8	1.51 ± 0.08	47.8 ± 3.2	31.6 ± 2.7	27.7 ± 0.9	18.3 ± 1.1
HRT5	Chleigrut	149-202	39	1.09 ± 0.02	2.55 ± 0.16	0.97 ± 0.03	10 ± 5	4	1.45 ± 0.07	45.6 ± 3.0	31.4 ± 2.6	33.1 ± 0.8	22.8 ± 1.3
HRT6	Markhof	149-202	42	1.02 ± 0.02	2.51 ± 0.21	0.93 ± 0.06	10 ± 5	6	1.35 ± 0.07	30.2 ± 1.8	22.3 ± 1.8	22.8 ± 0.5	16.8 ± 1.0
HRT7	Haltingen	149-202	45	0.89 ± 0.02	3.26 ± 0.19	1.22 ± 0.09	10 ± 5	15	1.30 ± 0.08	43.1 ± 3.0	33.2 ± 3.0	27.2 ± 0.7	20.9 ± 1.2
HRT8	Haltingen	149-202	38	0.78 ± 0.02	2.93 ± 0.18	1.04 ± 0.04	10 ± 5	12	1.15 ± 0.06	34.5 ± 3.8	29.9 ± 3.7	19.0 ± 0.5	16.5 ± 1.0
HRT9	Haltingen	149-202	39	1.32 ± 0.03	4.35 ± 0.27	1.39 ± 0.06	10 ± 5	5	1.85 ± 0.10	40.4 ± 2.5	21.8 ± 1.8	21.2 ± 0.5	11.4 ± 0.7
HRT10	Muttenz	149-202	39	0.76 ± 0.02	3.49 ± 0.18	1.17 ± 0.05	10 ± 5	18	1.18 ± 0.07	43.4 ± 2.3	36.7 ± 2.9	25.0 ± 0.9	21.1 ± 1.4
HRT11	Muttenz	149-202	40	1.02 ± 0.02	3.10 ± 0.21	1.16 ± 0.05	10 ± 5	7	1.43 ± 0.08	32.3 ± 1.5	22.5 ± 1.6	17.8 ± 0.7	12.4 ± 0.8
HRT12	Wallbach	149-202	37	1.09 ± 0.02	2.88 ± 0.31	1.11 ± 0.05	10 ± 5	7	1.47 ± 0.08	47.6 ± 2.2	32.4 ± 2.3	40.4 ± 1.1	27.5 ± 1.7
HRT13	Bellingen	150-200	37	1.58 ± 0.08	4.90 ± 0.12	1.32 ± 0.10	10 ± 5	3.5	2.10 ± 0.17	138.8 ± 10.9	66.0 ± 7.4	58.5 ± 0.6	27.8 ± 2.2
HRT14	Rheinweiler	150-200	39	1.12 ± 0.03	2.87 ± 0.07	0.87 ± 0.06	10 ± 5	0.5	1.52 ± 0.12	1.66 ± 0.24	1.1 ± 0.2	0.35 ± 0.01	0.23 ± 0.02
HRT15	Rheinweiler	150-200	38	1.06 ± 0.05	3.96 ± 0.10	1.56 ± 0.07	10 ± 5	2.0	1.65 ± 0.10	1.71 ± 0.31	1.0 ± 0.2	0.43 ± 0.02	0.26 ± 0.02
HRT16	Rheinweiler	150-200	41	1.18 ± 0.06	2.61 ± 0.07	0.89 ± 0.07	10 ± 5	3.0	1.51 ± 0.12	1.16 ± 0.26	0.76 ± 0.18	0.65 ± 0.03	0.43 ± 0.04
HRT17	Habsheim	150-200	40	1.16 ± 0.04	4.43 ± 0.11	1.58 ± 0.10	10 ± 5	0.6	1.84 ± 0.13	33.0 ± 2.3	18.0 ± 1.8	24.3 ± 0.6	13.2 ± 1.0

Age Model assumes 7.5 % scatter from lab reproducibility and 15 % scatter from microdosimetry (= 16.8 % total scatter) for samples HRT1-13 and HRT 17. For HRT14-16 21 % scatter in reproducibility have been identified (due to low counting statistics), which results in an overall scatter of 25.8 %.

Tab. 1: Results of dosimetry and luminescence measurement, and calculated median and model OSL ages. See Kock et al. (in review) for full details and discussion.

XIX[th] Century (Fig. 5). However, other radiocarbon datings from overbank deposits on the B3 and C sublevels yielded ages between 6160 ± 50 ^{14}C yr BP (7120 ± 160 cal. yr BP) and 2470 ± 100 ^{14}C yr BP (2600 ± 200 cal. yr BP, Tab. 2).

Two ages of 4.8 ± 0.1 ka and 6.2 ± 0.1 ka were obtained from two different speleothems from Tschamberhöhle (Fig. 16). Speleothems can start growing only when vadose conditions are established; hence the ages can be regarded as minimal age of the lowering of the water table below the cave. The water table must have been lower than the cave at least once before the Late Glacial, since a nearby Middle Pleistocene fluvial trough indicates that the base level was then several metres lower than the modern river bed, but we use the hypothesis that the cave was

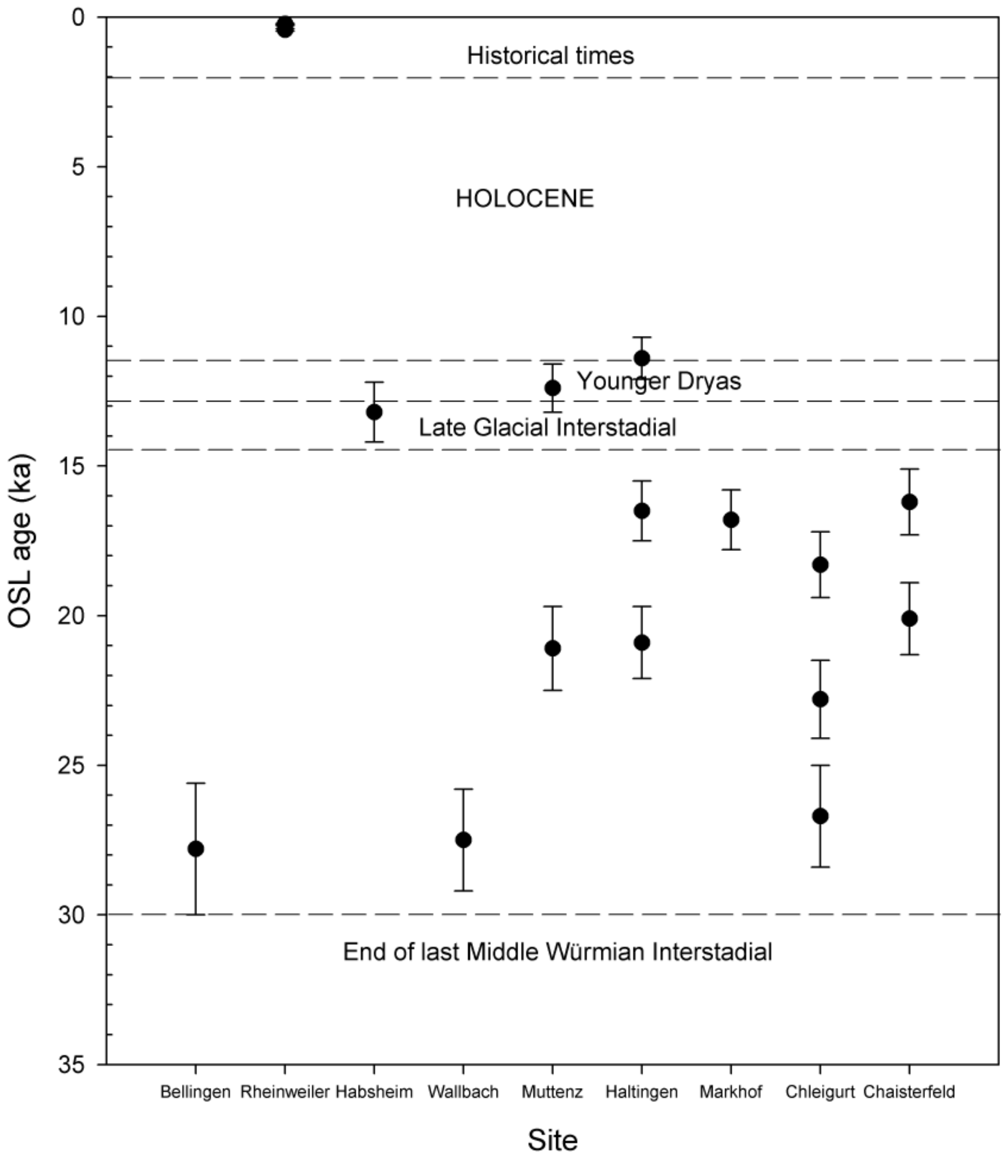

Fig. 17: Plot of OSL ages for the different sites investigated. OSL ages fall into three cluster correlating with the Last Glacial Maximum, the Younger Dryas and historical times, respectively.

formed during the same time as the Lower Terrace because the speleothems and the network of the Tschamberhöhle are very little developed, in contrast with the older "Erdmannshöhle" cave, which developed in the same lithologic unit (Middle Triassic "Muschelkalk" limestone) and in the same area, and where the speleothems are abundant and well developed, and the network much more complex (Piepjohn, 1995).

4.3 Aggradation-erosion chronology

OSL ages from the Hochrhein indicate aggradation between ca. 30 ka and 11 ka. The base of Lower Terrace is dated in Birmenstorf, outside the study area, to 32350 ± 280 ^{14}C yr BP (age beyond recent calibration) using a mammoth tooth found in a palaeosol predating gravel deposition (MBN AG, 1998). Upstream of the study area, at Hüntwangen, Huggenberger et al. (1997) and Preusser et al. (2007) document incision up to 30 m within a short time span in the Rafz terrace, attributed to an early phase of LGM, before the Hüntwangen terrace (dated by Preusser et al., 2007, between about 30 to 25 ka) was deposited (location 16 on Fig.1). Thus, it appears that the onset of accumulation coincides with the beginning of the LGM, and the end with the termination of the Younger Dryas (Fig. 18).

Although erosion phases most probably occurred during this time, aggradation must have been dominant until 11 ka, since sediments of that age are found atop the highest levels of the Lower Terrace (Fig. 6). A pause in the aggradation or an erosion phase may be documented by the absence of ages between 25 and 23 ka, and between 16 and 13 ka, although much more data would be needed to prove this (Fig. 17). Significant incision could hence have started only after 11 ka, as also indicated by the Holocene U-Th ages of speleothems (Fig. 16). The terraces were formed by incision of the River Rhine and afterwards covered by overbank sediments during the Holocene, which were conserved due to the general lowering of the water level. Palynological and radiocarbon ages (Tab. 2), as well as archaeological investigations indicate that the different sub-levels were covered by overbank deposits and soils between the Younger Dryas (A3 level) and the Subboreal (Rentzel, unpublished data; Rentzel 1994 and ref. therein). The chronology of aggradation and erosion presented here is in contrast to previous theories, in which the accumulation of the highest terrace level was assumed to be much older (e.g. about 45 ka in Witmann, 1961). The Bellingen outcrop (Fig. 7) highlights the fact that the age of the terrace sediment should not be taken for the age of the terrace surface (morphologic feature). Indeed, the terrace surface is less than 200 years old (it is still part of the river bed on the "Rheingränz-Carte"), while the sediment located about two metres below the surface has an age of about 27 ka (HRT 13), i.e. the oldest of our samples. This is what would be expected from a normal stratigraphic situation, where the oldest sediment is located at the base of the formation. However, the high density bedload sheet lying on top of the dated sediment is probably much younger, as its conservation and position on top of the terrace implies no subsequent deposition and thus deposition only after the main aggradation and incision

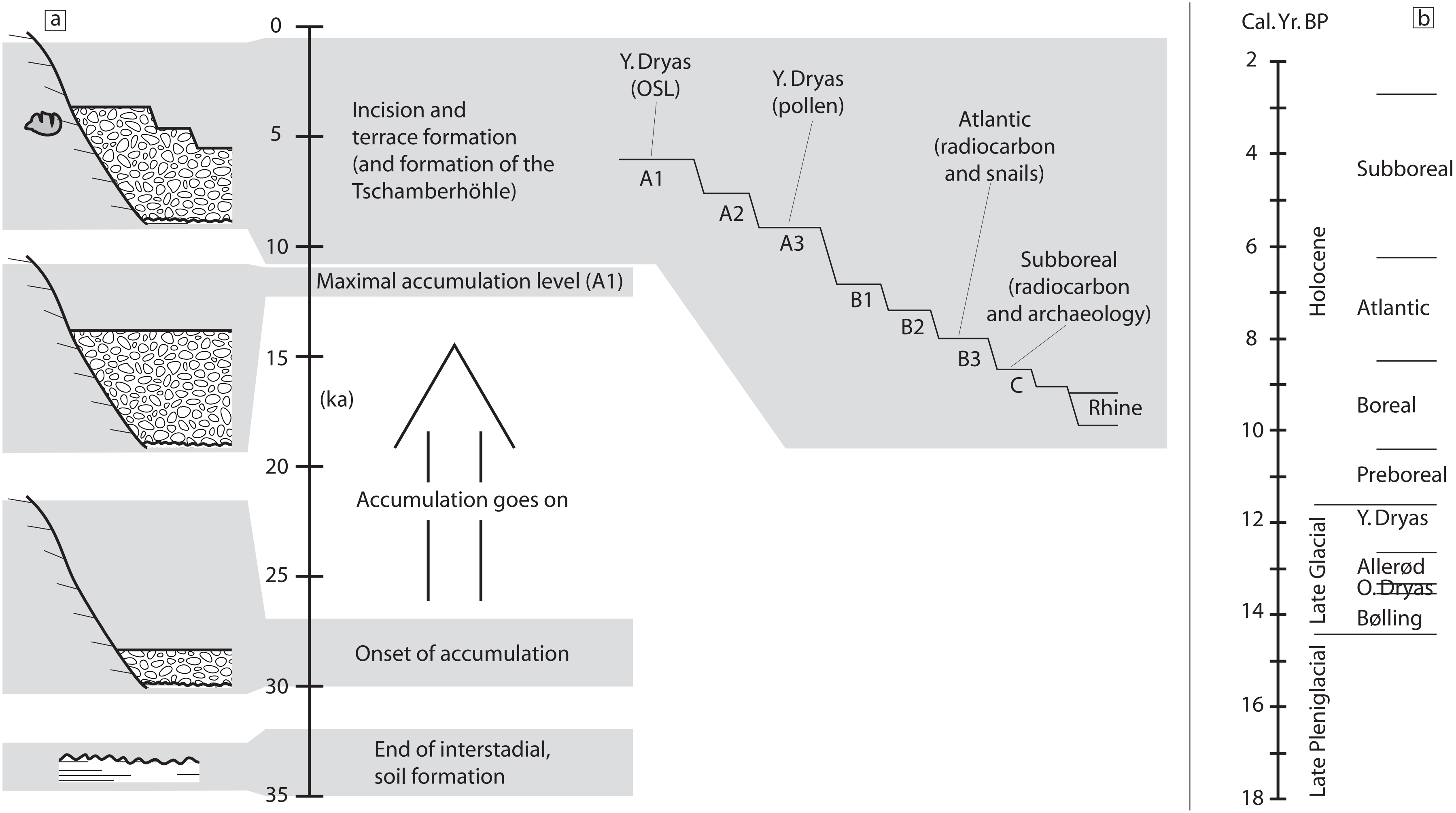

Fig. 18: (a) Reconstitution of the evolution of the Lower Terrace in the area of Basel: gravels started accumulating before 27 ka, and accumulation went on until 12 ka, although some small erosion phases may have happened during this time, that are not documented. The highest accumulation level is thus reached at 12 ka. Then, erosion became dominant and terrace formation began. The water level was located below the level of the Tschamberhöhle at 6 ka. (b) Late Pleistocene and Holocene climatic stages are given for reference, compiled after Litt et al. (2003) and Bos et al. (2008).

events.
The highest level of the Lower Terrace (accumulation surface) is approximately 30 m higher than present Rhine level. The Lower Terrace was thus incised by about 30 m within not more than 12 ka, which represents a mean incision rate of 2.5 mm yr^{-1}. However, incision was most probably irregular and distributed on a series of exceptional events, as terraces have been shown to form very quickly (Born and Ritter, 1970).

4.4 River regime
Recently, Late Glacial to Holocene changes in European river dynamics has been connected to changes in climatic conditions (Kasse et al., 1995; Andres et al., 2001; Houben et al., 2003; Litt et al., 2003). These studies showed that meandering rivers dominated by incision and fine-grained overbank deposition prevailed during warmer phases (Bølling-Allerød, Holocene), whereas braided rivers and coarse sediments were common during colder phases (Late Pleniglacial, Younger Dryas). In the present case, no evidence for a meandering phase during the Late Glacial could be found and such flow regimes are known from the Holocene only (Fig. 4) (cf., Rentzel, 1994). Overbank deposits and soils are located on top of the different sub-levels, thus correlating with the onset of Boreal and Atlantic. However, it is known that the part of the Rhine located downstream of Basel was braided in historical times (until the XIX^th^ Century and before the correction of the river, Fig. 5). Clearly, climate is not the sole controlling factor of river regime in the Basel area and other factors are possibly regional slope and width of the river bed, which in turn may be controlled by recent tectonic movements.

5. Conclusion

A terrace formation process has been described, where flood events are important agents of terrace building, their eroding effects as well as their accumulation effects. A precise aggradation-erosion history has been proposed for the Lower Terrace in the area of Basel, where the gravel input is correlated with the LGM, and the main change from aggradation-dominated to erosion-dominated conditions occurs at the end of the Younger Dryas, after which all the cut-terraces of the Lower Terrace were formed. It has been shown that sediment ages should not be used as cut-terrace ages in a geomorphological view, since their respective ages are actually inversely correlated. Only the age of the accumulation surface is comparable with that of its highest (youngest) sediments.

Acknowledgments

Table 2. Radiocarbon ages for organic material found below (1), in (2) and on top (3) of Lower Terrace sediment of River Rhine in the Basel area. Calibration was carried out using OxCal 4.0 online (C. Bronk Ramsey, Oxford) that is based on INTCAL04 (Reimer et al. 2004). * Radiocarbon age on plateau, the most likely calibration has been used considering the geological and chronological context..

Location	Sample code	^{14}C age (yr BP)	Calibrated age (cal. yr BP)	Material	Host sediment	Stratigraphic position	Dated event	Source	Note
17	ETH-17251	32350 ± 280	n.a.	Mammoth tooth	Buried palaeosol	1	Formation of soil	MBN AG (1998)	
16	ETH-17255	22190 ± 170	n.a.	Mammoth tibia	Gravel	2	Accumulation	MBN AG (1998)	agrees with OSL age
15	UZ-2416	20550 ± 250	24800 ± 700	Mammoth skull	Gravel	2	Accumulation	Bitterli et al. (2000)	
14	ETH-17250	19850 ± 150	23840 ± 470	Mammoth tusk	Gravel	2	Accumulation	MBN AG (2001)	
close to 6	Basel_98_22_9a	6160 ± 50	7120 ± 160	Organic debris	Overbank (B3)	3	Abandonment of terrace	Rentzel (unpubl.)	
close to 6	B-2195	5860 ± 110	6730 ± 270	Wood debris	Gravel	2	Accumulation	Hauber (1971)	
close to 6	Basel_98_1_1	4496 ± 47	5200 ± 170	Organic debris	Overbank (C)	3	Abandonment of terrace	Rentzel (unpubl.)	
6	ETH-19324	3320 ± 60	3600 ± 150	Tree trunk	Gravel	2	Flood accumulation	Schwarz (1998)	
close to 6	B-2194	2470 ± 100	2600 ± 200	Wood debris	Overbank (C)	3	Abandonment of terrace	Hauber (1971)	
4	ETH-34367	870 ± 60	850 ± 110	Organic debris	Overbank (C)	3	Abandonment of terrace	This study	probably reworked
4	ETH-34582	310 ± 40	440 ± 100	Tree stem	Gravel	2	Accumulation	This study	
4	ETH-34366	260 ± 50	420 ± 100*	Organic debris	Sand lens	2	Accumulation	This study	agrees with OSL age
4	ETH-34581	255 ± 40	410 ± 100*	Tree trunk	Gravel	2	Accumulation	This study	agrees with OSL age

The authors wish to thank Philippe Rentzel (IPNA, Universität Basel) for the data and the fruitful discussions about the terrace covers, and the NAGRA (Swiss National Cooperative for the Disposal of Radioactive Waste) who provided the DEM. Gamma spectrometry for the luminescence dating was carried out by J. Lomax at Geographisches Institut, Universität zu Köln, and the radiocarbon dating was performed by I. Hajdas, Institut for Particle Physics, ETH Zürich. Jan Kramers (Institut für Geologie, Universität Bern) is thanked for the U/Th dating. The authors are grateful to the companies for giving access to their gravel pits, sometimes even giving a hand with their excavator. S.K. acknowledges financial support from the Freiwillige Akademische Gesellschaft of Basel.

References

Andres, W., Bos, J.A.A., Houben, P., Kalis, A.J., Nolte, S., Rittweger, H. & Wunderlich, J. 2001: Environmental change and fluvial activity during the Younger Dryas in central Germany. Quaternary International 79, 89-100.

Bitterli, T., Graf, H.R., Matousek, F. & Wanner, M. 2000: Blatt 1050 Zurzach.

Born, S. M. & Ritter, D.F. 1970: Modern Terrace Development Near Pyramid Lake, Nevada, and its Geologic Implications. GSA Bulletin 81, 1233-1242.

Bos, J. A. A., Dambeck, R., Kalis, A.J., Schweizer, A. & Thiemeyer, H. 2008: Palaeoenvironmental changes and vegetation history of the northern Upper Rhine Graben (southwestern Germany) since the Lateglacial. Netherlands Journal of Geosciences - Geologie en Mijnbouw 87, 67-90.

Choi, S.-W., Preusser, F. & Radtke, U. 2007: Dating of lower terrace sediments from the Middle Rhine area, Germany. Quaternary Geochronology (Quaternary Science Reviews) 2, 137-142.

Criqui, G. 1981: Le régime hydraulique, les crues et les inondations du Rhin. Une histoire du Rhin. Ayçoberry, P. & Ferro, M. Paris, Ramsay: 317-336.

Fleitmann, D., Burns, S.J., Mangini, A., Mudelsee, M., Kramers, J.D., Villa, I., Neff, U., Al-Subbary, A. A., Buettner, A., Hippler, D. & Matter, A. 2007: Holocene ITCZ and Indian monsoon dynamics recorded in stalagmites from Oman and Yemen (Socotra). Quaternary Science Reviews 26, 170-188.

Fracassi, U., Nivière, B. & Winter, T. 2005: First appraisal to define prospective seismogenic sources from historical earthquake damages in southern Upper Rhine Graben. Quaternary Science Reviews 24, 403-425.

Frechen, M., Ellwanger, D., Hinderer, M., Lämmermann, J., Neeb, I., 2004. Late Pleistocene fluvial dynamics in the Upper Rhine Graben and the Hochrhein area – chronological frame. Abstracts DEUQUA meeting Nijmegen, p. 34.

Giamboni, M.E., Ustaszewski, K., Schmid, S.M., Schumacher, M.E. & Wetzel, A. 2004a: Plio-

Pleistocene transpressional reactivation of Paleozoic and Paleogene Structures in the Rhine-Bresse transform zone (northern Switzerland and eastern France. International Journal of Earth Sciences 93, 207-223.

Giamboni, M.E., Wetzel, A., Nivière, B. & Schumacher, M.E. 2004b: Plio-Pleistocene folding in the southern Rhinegraben recorded by the evolution of the drainage network (Sundgau area; northwestern Switzerland and France). Eclogae geol. Helv. 97, 17-31.

Gross, H. 1958: Die bisherigen Ergebnisse von C14-Messungen und paläontologischen Untersuchungen für die Gliederung und Chronologie des Jungpleistozäns in Mitteleuropa und den Nachbargebieten. Eiszeitalter und Gegenwart 9, 155-187.

Hajdas, I., Bonani, G., Thut, H., Leone, G., Pfenninger, R. & Maden, C. 2004: A Report on Sample Preparation at the Eth/Psi Ams Facility in Zurich. Nuclear Instruments & Methods in Physics Research Section B-Beam Interactions with Materials and Atoms 223-224, 267-271.

Haldimann, P., Naef, H. & Schmassmann, H. 1984: Fluviatile Erosions- und Akkumulationsformen als Indizien jungpleistozäner und holozäner Bewegungen in der Nordschweiz und angrenzenden Gebieten. Nagra Technischer Bericht 84-16.

Hauber, L. 1971: Das Alter des Rhein- und Wiesenbettes beim Eglisee in Basel. Regio Basiliensis XII, 316-319.

Houben, P. 2003: Spatio-temporally variable response of fluvial systems to Late Pleistocene climate change: a case study from central Germany. Quaternary Science Reviews 22, 2125-2140.

Huggenberger, P. & Regli, C. 2006: A sedimentological model to characterize braided river deposits for hydrogeological application. Braided Rivers. Sambrook Smith, G. H., Best, J. L., Bristow, C. S. & Petts, G. E., International Association of Sedimentologists. 36: 51-74.

Huggenberger, P., Siegenthaler, C. & Aigner, T. 1997: Quaternary fluvial sedimentation in northern Switzerland and southern Germany: an integrated approach of sedimentological analysis and ultra-high resolution geophysical techniques. Gaea heidelbergensis 4, 141-157.

Ivy-Ochs, S., Schäfer, J., Kubik, P.W., Synal, H.-A. & Schlüchter, C. 2004: Timing of deglaciation on the northern alpine foreland (Switzerland). Eclogae geol. Helv. 97, 47-55.

Kasse, K., Vandenberghe, J. & Bohncke, S. 1995: Climatic change and fluvial dynamics of the Mass during the Late Weichselian and Early Holocene. In: Frenzel, B., Vandenberghe, J., Kasse, K., Bohncke, S., Gläser, B. (Eds.), European River Activity and Climatic Change During the Lateglacial and Early Holocene. Fischer, Stuttgart, 123–150.

Kock, S., Kramers, J.D., Preusser, F. & Wetzel, A. submitted: Dating of Late Pleistocene terrace deposits of the River Rhine using uranium series and luminescence methods: potential and limitations. Quaternary Geochronology (Quaternary Science Reviews).

Lambert, J., Winter, T., Dewez, T.J.B. & Sabourault, P. 2005: New hypotheses on the maximum damage area of the 1356 Basel earthquake (Switzerland). Quaternary Science Reviews 24, 383-401.

Litt, T., Schmincke, H.-U. & Kromer, B. 2003: Environmental response to climatic and volcanic events in central Europe during the Weichselian Lateglacial. Quaternary Science Reviews 22, 7-32.

MBN AG, 1998: Zur Stratigraphie des jüngeren Pleistozäns im Gebiet des Zusammenflusses von Aare, Surb, Rhein und Wutach. Bericht G819B z. Hd. Landeshydrologie und -geologie, Bern

Murray, A.S. & Wintle, A.G. 2000: Luminescence dating of quartz using an improved single-aliquot regenerative-dose protocol. Radiation Measurements 32, 57-73.

Murray, A.S. & Wintle, A.G. 2003: The single aliquot regenerative dose protocol: potential for improvements in reliability. Radiation Measurements 37, 377-381.

Ollive, V., Petit, C., Garcia, J.-P. & Reddé, M. 2006: Rhine flood deposits recorded in the Gallo-Roman site of Oedenburg (Haut-Rhin, France). Quaternary International 150, 28-40.

Penck, A. & Brückner, E. 1909: Die Alpen im Eiszeitalter. Leipzig, Tauchnitz.

Piepjohn, K. 1995: Die Erdmannshöhle bei Hasel (Südbaden) und die Abhängigkeit ihrer Entwiklung von den quartären Klima-Ereignissen. Münster. Forsch. Geol. Paläont. 77, 155-171.

Prescott, J.R. & Hutton, J.T. 1994: Cosmic ray contributions to dose rates for luminescence and ESR dating: Large depths and long-term time variations. Radiation Measurements 23, 497-500.

Preusser, F. 2004: Towards a chronology of the Late Pleistocene in the northern Alpine Foreland. Boreas 33, 195-210.

Preusser, F. 2008: Characterisation and evolution of the River Rhine system. Netherlands Journal of Geosciences - Geologie en Mijnbouw 87, 7-19.

Preusser, F. & Kasper, H.U. 2001: Comparison of dose rate determination using high-resolution gamma spectrometry and inductively coupled plasma mass spectrometry. Ancient TL 19, 19-23.

Preusser, F., Blei, A., Graf, H. R. & Schlüchter, C. 2007: Luminescence dating of Würmian (Weichselian) proglacial sediments from Switzerland: methodological aspects and stratigraphical conclusions. Boreas 36, 1-13.

Preusser, F., Geyh, M. A. & Schlüchter, C. 2003: Timing of Late Pleistocene climate change in lowland Switzerland. Quaternary Science Reviews 22, 1435-1445.

Rentzel, P. 1994: Geologisch-bodenkundliche Untersuchungen an den Niederterrassenfeldern bei Basel unter besonderer Berücksichtigung der spätlatènezeitlichen Fundstelle Basel-Gasfabrik. Jahresbericht Archäologische Bodenforschung des Kanton Basel-Stadt 1994, 31-52.

Schumacher, M.E. 2002: Upper Rhine Graben: Role of preexisting structures during rift evolution. Tectonics 21, 6-1 - 6-17.

Schwarz, P.-A. (1998). Tätigkeitsbericht der Archäologischen Bodenforschung Basel-Stadt für das

Jahr 1998. Basel: 67.

Siegenthaler, C. & Huggenberger, P. 1993: Pleistocene Rhine gravel: deposits of a braided river system with dominant pool preservation. Braided Rivers. Best, J. L. & Bristow, C. S., Geological Society. 75: 147-162.

Theobald, N. 1933: Observations sur la Basse Terrasse du Rhin en aval de Bâle. Bull. Soc. industr. Mulhouse, 21-27.

Todd, S.P. 1989: Stream-driven, high-density gravelly traction carpets: possible deposits in the Trabeg Conglomerate Formation, SW Ireland and some theoretical considerations of their origin. Sedimentology 36, 513-530.

Ustaszewski, K. & Schmid, S.M. 2007: Latest Pliocene to recent thick-skinned tectonics at the Upper Rhine Graben - Jura Mountains junction. Swiss j. geosci. 100, 293-312.

Wallinga, J. 2002: Optically stimulated luminescence dating of fluvial deposits: a review. Boreas 31, 303-322.

Wallinga, J., Murray, A.S., Duller, G.A.T. & Törnqvist, T.E. 2001: Testing optically stimulated luminescence dating of sand-sized quartz and feldspar from £uvial deposits. Earth and Planetary Science Letters 193, 617-630.

Wittmann, O. 1961: Die Niederterrassenfelder im Umkreis von Basel und ihre kartographische Darstellung. Basler Beiträge zur Geographie und Ethnologie 3, 46.

Chapter 3

Chapter 3

Neotectonic activity in the area of Basel as inferred from morphological analysis of fluvial terraces of the Rhine River

Kock, S., Schmid, S.M., Fraefel, M., Wetzel, A.

Abstract

The southern Upper Rhine Graben (URG) and neighbouring regions are tectonically still active, though low displacement rates renders it difficult to assess neotectonic activity. Pleistocene fluvial deposits of the Rhine river that are present upstream from the URG are used to solve this problem: The geometry of these deposits shows that a Paleogene depocenter in the southern URG underwent renewed subsidence during the Pleistocene, while the Rhine valley upstream of the URG incised into bedrock. In the area of Basel, the eastern main border fault of the URG or a parallel fault (Allschwil fault) was possibly active during Pleistocene times, as terrace deposits of the Rhine occur on its down-throw side at an altitude lower than expected. Analyses of the youngest terrace system (Late Glacial Lower Terrace) using a high precision digital elevation model (DTM-AV) suggests possible Pleistocene-Holocene fault activity upstream from the URG near the southern border of the Black Forest Massif. NW of Basel, within the URG, field evidence indicates recent NE-SW extension.

1 Introduction

The Basel area, located at the border between Switzerland, France and Germany is also located at the intersection point of four main tectonic features within Central Europe: the Jura Mountains (Laubscher, 1992; Philippe et al., 1996; Affolter and Gratier, 2004), the NNE-SSW striking Upper Rhine Graben (Ziegler, 1994), the Black Forest and Vosges Massifs (Ziegler and Dèzes, 2007), and a ENE-WSW striking late Palaeozoic (Permo-Carboniferous) graben system (Lutz, 1964; Diebold, 1989; Laubscher and Noack, 1997) mostly defined by subsurface data (Fig.1). Hence, it represents a tectonically complex area that is prone to reactivation under the present-day NW directed compressional stress field (Schumacher, 2002; Ustaszewski and Schmid, 2006; 2007; Madritsch et al., accepted). Some of this stress was dramatically released in 1356 when a major earthquake destroyed the city of Basel (Meyer et al., 1994; Lambert et al., 2005), and minor earthquakes are regularly recorded and felt nowadays in this area, which is densely populated and of high economic value (Baer et al., 2007). It is therefore crucial to refine the

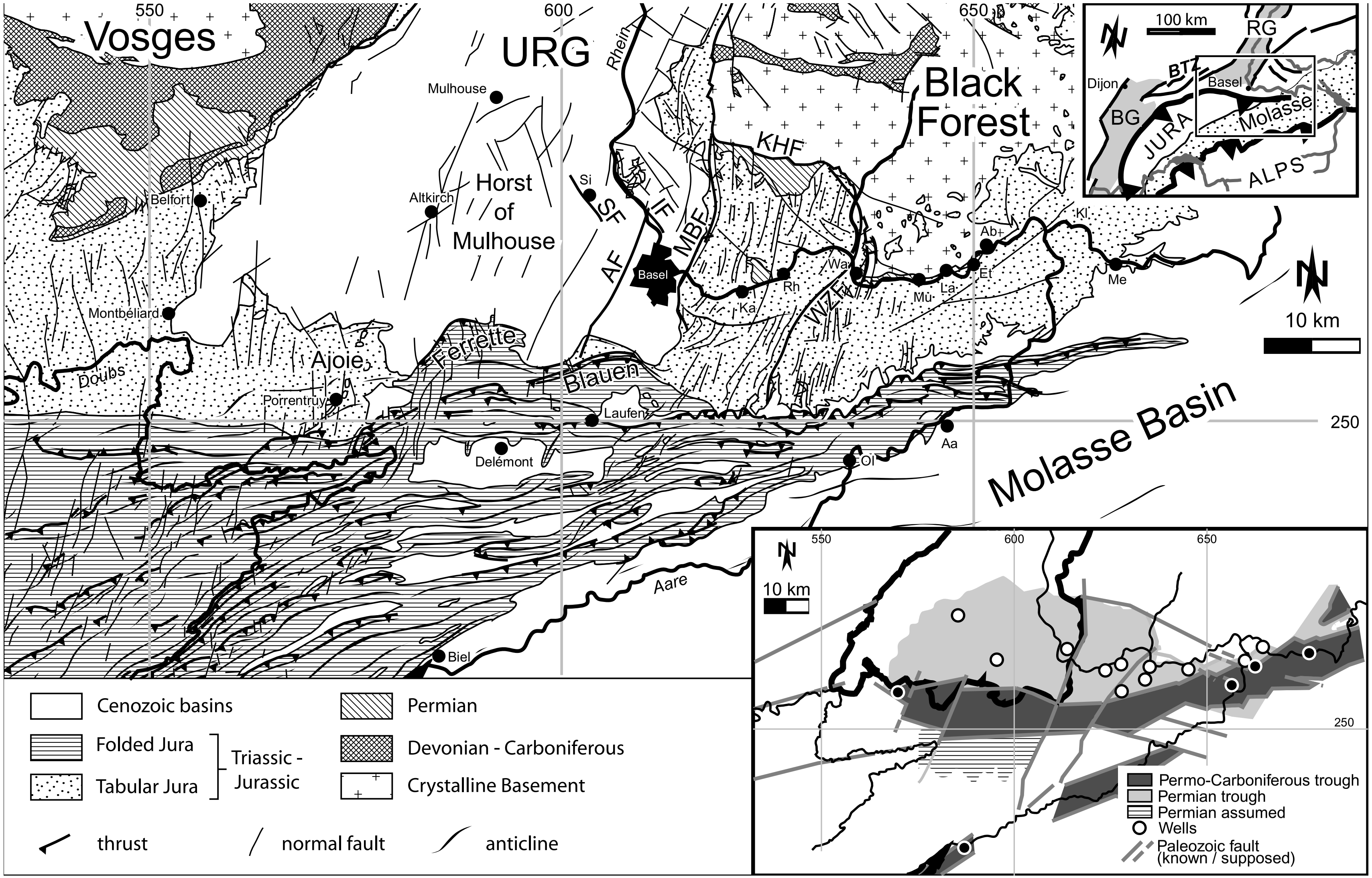

Fig. 1: Geographic and geological settings. AF: Allschwil Fault; IF: Istein Fault; KHF: Kandern Hausen Fault; MBF: Main Border Fault; SF: Sierentz Fault; URG: Upper Rhine Graben; WZF: Wehra-Zeiningen Fault. Localities cited in the text: Aa: Aarau; Ab: Albbruck; Et: Etzgen; Ka: Kaiseraugst; Kl: Klettgau area; La: Laufenburg; Me: Mellikon; Mu: Murg; Ol: Olten; Rh: Rheinfelden; Si: Sierentz; Wa: Wallbach. Inset top right is an overview map, inset bottom right is a map of the Permo-Carboniferous trough system.

assessment of geohazards. This includes studying the Quaternary deformation history of the area. Accordingly, it is the aim of this work to provide new constraints on neotectonic activity in the area using Quaternary-age marker beds.

Fluvial and marine terraces have been recognized to record neotectonic activity (Bull, 1991; Schumm, 1993, Wang and Grapes, 2008), as they form rather regular surfaces, which can sometimes be traced for several tens of kilometres. These may be displaced or disturbed by tectonic events, depending on the intensity of such events. Other morphological features, such as stream gradients are also useful indicators of neotectonic activity (Hack, 1957; Seeber and Gornitz, 1983; Snyder et al., 2000).

Previous studies that applied similar methodologies to the nearby Sundgau area, which borders the Folded and Tabular Jura and the Upper Rhine Graben, were able to demonstrate that tectonic activity persisted until at least latest Pliocene times (Meyer et al., 1994, Giamboni et al., 2004a; 2004b; 2005; Ustaszewski and Schmid, 2007). This study applies a similar approach but concentrates on the the Upper Rhine Valley between the Aare-Rhine junction (N-Switzerland) and Mulhouse (E-France).

1.2 Geological setting

From a geological point of view, the study area comprises two main tectonic settings. From the junction of the Aare and Rhine to the city of Basel, the Rhine River follows the boundary between the almost undeformed Mesozoic sediments of the Tabular Jura (mainly limestones and marls) and the uplifted Black Forest Massif and its sedimentary cover (crystalline rocks, sandstones and limestones). Immediately east of Basel the Rhine crosses a southern portion of the eastern Main Border Fault (MBF or “Rheintal Flexur”) of the Upper Rhine Graben (URG) and thereafter enters the Tertiary graben fill (limestones, sandstones and conglomerates).

The NNE trending URG is a key feature of the European Cenozoic Rift System, which extends from the North Sea to the Mediterranean (Ziegler, 1990, 1992; Dèzes et al. 2004, Ziegler and Dèzes, 2007). The URG is limited to the North by the Rhenish Massif and to the south by the Rhine-Bresse Transfer Zone (Ustaszewski et al., 2005; Madritsch et al., submitted) that kinematically links the URG to the Bresse graben via sinistrally transtensional deformations (Laubscher, 1970; Bergerat and Chorowicz, 1981). This transfer zone coincides with the Permo-Carboniferous ENE-WSW striking Burgundy Trough (Boigk and Schöneich, 1970; Allenbach and Wetzel, 2006) and more or less coincides with the front of the Jura Mountains (Ziegler, 1992, 1994, Ustaszewski & Schmid, 2006; Madritsch et al., submitted). In the southern Black Forest, a major Paleozoic structure is the WNW-ESE striking Kandern-Hausen Fault (KHF), which separates the crystalline footwall to the North from the hanging-wall Dinkelberg Block, which is still covered by Permian and Triassic sediments (Echtler and Chauvet, 1992; Hinsken et al., 2007).

Tensional subsidence in the URG commenced during the late Middle Eocene (e.g. Pflug, 1982; Duringer, 1988; Hinsken et al., 2007). During the Burdigalian, the southern URG, together with the flanking Vosges and Black Forest massifs, were uplifted and subjected to erosion (Dèzes et al., 2004; Dèzes & Ziegler, 2007). Correspondingly, Late Chattian and Miocene deposits are missing in the southern URTG (Fischer, 1965; Villemin et al., 1986; Berger et al., 2005a; Hinsken et al., 2007). During the Middle and Late Miocene a south-directed fluvial network developed on the southern flanks of the Vosges-Black Forest arch and debouched into the Swiss Molasse Basin (Liniger, 1967; Berger et al., 2005b; Ziegler & Fraefel, submitted). During the middle Tortonian deformation of the thin-skinned Jura fold-and-thrust belt commenced, controlling a reorganization of this drainage system. By Early Pliocene times the river Aare-Doubs started to flowed westward along the southern margin of the Black Forest and deposited in the foreland of the evolving Jura fold-and-thrust belt the Sundgau gravels (e.g. Villinger, 1998, 2003; Ziegler and Fraefel, submitted). These gravels were folded during late Pliocene to Pleistocene times (e.g. Giamboni et al., 2004; Ustaszewski & Schmid, 2006, 2007) whilst the river Aare flowed from Basel northward in the URG in response to subsidence of its southern parts, resuming during the Late Pliocene (Dèzes et al., 2004; Ziegler & Dèzes, 2007). Around 1.7 Ma tributaries of the river Aare captured the Alpine headwaters of the river Rhine (Villinger, 1998, 2003). With this, the water and sedimentary load of the newly formed Alpine Rhine increased strongly (Müller et al., 2002; Hagedorn & Boenigk, 2008; Ziegler & Fraefel, submitted).

During the Pleistocene, a complex flight of fluvial terraces developed in the Rhine Valley upstream from Basel, reflecting alternating phases of river incision and aggradation. These terraces, which are the focus of this study, are genrally divided into four units (Fig. 2): the Higher Deckenschotter, the Lower Deckenschotter, the High Terrace and the Lower Terrace (e.g. Bitterli et al., 2000).

The Higher and Lower Deckenschotter have a complex stratigraphy (Graf, 1993; Bitterli et al., 2000; Graf et al., 2007) that includes fine sediments and paleo-soils typical for temperate climates as well as coarse sediments typical for cold climates. As such, this indicates a polyphase accumulation history during several climatic cycles. The most important outcrops are located along the southern side of the Rhine River between the confluence of the rivers Thur and Aare, in the lower Aare Valley between the confluence of the Reuss into the Aare, and near the confluence of the Aare with the Rhine. Other outcrops are located further downstream between Wallbach and Rheinfelden, though now on the northern bank of the Rhine, as well as between Rheinfelden and Kaiseraugst on the southern side, and finally, south and west of Basel (Fig. 3). In the Aare valley these outcrops are often covered by moraines, or by loess in the Rhine valley.

The stratigraphy of the High Terrace indicates deposition over at least two climatic cycles, as suggested by the occurrence of moraines that are interbedded with other deposits (Bugmann,

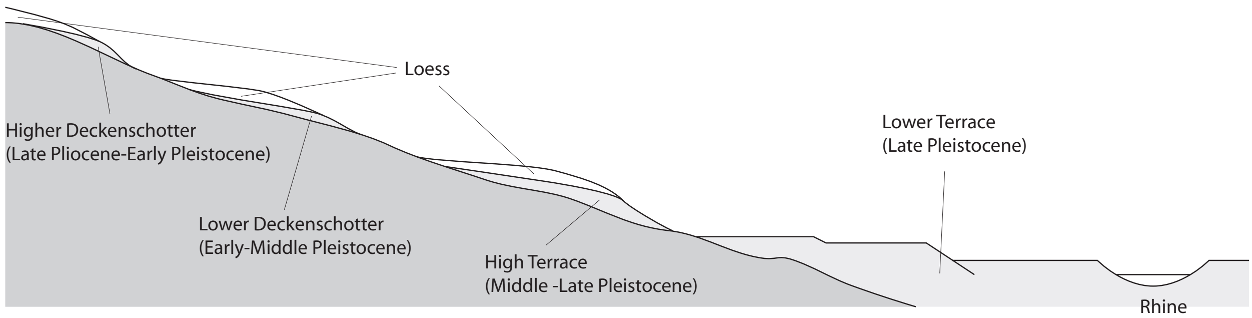

Fig. 2 Schematic cross-section without scale showing the relative positions of the Pleistocene fluvial deposits in the Rhine valley.

1961; MBN AG, 1998; Bitterli et al., 2000; Graf and Hofmann, 2000). It is during one of these climatic cycles that river incision was most severe, cutting deeply into the substratum and forming channels which are filled by Quaternary sediments, as evidenced by boreholes (Haldimann et al., 1984). The most significant outcrops of the High Terrace are located in the Klettgau depression, in the lower Aare valley, between the confluence of the Reuss and Rhine. Other outcrops are located in the Aare valley between Olten and Aarau, in the Rhine valley between the inlet of the Töss and Mellikon, between Albbruck and Murg, between Wallbach and Rheinfelden (Switzerland), and south and west of Basel.

The Lower Terrace, which is exclusively characterized by fluvioglacial sediments, was possibly deposited during a single climatic cycle in the area, although evidence for erosion and re-accumulation is repeatedly found (Bitterli et al., 2000; Kock et al., in prep). Huggenberger and Regli (2006) investigated related sedimentological processes. The Lower Terrace constitutes most of the flat areas flanking the Rhine River and its tributaries in northern Switzerland, with numerous gravel pits offering plentiful fresh outcrops. These terraces are generally covered by about one meter of soil. The gravels of the Lower Terrace were deposited partly on bedrock, partly on older Pleistocene sediments attributed to the High Terrace. They formed a braid plain that was constantly reworked due to channel migration during the accumulation phases and reworked during incision phases until the area was abandoned. These terraces were covered by soil or finer river sediments during the Holocene.

Different types of fluvial formations are known from drillings into the Quaternary deposits of the southern Upper Rhine Graben (Geisswasser Basin, Fig. 4), the stratigraphic position of which has been inferred from their heavy mineral spectrum. These can partly be correlated with the fluvial terraces of the Rhine. The Iffezheim Formation has a late Pliocene age and is a potential equivalent of the oldest part of the Higher Deckenschotter; the Breisgau Formation can be correlated with the Higher and Lower Deckenschotter; the Neuenburg Formation can be correlated with the High Terrace as well as the Lower Terrace (LGRB Baden-Würtemberg, 2004; Hagedorn and Boenigk, 2008). The Iffezheim Formation contrasts with the Breisgau and Neuenburg Formations due to its non-alpine heavy mineral spectrum.

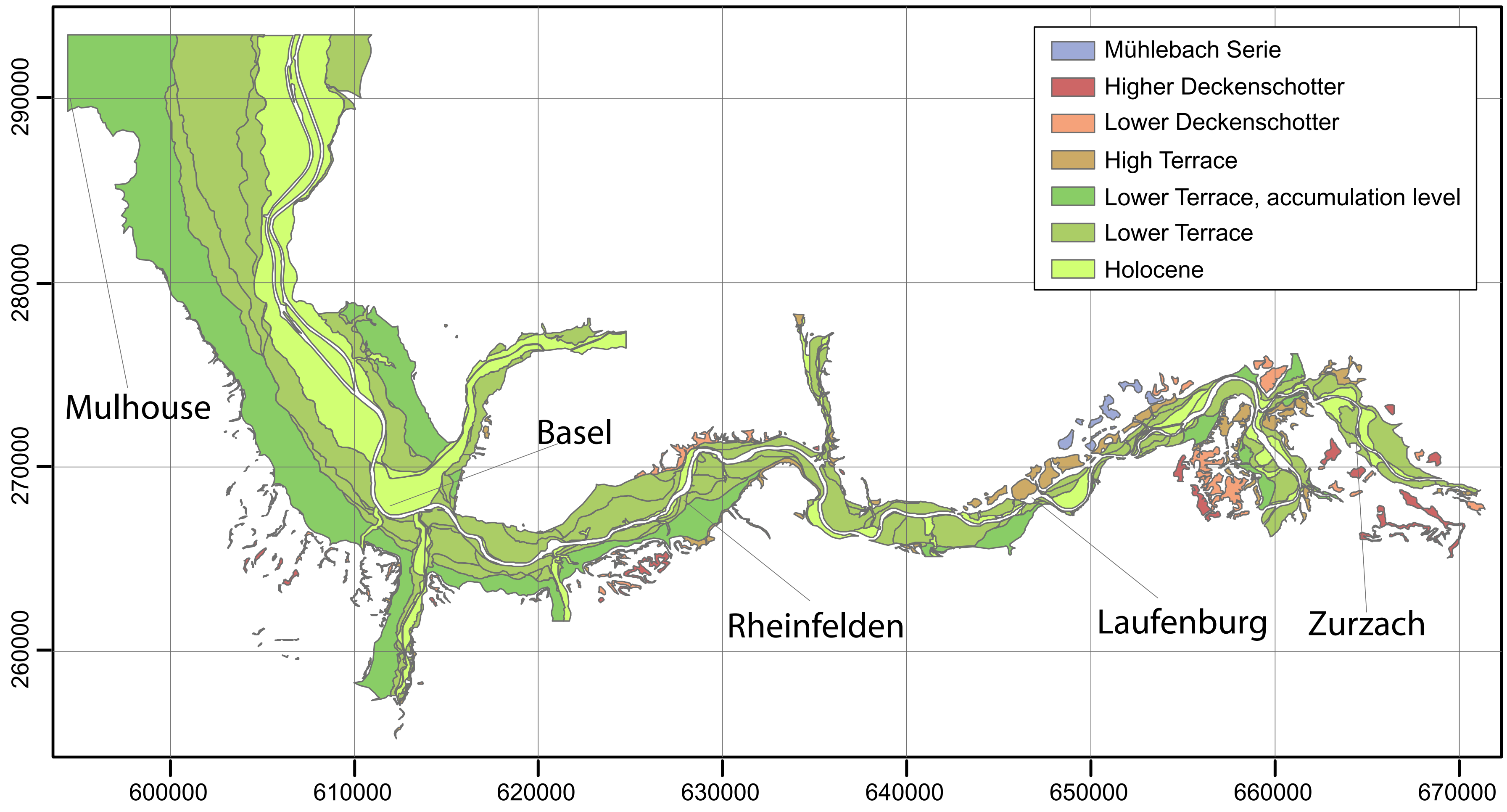

Fig. 3 Map of Late Pliocene and Pleistocene fluvial deposits in the Hochrhein area. The Mühlebach Serie is described in Groschopf and Sawatzki (1989), Hofmann (1996) and Verderber (2003).

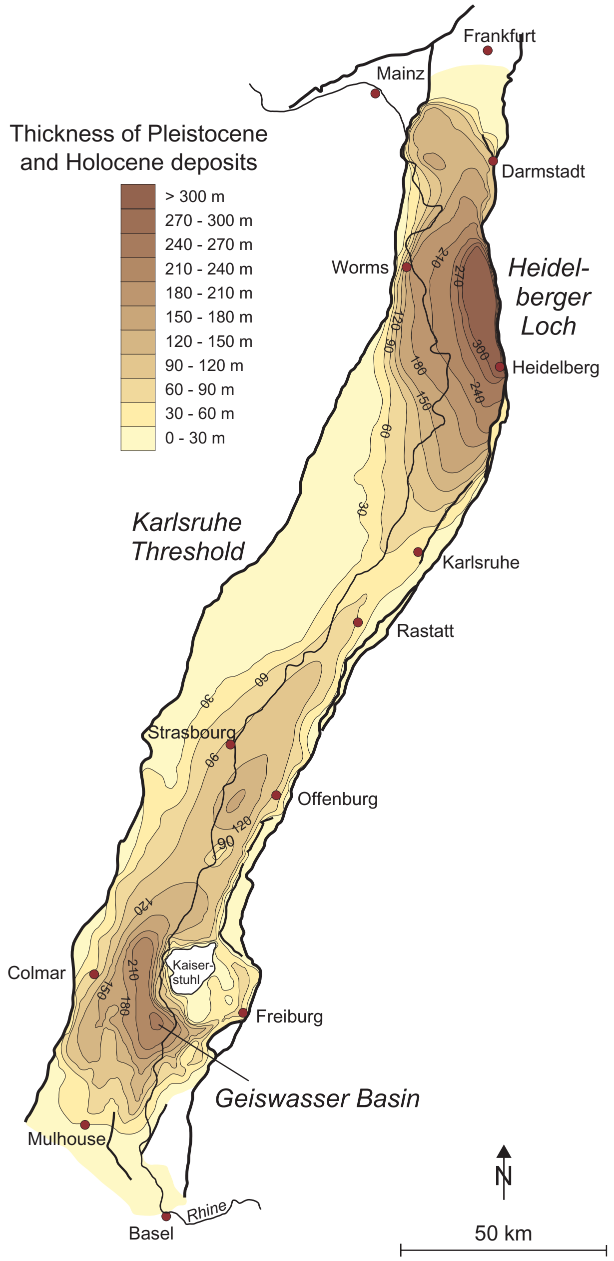

Fig. 4 Map of the URG showing the thickness of Pleistocene and Holocene deposits. Two depocenters can be seen: the Geiswasser Basin in the South, and the "Heidelbergerloch" in the North. Modified after Bartz (1974) and Hagedorn and Boenigk (2008).

1.3 Age control on the terraces

1.3.1 Deckenschotter

According to Penck and Brückner (1909), and based on stratigraphic records, the Higher and Lower Deckenschotter are usually attributed to the Günz and Mindel glacial stages. However, the attribution of the Lower Deckenschotter to the Mindel glacial event was contested by Bibus (1990), who proposed an older age, based on the presence of five paleosols on top of this highest terrace. Biostratigraphical and chronometric ages could be obtained only much later: Palaeontological findings from the Higher Deckenschotter indicate an age 1.8 Ma (Bolliger et al., 1996); paleomagnetic analysis indicates a reverse magnetic field, and thus a minimum age of 0.78 Ma (Villinger, 2003). The new cosmogenic nuclide method recently yielded an age of 2.35 Ma for the Higher Deckenschotter, and 0.68 Ma for the Lower Deckenschotter (Häuselmann et al., 2007). Other authors (e.g. van Husen 2004), however, attribute the Lower Deckenschotter to the marine isotope stage MIS 12 (0.45 Ma) and the Higher Deckenschotter to MIS 16 (0.65 Ma).

1.3.2 High Terrace

Based on stratigraphic records, the High Terrace is usually attributed to the Riss glacial stage (Blösch, 1911; Bugmann, 1961) that represents the maximum extent of ice sheets (Schlüchter 1989). Chronometric ages for the gravels are, however, generally lacking. Van Husen (2004) attributes the High Terrace to MIS 6 (150 ka). Fiebig and Preusser (2003) obtained very young luminescence ages from sediments attributed to the High Terrace in Bavaria (62 and 75 ka). They noted that a better definition of this formation is necessary. On the other hand, the loess sequence deposited on a terrace close to Basel, correlated with the High Terrace, was recently dated by Rentzel et al. (submitted) by OSL (Optically Stimulated Luminescence) ages which range up to 236 ka. Thus, these authors concluded that the underlying gravel has a minimum age of 250 ka (MIS 8), possibly even 340 ka (MIS 10).

1.3.3 Lower Terrace

In contrast to the older terraces, the age of the Lower Terrace is by now reasonably well constrained, mostly by radiocarbon and OSL dating. Moreover, mammoth remains were found in Mellikon (20550 ± 250 BP, Bitterli et al., 2000), Böttstein (19850 ± 150 BP, MBN AG, 1998), Turgi (18150 ± 140 BP, MBN AG, 1998) and Birmenstorf (32350 ± 280 BP, MBN AG, 1998). The findings of Mellikon, Böttstein and Turgi come from the Lower Terrace gravels themselves, while the Birmenstorf finding comes from a paleosoil that predates the deposition of the Lower Terrace. In the Basel area, the gravels attributed to the Lower Terrace accumulated between 27 and 12 ka, whereupon a series of cut-terraces were formed (Kock et al., submitted). These cut-terraces are covered by sediments of younger Dryas to Subboreal age (Rentzel, 1994). Other studies from a wider area (Litt et al., 2003; Choi et al., 2007; Preusser et al., 2007) confirm the Late Glacial to Younger Dryas depositional age of these gravels.

2 Methods

2.1 Field evidence for neotectonic deformation

Given (1) the young age of the studied sediments, which are often not cemented and coarse-grained and (2) the intraplate setting with relatively low deformation rates, distinct and sharp tectonic structures are expected to be very rare or inexistent Nevertheless, Théobald et al.

(1977) reported recent fault movement along the Mulhouse-Sierentz line, and one clear tectonic structure was found nearby in older but also unconsolidated Sundgau gravels (Ustaszewski and Schmid, 2007). During this study, outcrops of fluvial deposits were systematically analysed for evidence of late-stage tectonic movements.

2.2 Geomorphology

An indirect way of gathering evidence for tectonic activity is to look for potential controls of neotectonic deformation on landforms on a local to regional scale. Such a study successfully evidenced neotectonic movements in the northernmost parts of the URG (Peters and van Balen, 2007). In the study area, the position and shape of the different terraces was analysed using topographic maps and a high precision Digital Elevation Model (DEM) with 1 m resolution: the DTM-AV provided by the Swiss Federal Office of Topography (Swisstopo). In particular the Lower Terrace was remapped based on this DEM, which permitted very precise positioning of the terrace limits.

Two different approaches had to be used to map the different terraces owing to their variable states of preservation. A high precision longitudinal profile was constructed for the Lower Terrace, the surfaces of which are still preserved and clearly visible in the landscape, and within which the original braided structure can still be seen on the DTM-AV. By contrast, applying the same process to the older terraces turned out to be impossible because their original surfaces are not preserved. Older terraces are usually covered by a few meters of loess, the surface of which is in turn modified by subsequent erosion or colluvial deposition. Thus, the elevation of the individual outcrops was used instead of the altitude of the terrace surface, although this does not necessarily reproduce the elevation of the surface, but the envelope of all the outcrops plotted on a longitudinal profile provides nevertheless a realistic approximation.

For the Lower Terrace, the profile was constructed along the reference line used by Haldimann et al. (1984) in order to permit a precise comparison of our results with those of these authors (Fig. 5). However, for the older terraces, a different, composite reference line was selected. Upstream from Sierentz, the line was located in order to fit the occurence of the outcrops, which are located further from the Rhine than the Lower Terrace, whereas downstream from Sierentz, the line follows the Rhine, since no outcrop exists in this area and since, on the other hand, bore holes and river seismic data are available (Wirsing et al., 2007) along the Rhine.

2.3 Investigations using the high precision digital elevation model (DTM-AV)

This part of the study builds on the data of Haldimann et al. (1984). These authors studied the longitudinal profile of the Lower Terrace in the same area and with the scope of constraining neotectonics. The present study uses the same terrace surfaces along the same reference line, but is based on much more elevation data, thanks to the availability of the DTM-AV. This allows for a

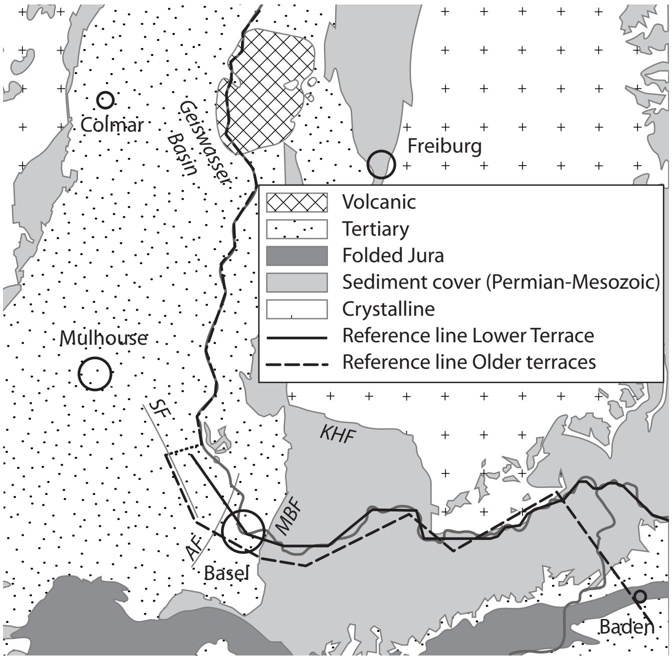

Fig. 5 Map showing the two reference lines used in this paper. Plain line: reference line of Haldimann et al. (1984), used for the longitudinal profile of the Lower Terrace (Fig. 7); Dashed line: reference line used for the longitudinal profile of the older terraces (Fig. 8).

direct comparison of the results of both studies.

2.3.1 Processing of the high precision digital elevation model (DTM-AV)

The DTM-AV was processed as follows using ArcGIS:

1) The outlines of individual surfaces of the Lower Terrace were mapped. The limits of these surfaces were set such as to include only those surfaces that are most likely to represent the original terrace surface. Thus, terrace risers, colluvial slopes, alluvial fans and areas heavily disturbed in elevation by human activity were excluded. However, urbanised areas could mostly be taken into account as the DTM-AV compensated for the heights of buildings.

2) Discrete points were selected within the surfaces of the terraces, whenever possible aligned with the probable flow direction of the river that created the surface, and was attributed its elevation. Again elevation artefacts, if not previously excluded from the mapping, were avoided.

3) The elevation of the selected points was orthogonally projected onto a plane coinciding with the reference line, which is identical with the one used by Haldimann et al. (1984)

4) Simultaneously, each terrace surface was averaged into a plane, whose exposition was measured.

2.3.2 Possible bias that may appear in the longitudinal profile

Using a high precision DEM and an automated method helps to cover a large area and to reach high precision of details; but it also introduces the following unwanted effects:

1) The reference line is not straight, but features several breaks, which causes distortions in the terrace projections. In case a projected terrace is located in the inner part of a break in the

reference line, the profile will show a parted line with a lower gradient. If, however, the terrace is in the outer part of the break, the profile will show a concentration of points at the same location, and thus an over-steepened segment (Fig. 6).

2) The alluvial cone of a tributary river may influence the dip of a terrace surface. In this case, a line set parallel to the main flow direction will appear with a lower, or even reverse, gradient, since the relevant gradient will be that of the tributary.

3) The original surface of a braided river is criss-crossed by channels. These appear on the high precision DEM, causing elevation fluctuations on the profile.

2.3.3 Expected exposition of a terrace

The exposition (dip direction) of a terrace surface can be relevant for constraining recent displacements. However, in the first place exposition is controlled by two different sedimentary processes. Firstly, the river flow tends to give the terrace its own dip direction, and secondly, material input and riser erosion from the side tend to expose the terrace perpendicularly to the flow direction. In fact, the terraces often show composite influence of these processes, with an exposition component parallel to the flow direction and a component perpendicular to it. Here the width of a terrace is a key issue: the exposition of a very narrow strip of terrace is extremely sensitive to side input and riser erosion, whereas this has generally only a marginal and thus negligible effect on the exposition of a wide terrace.

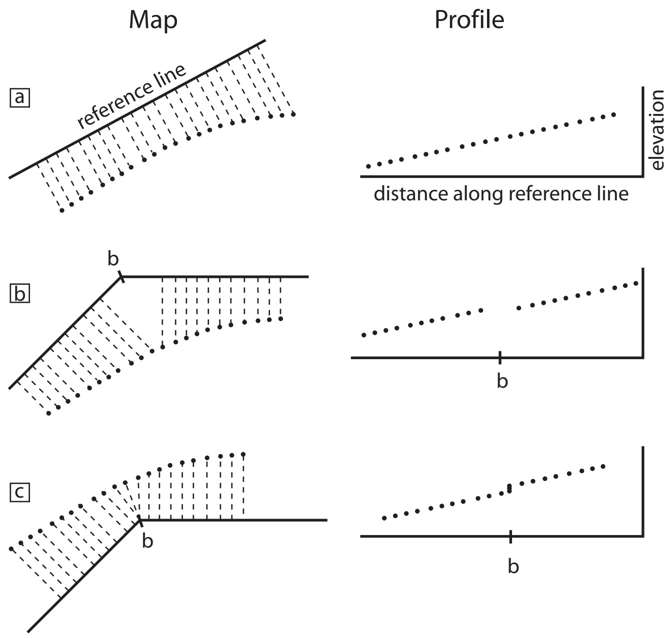

Fig. 6 Effect of a break point marked “b” on the orthogonal projection of a series of points with a gradient. a) projection onto a reference line without a break of a regular gradient; b) projection of a series of points located in the inner side of a reference line with break: the resulting gradient is smaller around the location of the knick point; c) projection of a series of points located in the outer side of a reference line with break: the resulting gradient is steeper at the location of the break point.

3 Results

3.1 Lower Terrace

Comparison of our data with those presented by Haldimann et al. (1984) shows that longitudinal profiles derived from the DTM-AV mostly confirm the longitudinal profile of the Rhine river of Haldimann et al. (1984). However, the projections of a group of terraces in the area SW of Albbruck differ significantly by showing a reverse gradient along a four km long segment of the reference line (Fig. 7).

The tilt directions of different blocks along the Rhine suggested by Haldimann et al. (1984) can neither be confirmed nor refuted by the dip of the terraces, which appears to be mostly controlled by sedimentary processes.

Haldimann et al. (1984) noted that the accumulation surface between Kaiseraugst and Basel is a few meters lower than expected, and suggested that this is the effect of subsidence. Actually, the important feature is that the accumulation surface has a steeper gradient downstream from Kaiseraugst compared to the upsteam part of the profile.

3.2 Older terraces

By contrast to the Lower Terrace, which constitutes most of the flat areas in the area under consideration, the older terrace levels (High Terrace and Deckenschotter) are mostly represented by badly outcropping remnants on hill slopes, and the surfaces that may still exist are always covered by several meters of loess. Thus, no surface can be investigated for assessing potential neotectonic activity. Nevertheless, the elevation of each outcrop in the Rhine valley can be plotted onto a longitudinal profile (Fig. 8). Combined, the Higher and Lower Deckenschotter and the High Terrace show an over-steepened gradient at the point where the Rhine crosses the main border fault of the URG and the Allschwil fault.

It appears that the gradient of the terrace groups increases together with their age. Thus they are not parallel and intersect each other at a single point located about 2 km north of Sierentz. Beyond this point, these formations do no longer crop out above the Lower Terrace, as their equivalents occur in the subsurface of the Geisswasser basin, as is evidenced by boreholes (LGRB Baden-Württemberg, 2004; Hagedorn, 2004; Lang et al., 2005; Hagedorn and Boenigk, 2008). Significantly, the depth position of these units place them on a gradient similar to that of the equivalent terraces (Fig. 8).

3.3 Outcrop evidence

Two outcrops located on the Sierentz fault (in Blotzheim and Sierentz), where the loess and soil stratigraphy has been recently refined, and for which ages are now available (Rentzel et al., submitted), displayed tectonic features. The Blotzheim outcrop is a road-cut featuring graben

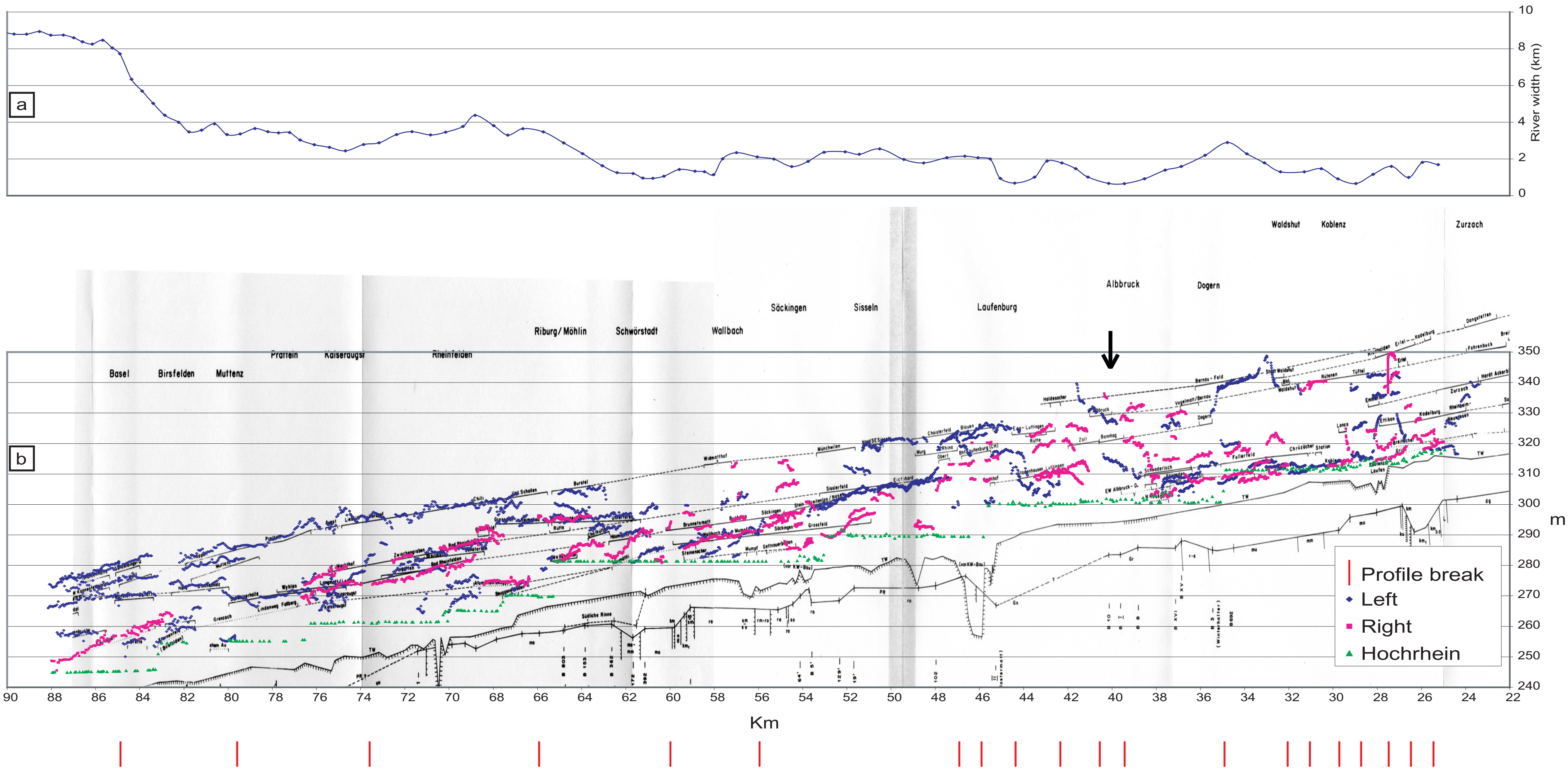

Fig. 7 Longitudinal profile of the Lower Terrace: a) River width along the longitudinal profile, b) Longitudinal profile of the Lower Terrace as obtained from the DTM-AV, superposed to the same profile as published by Haldimann et al. (1984). Blue dots indicate terraces on the left side of the river, red dots indicate terraces on the right side of the river, green dots indicate the modern level of the Rhine river with barrages steps. The reference line is shown on Fig 5. The arrow indicates the position of the Etzgen terraces.

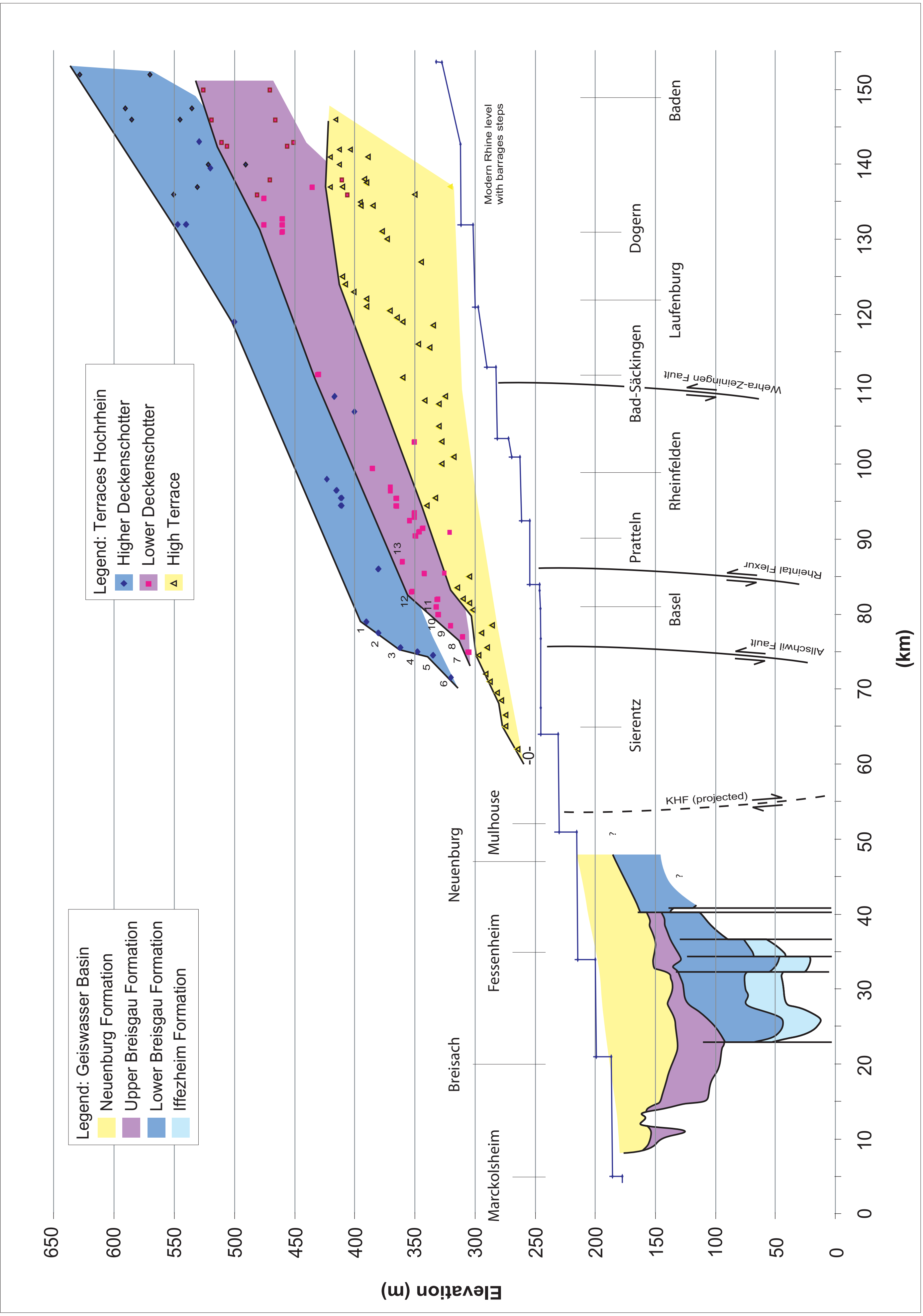

Legend: Geiswasser Basin
Neuenburg Formation
Upper Breisgau Formation
Lower Breisgau Formation
Iffezheim Formation
Legend: Terraces Hochrhein
Higher Deckenschotter
Lower Deckenschotter
High Terrace
Modern Rhine level with barrages steps
Marckolsheim
Breisach
Fessenheim
Neuenburg
Mulhouse
Sierentz
Basel
Pratteln
Rheinfelden
Bad-Säckingen
Laufenburg
Dogern
Baden
KHF (projected)
Allschwil Fault
Rheintal Flexur
Wehra-Zeiningen Fault
Elevation (m)
(km)

Fig. 8 (*opposite*) Longitudinal profile of the Higher Deckenschotter, the Lower Deckenschotter and the High Terrace between the inlet of the Aare and the Kaiserstuhl. Especially in the case of the Deckenschotter, the points represent the altitude of an outcrop, not of a surface, they give thus a minimal elevation. Incision is dominant in the upper reach, while subsidence is dominant in the lower reach, known as the Geiswasser Basin. All three formations have an over steepened gradient in the area of the Rheintal Flexure and the Allschwil Fault. -0- is the concordance point. The reference line is shown on Fig. 5. The location of the numbered outcrops is shown on Fig. 12. Geometry of the Geiswasser Basin after Lang et al. (2005).

structures that affect the High Terrace gravels as well as a loess unit lying on top of the gravel (Fig. 9). The fault planes are oriented 240/ 63 and 049/70. The Sierentz outcrop is a construction site featuring a normal fault oriented 066/65 that affects the High Terrace gravels (Fig. 10). Both structures strike parallel to the Sierentz fault.

4 Discussion

Generating longitudinal profiles of the Lower Terrace with the high precision DEM highlights the complexity of the morphology of terrace units. Indeed, while the accumulation surface seems somewhat regular, the numerous erosion surfaces give a first impression of being disturbed or offset. Actually, sedimentological processes can be invoked to explain most of the surprising features of terrace elevations. Indeed, on a local scale, accumulation and erosion processes are restricted to the active channel of a river, thus creating a discrepancy with other parts of the river bed that are provisionally inactive. These discrepancies can lead to apparently abnormal gradients.

The surprising exposition and inverse gradient of the terraces between Etzgen and Albbruck, however, needs further explanations. An effect of subrosion can be ruled out although subrosion features have frequently been identified in the study area. At this location the terraces rest directly on the stable crystalline basement and Lower Triassic Buntsandstein, while sedimentary strata that can potentially be subjected to subrosion (Middle and Upper Triassic Muschelkalk and Keuper) lay above them. Field observations confirm that the terraces consist of fluvial gravels containing a significant proportion of Alpine pebbles. This excludes a local alluvial fan or gravitational movements. These terraces were formed by a SW-flowing river, though there is very little room for such a river, as the right side of the valley is limited by crystalline rocks forming a steep flank (Fig. 11). This concept either suggests that the exposition of the terrace has changed, or that the crystalline flank has appeared subsequently by uplift. This is, however, highly hypotetical, as no other evidence support this interpretation. Rather, an unexpected sedimentological process, not

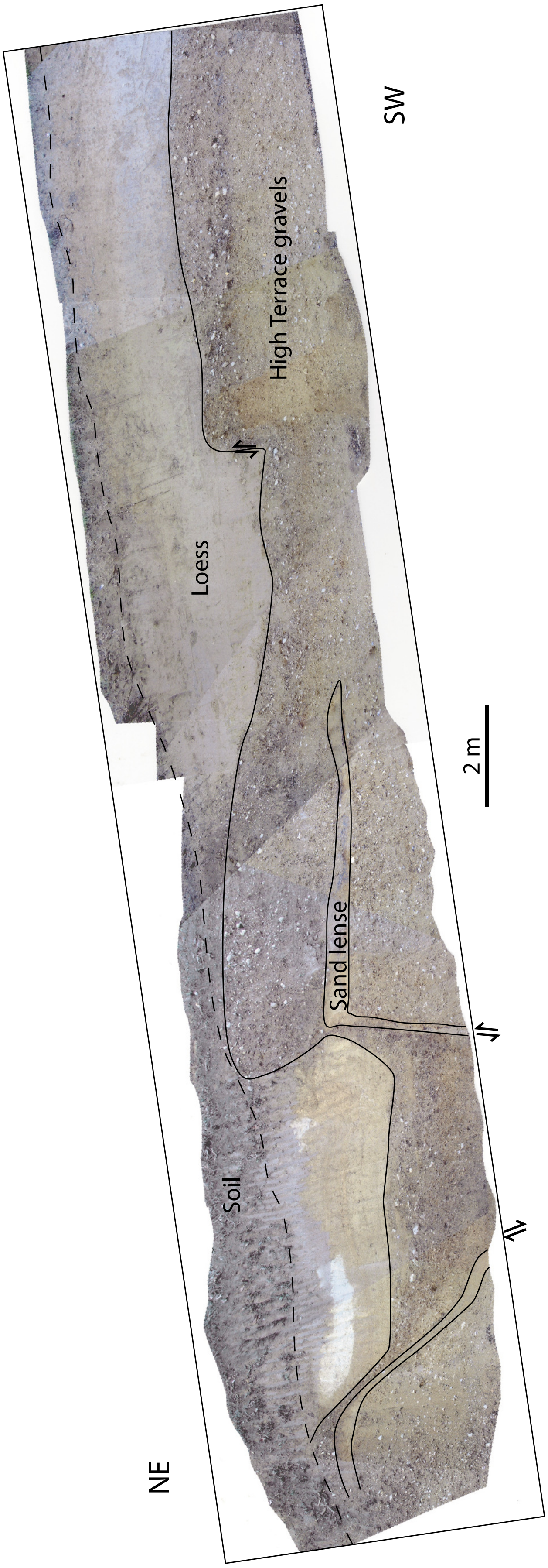

Fig. 9 Field evidence at the Blotzheim outcrop. The road-cut features two normal faults and a conjugated normal fault. The gravels belong to the High Terrace, and the loess sequence on top of the gravel has been dated by Rentzel et al. (subm.), with ages up to 236 ka. The fault plane dips are 240/63 (left of the graben structure) and 049/70 (right of the graben structure).

Fig. 10 (*opposite*) Field evidence at the Sierentz. The construction site in Sierentz features a normal fault. The fault plane dip is 066/65. The gravels belong to the High Terrace, and the loess sequence on top of the gravel has been dated by Rentzel et al. (subm.), with ages up to 236 ka.

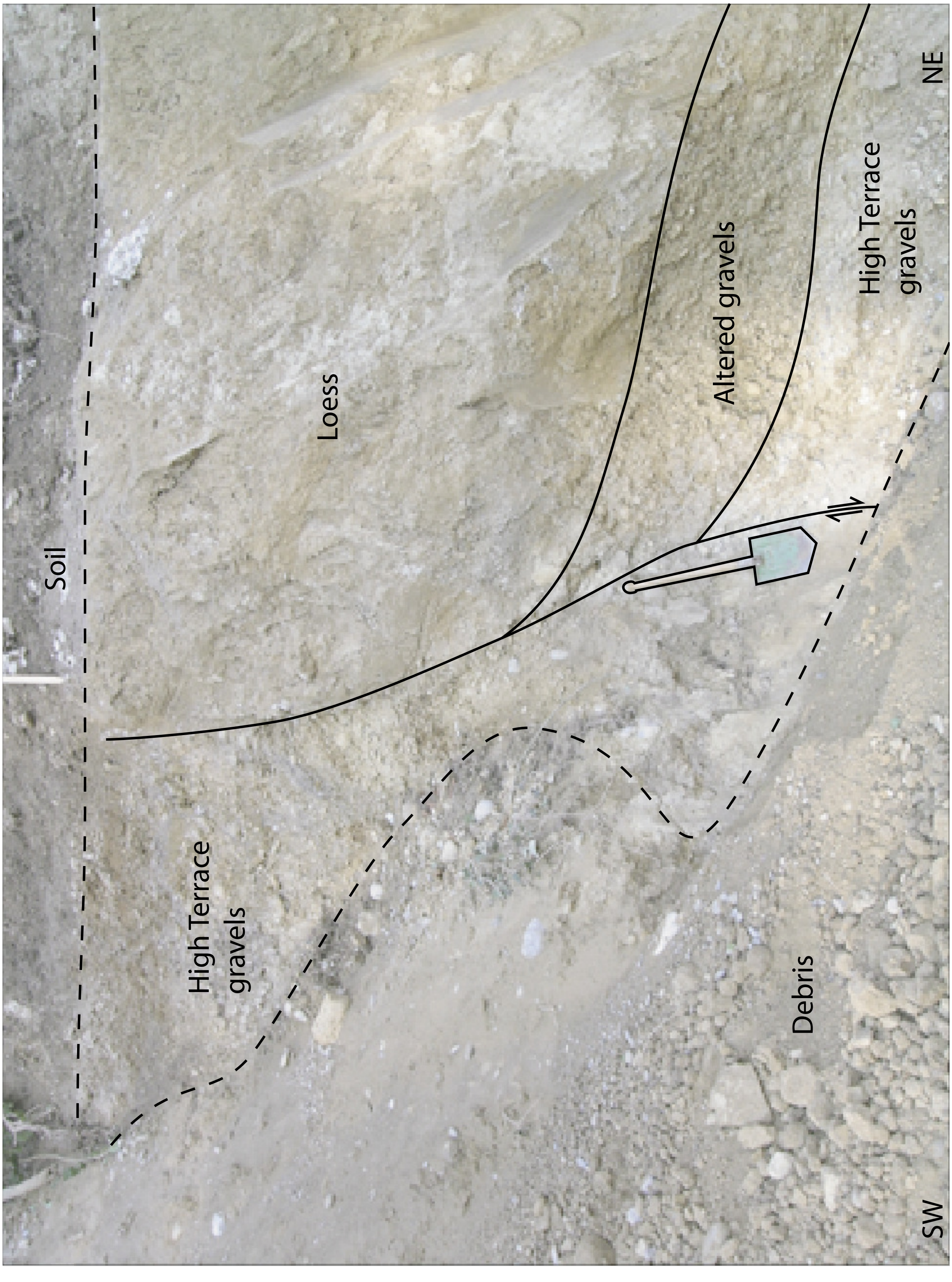
NE
High Terrace gravels
Altered gravels
Loess
Soil
High Terrace gravels
Debris
SW

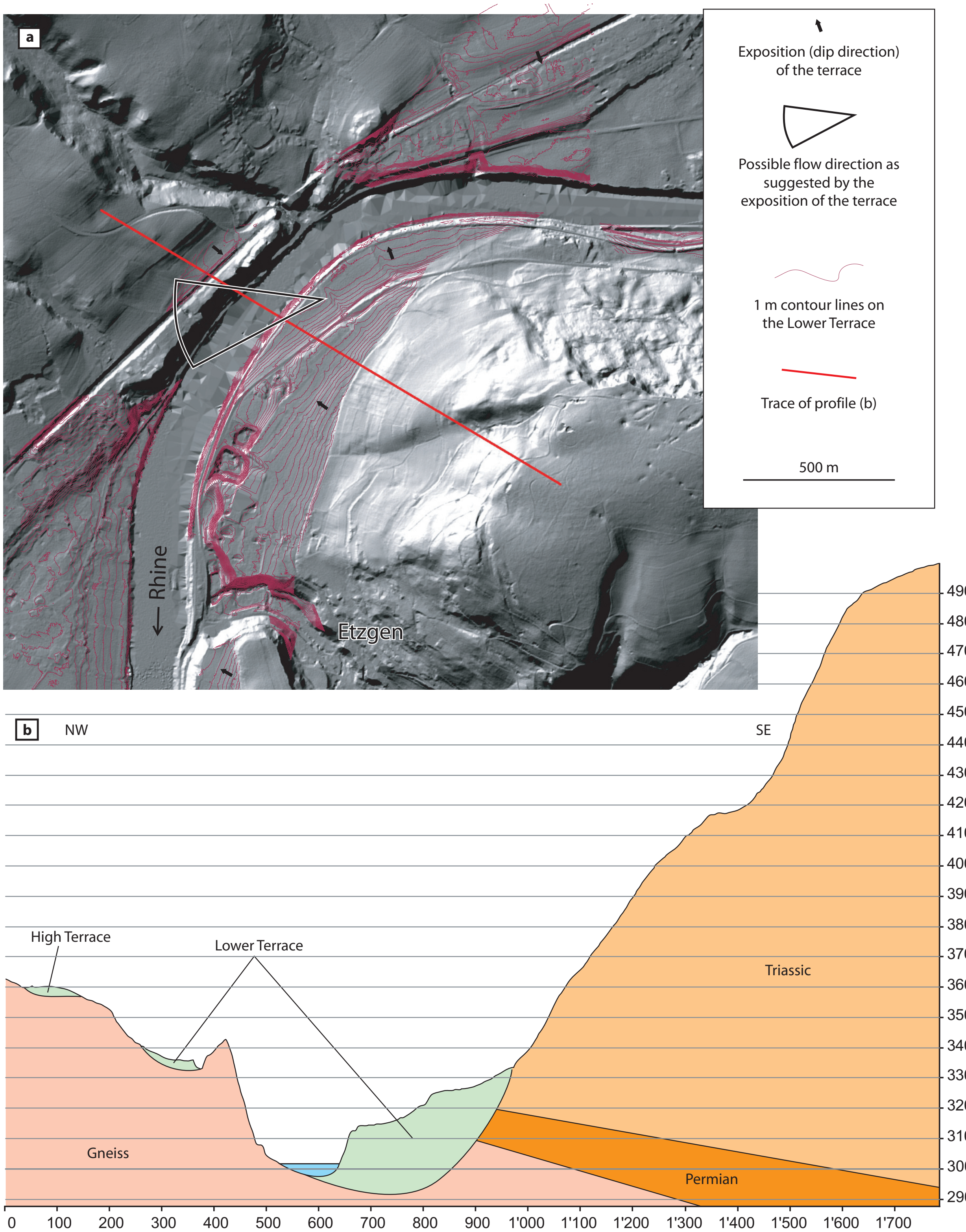

Fig. 11 (a) Shaded display of the DEM showing the exposition (arrows) and position (presence of contour lines) of the Lower Terrace. (b) Cross-section through the Etzgen terraces. Reproduced by permission of Swisstopo (BA081589).

considered in the concept, may be the cause.

The over-steepened gradients of the Higher and Lower Deckenschotter and high Terrace above the Allschwil Fault and the Main Border Fault of the URG (Fig. 8 and 12) suggest that they were active during the Pleistocene with a normal fault component, although repeated precision levelling could not detect significant movements in recent times in the area of Basel (Schlatter et al., 2005; Zippelt and Dierks, 2007). Moreover, the Main Border Fault has a strike that would rather accommodate senestral strike-slip movement in the present-day stress-field (Schumacher, 2002; Müller et al., 2002; Ustaszewski and Schmid, 2007). A compaction effect of the thick Eocene and Oligocene syn-rift sequence that occur in the URG west of the fault is unlikely, since a considerable overburden (several 100 m) has been removed by erosion during the Neogene, by far exceeding the thickness of Neogene deposits that rest on the corresponding erosional surface. Wittmann (1961) already noted that the height of the terrace scarp or the elevation difference between the terraces notably decreases across the URG Main Border Fault near Basel. Further to the North, in the area of Freiburg-in-Brisgau, Pleistocene normal faulting has been recently observed along a NNE-SSW striking fault (Nivière et al., 2008), and precision levelling data indicate subsidence of the URG respective to the Black Forest (Zippelt and Dierks, 2007). Assuming that over-steepening of the terraces is exclusively due to 50 meters downfaulting, and that the Higher Deckenschotter has a potential age of 1 Ma, this would imply average vertical movement rate of 0.05 mm/year.

The gradients of the terraces (Fig. 8) suggest either uplift of the eastern parts of the study area (or upstream of it) or subsidence of the URG, or a combination thereof. Théobald et al. (1977) and Haldimann et al. (1984) already noted that the terraces between Basel and Mulhouse have different gradients and converge northwards; they concluded that the Sundgau region underwent late-stage uplift. This is essentially compatible with the findings of Giamboni et al. (2004), Carretier et al. (2006) and Ustaszewski and Schmid (2007). However, these gradients can be followed much further upstream along the Rhine, and can thus be seen as an indication for relative uplift of an area further upstream. In the area of the Aare-Rhine confluence, the bedrock was incised by about 300 meters since the deposition of the Higher Deckenschotter. There is, however, only little geomorphologic evidence for Pleistocene uplift of the Black Forest and its surroundings (Müller et al., 2002; Ziegler & Fraefel, submitted). Precision leveling data indicate that the Black Forest is currently stable with respect to a reference point at Laufenburg, whilst the Dinkelberg block, delimited by the Kandern-Hausen and Wehra-Zeiningen faults gently subsides (Zippelt & Dierks, 2007). The gradients of the Rhine terraces reflect, however, no neotectonic activity along the Wehra-Zeiningen fault.

Significantly, all terraces intersect at a concordance point in the URG just north of Sierentz and in the westward prolongation of the Kandern-Hausen Fault (Fig. 1). North of this point, the Geisswasser Basin, containing up to 250 m deposits, shows that the southern parts of the URG resumed to subside during the Late Pliocene and continued to subside up to present (Bartz, 1974;

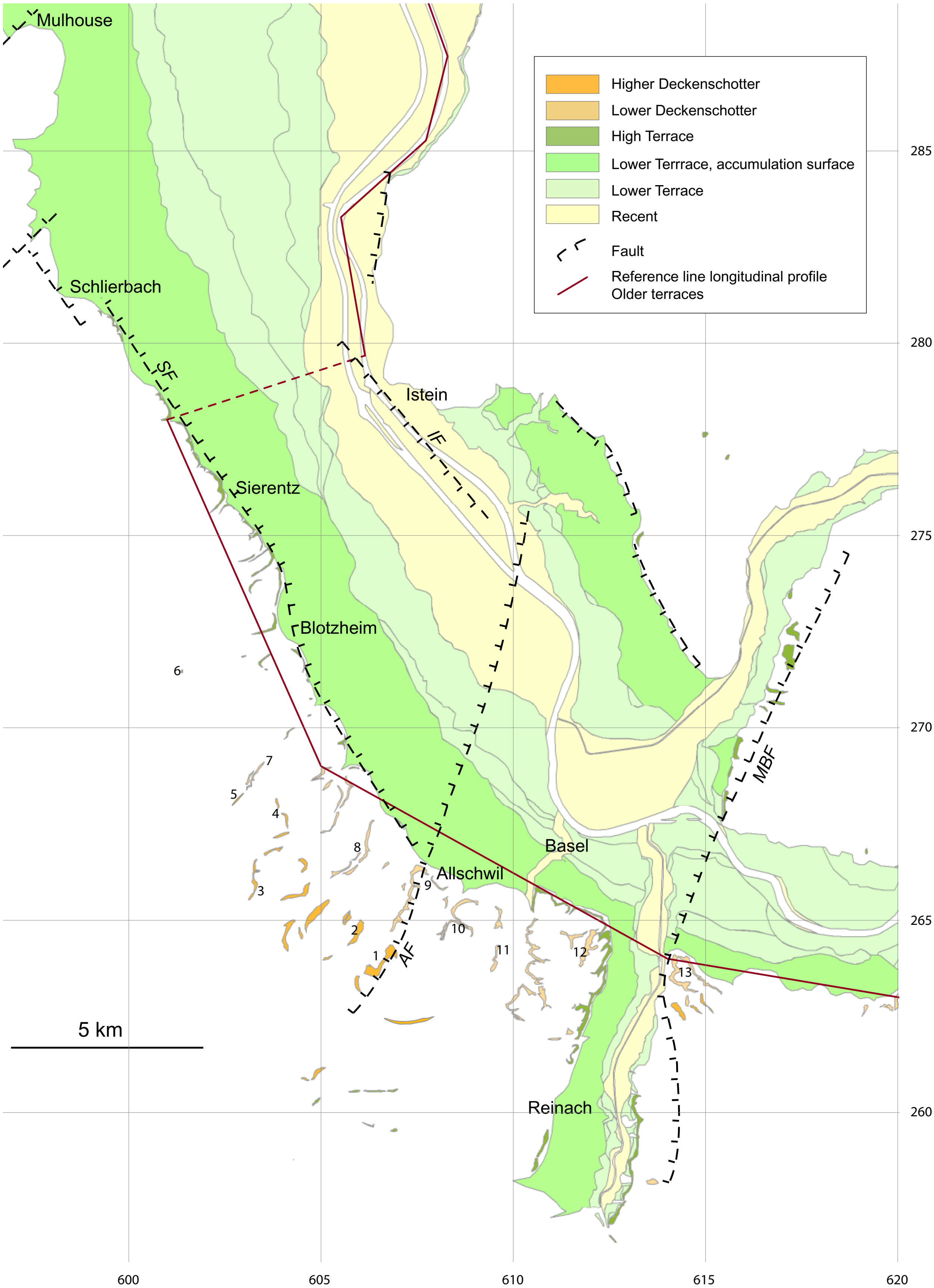
Mulhouse
Schlierbach
SF
Sierentz
Blotzheim
Istein
IF
Basel
Allschwil
AF
MBF
Reinach
1
2
3
4
5
6
7
8
9
10
11
12
13
5 km
Higher Deckenschotter
Lower Deckenschotter
High Terrace
Lower Terrrace, accumulation surface
Lower Terrace
Recent
Fault
Reference line longitudinal profile Older terraces
285
280
275
270
265
260
600
605
610
615
620

Fig. 12 (*opposite*) Map of Pleistocene fluvial deposits in the transition area between the Hochrhein and the URG, showing the position of the numbered outcrops of Fig. 8, as well as the reference line of the longitudinal profile of older terraces, relative to the position of the main fault.

Hagedorn & Boenigk, 2008). Borehole and reflection seismic data document that this subsidence was accompanied by tensional faulting (Lutz and Cleintuar, 1999; Wirsing et al., 2007). Precision levelling data indicate that in the area of the Geiswasser Basin the alluvial plain of the URG is presently subsiding at rates of 0.5-0.6 mm/y with respect to the Black Forest (Rózsa et al., 2005). This clearly illustrates that subsidence of the southern parts of the URG exerted strong controls on the evolution of the terrace systems by progressively lowering the erosional base level of the river Rhine and its tributaries (Ziegler & Fraefel, submitted).

Théobald et al. (1977) already suggested the presence of active faults along the eastern scarp of the Mulhouse horst. It can be argued that an extensional structure that occurs near a topographic scarp and strikes parallel to it has a gravitational origin. In the case of the Blotzheim fault, this can be ruled out for the following reasons: A sand layer within the gravels appears to have been plastically deformed, suggesting deformation under frozen conditions, under which a landslide would be impossible. Furthermore, the very steep dip of the exposed normal fault would imply a listric fault, which soles out at considerable depths, far beneath the foot of the topographic scarp which rises only 1 m above the Lower Terrace. A gravitational origin is also very unlikely in Sierentz, as the down-faulted gravel is located only one meter above modern surface of the Lower Terrace. Extension on a NE-SW axis is coherent with the orientation of the modern stress-field (Müller et al., 2002; Kastrup et al., 2004; Laubscher et al., 2006). A significant part of fault plane solutions of recent earthquakes in the southern URG indicate indeed NW-SE striking normal faulting, although sinistral strike-slip movements are dominant in the vicinity of the Sierentz fault (Plenefisch and Bonjer, 1997; Deichmann et al., 2000).

The general orientation of the deepest part of the Geiswasser Basin (Fig. 4), striking NNW-SSE (Bartz, 1974), also suggests the existence of normal fault along this axis, and thus extension on an ENE-WSW axis. Alltogether, the fact that both the Sierentz fault and the MBF or Allschwil Fault show signs of extension, suggests that the orientation of σ_3 (extension) in the Southern URG is close to an ENE-WSW direction.

5 Conclusion

During the Pleistocene, several units of fluvial deposits were formed in a tectonically active area. The geometry of these deposits suggests that the Main Border Fault of the URG near Basel (Rheintal Flexur), or the Allschwil Fault has been active with a normal fault component during Pleistocene. Pleistocene normal faulting is also evidenced along NW-SE striking faults.

During the same time, active subsidence is recorded in the URG north of Basel in the "Geiswasser Basin". Progressive lowering of the erosional base level during Late Pliocene and Pleistocene times controlled incision of the Rhine and its tributaries upstream from Basel. The concordance point between erosion and accumulation is located between the westward prolongation of the Kandern-Hausen Fault and the Mulhouse horst.

The use of high precision digital elevation model proved valuable in the study of fluvial terraces, but such data should not be interpreted in terms of tectonic activity without good knowledge and understanding of the sedimentary and anthropogenic processes that led to the formation of these landforms.

Acknowledgment

P. Ziegler, P. Jordan, M. Schnellmann, S. Hinsken and H. Madritsch are thanked for numerous fruitful discussions. The NAGRA (Swiss National Cooperative for the Disposal of Radioactive Waste) provided the DTM-AV, and P. Jordan helped greatly in processing it. S.K. acknowledges financial support from the Freiwillige Akademische Gesellschaft of Basel.

References

Affolter, T. & Gratier, J.-P. 2004: Map view retrodeformation of an arcuate fold-and-thrust belt: The Jura case. Journal of Geopysical Research 109, B03404.

Allenbach, R. & Wetzel, A. 2006: Spatial patterns of Mesozoic facies relationships and the age of the Rhenish Lineament: a compilation. International Journal of Earth Sciences 95, 803-813.

Baer, M., Deichmann, N., Braunmiller, J., Clinton, J., Husen, S., Fäh, D., Giardini, D., Kästli, P., Kradolfer, U. & Wiemer, S. 2007: Earthquakes in Switzerland and surrounding regions during 2006. Swiss journal of geosciences 100, 517-528.

Bartz, J. 1974: Die Mächtigkeit des Quartärs im Oberrheingraben. Approaches to Taphrogenesis. Fuchs, K. & Illies, J. H. Stuttgart: 78-87.

Berger, J.-P., Reichenbacher, B., Becker, D., Grimm, M., Grimm, K., Picot, L., Storni, A., Pirkenseer, C., Derer, C. & Schäfer, A. 2005b: Paleogeography of the Upper Rhine Graben (URG) and the Swiss Molasse Basin (SMB) from Eocene to Pliocene. International Journal of Earth Sciences 94, 697-710.

Bergerat, F. & Chorowicz, J. 1981: Etude des images Landsat de la zone transformante Rhin-Saône (France). Geol. Rdsch. 70, 354-367.

Bibus, E. 1990: Das Mindesalter des «jüngeren Deckenschotters» bei Basel aufgrund seiner Deckschichten in der Ziegelei Allschwil. Jh. geol. Landesamt Baden-Würtemberg 32, 223-234.

Bitterli, T., Graf, H.R., Matousek, F. & Wanner, M. 2000: Blatt 1050 Zurzach.

Blösch, E. 1911: Die grosse Eiszeit in der Nordschweiz. Beitr. geol. Karte Schweiz 31.

Boigk, H. & Schöneich, H. 1970: Die Tiefenlage der Permbasis im nördlichen Teil des Oberrheigrabens. Graben Problems. In: Illies, J. H. & Mueller, S.: Graben problems Stuttgart: 45-55.

Bolliger, T., Fejfar, O., Graf, H.R. & Kälin, D. 1996: Vorläufige Mitteilung über Funde von pliozänen Kleinsäugern aus den höheren Deckenschottern. Eclogae geol. Helv. 89, 1043-1048.

Bugmann, E. 1961: Beiträge zur Gliederung der risszeitlichen Bildungen in der Nordschweiz. Mitt. aargau. natf. Ges 26, 105-119.

Bull, W.B. 1991: Geomorphic responses to climatic change. New York, Oxford University Press.

Carretier, S., Nivière, B., Giamboni, M.E. & Winter, T. 2006: Do river profiles record along-stream variations of low uplift rate? Journal of Geopysical Research 111, F02024.

Choi, S.-W., Preusser, F. & Radtke, U. 2007: Dating of lower terrace sediments from the Middle Rhine area, Germany. Quaternary Geochronology (Quaternary Science Reviews) 2, 137-142.

Deichmann, N., Ballarin Dolfin, D. & Kastrup, U. (2000). Seismizität der Nord- und Zentralschweiz. Nagra Technischer Bericht. Wettingen, NAGRA. 00-05.

Dèzes, P., Schmid, S.M. & Ziegler, P.A. 2004: Evolution of the European Cenozoic Rift System: interaction of the Alpine and Pyrenean orogens with their foreland lithosphere. Tectonophysics 389, 1-33.

Diebold, P. 1989: Der Nordschweizer Permokarbon-Trog und die Steinkohlenfrage der Nordschweiz. Vierteljahrsschrift der Naturforschenden Gesellschaft in Zürich 133, 143-174.

Echtler, H.P. & Chauvet, A.C. 1992: Carboniferous convergence and subsequent crustal extension in the southern Schwarzwald (SW Germany). Geodinamica Acta 5, 37-49.

Fiebig, M. & Preusser, F. 2003: Das Alter fluvialer Ablagerungen aus der Region Ingolstadt (Bayern) und ihre Bedeutung für die Eiszeitenchronologie des Alpenvorlandes. Zeitschrift Für Geomorphologie 47, 449-467.

Giamboni, M.E., Ustaszewski, K., Schmid, S.M., Schumacher, M.E. & Wetzel, A. 2004a: Plio-Pleistocene transpressional reactivation of Paleozoic and Paleogene Structures in the Rhine-Bresse transform zone (northern Switzerland and eastern France. International Journal of Earth Sciences 93, 207-223.

Giamboni, M.E., Wetzel, A., Nivière, B. & Schumacher, M.E. 2004b: Plio-Pleistocene folding in the southern Rhinegraben recorded by the evolution of the drainage network (Sundgau area; northwestern Switzerland and France). Eclogae geol. Helv. 97, 17-31.

Giamboni, M.E., Wetzel, A. & Schneider, B. 2005: Geomorphic response of alluvial rivers to active tectonics: Example from the southern Rhinegraben. Austrian Journal of Earth Sciences 97, 24-37.

Graf, H.R. (1993). Die Deckenschotter der zentralen Nordschweiz. Zürich, Eidgenössische

Technischen Hochschule Zürich: 187.

Graf, H.R., Bitterli-Dreher, P., Burger, H., Bitterli, T., Diebold, P. & Naef, H. 2007: Blatt 1070 Baden.

Graf, H.R. & Hofmann, F. 2000: Zur Eiszeitgeologie des oberen Klettgau (Kanton Schaffhausen, Schweiz). Jahresbericht und Mitteilungen des oberrheinischen geologischen Vereins NF 82, 279-315.

Groschopf, R. & Sawatzki, G. 1989: Quartär und Grundgebirge im zentralen Hotzenwald. Jber. Mitt. oberrheinische geologische Ver. N.F. 71, 55-109.

Hack, J.T. 1957: Studies of longitudinal streams profiles in Virginia and Maryland. Prof. Pap. U. S. geol. Surv. 294-B: 97.

Hagedorn, E.-M. (2004). Sedimentpetrographie und Lithofazies der jungtertiären und quartären Sedimente im Oberrheingebiet. PhD thesis, Mathematisch-Naturwissenschaftliche Fakultät. Köln, Universität zu Köln: 310 pp.

Hagedorn, E.-M. & Boenigk, W. 2008: The Pliocene and Quaternary sedimentary and fluvial history in the Upper Rhine Graben based on heavy mineral analyses. Netherlands Journal of Geosciences - Geologie en Mijnbouw 87, 21-32.

Haldimann, P., Naef, H. & Schmassmann, H. 1984: Fluviatile Erosions- und Akkumulationsformen als Indizien jungpleistozäner und holozäner Bewegungen in der Nordschweiz und angrenzenden Gebieten. Nagra Technischer Bericht 84-16.

Häuselmann, P., Fiebig, M., Kubik, P.W. & Adrian, H. 2007: A first attempt to date the original ‘‘Deckenschotter’’ of Penck and Brückner with cosmogenic nuclides. Quaternary International 164-165, 33-42.

Hinsken, S., Ustaszewski, K. & Wetzel, A. 2007: Graben width controlling syn-rift sedimentation: the Palaeogene southern Upper Rhine Graben as an example. International Journal of Earth Sciences 96, 979-1002.

Hofmann, F. 1996: Zur plio-pleistozänen Landschaftsgeschichte im Gebiet Hochrhein-Wutach-Donau: Geomorphologische Überlegungen und sedimentpetrographische Befunde. Eclogae geol. Helv. 89, 1023-1041.

Huggenberger, P. & Regli, C. 2006: A sedimentological model to characterize braided river deposits for hydrogeological application. Braided Rivers. Sambrook Smith, G. H., Best, J. L., Bristow, C. S. & Petts, G. E., International Association of Sedimentologists. 36: 51-74.

Kastrup, U., Zoback, M.L., Deichmann, N., Evans, K.F., Giardini, D. & Michael, A.J. 2004: Stress field variations in the Swiss Alps and the northern Alpine foreland derived from inversion of fault plane solutions. Journal of Geopysical Research 109, B01402.

Kock, S., Kramers, J.D., Preusser, F. & Wetzel, A. submitted: Dating of Late Pleistocene terrace deposits of the River Rhine using uranium series and luminescence methods: potential and limitations. Quaternary Geochronology (Quaternary Science Reviews).

Lambert, J., Winter, T., Dewez, T.J.B. & Sabourault, P. 2005: New hypotheses on the maximum damage area of the 1356 Basel earthquake (Switzerland). Quaternary Science Reviews 24, 383-401.

Lang, U., Gudera, T., Elsass, P. & Wirsing, G. 2005: Numerical modelling of chloride propagation in the quaternary aquifer of the southern Upper Rhine Graben. International Journal of Earth Sciences 94, 550-564.

Laubscher, H. 1970: Grundsätzliches zur Tektonik des Rheingrabens. In: Illies, J. H. & Mueller, S.: Graben Problems. Stuttgart, Proceedings 1174 of an International Rift Symposium held in Karlsruhe 1968, International Upper Mantle Project.

Laubscher, H. 1992: Jura kinematics and the Molasse Basin. Eclogae geol. Helv. 85, 653-675.

Laubscher, H. 2006: Zur Geologie des Erdbebens von Basel. Da verfiele Basel überall. Meier, W. Basel. Neujahrsblatt der GGG 184: 207-230.

Laubscher, H. & Noack, T. 1997: The deep structure of the Basel Jura. Deep structure of the Swiss Alps. Results of NRP 20. Pfiffner, O. A., Lehner, P., Heitzmann, P., Mueller, S. & Steck, A., Birkhäuser: 54-58.

LGRB Baden-Württemberg 2004: Lithostratigraphische Übersicht des Quartärs in Baden-Württemberg. Freiburg i. Br. www.lgrb.uni-freiburg.de

Liniger, H. 1967: Pliozän und Tektonik des Juragebirges. Eclogae geol. Helv. 60, 407-490.

Litt, T., Schmincke, H.-U. & Kromer, B. 2003: Environmental response to climatic and volcanic events in central Europe during the Weichselian Lateglacial. Quaternary Science Reviews 22, 7-32.

Lutz, M. 1964: Stratigraphische und tektonische Untersuchungen am südwestlichen Schwartzwald zwischen Wiesental und Hochrhein. Oberrheinische Geologische Abhandlungen 13, 75-122.

Lutz, M. & Cleintuar, M. 1999: Geological results of a hydrocarbon exploration campaign in the souther Upper Rhine Graben. Bulletin für Angewandte Geologie 4, 3-80.

Madritsch, H., Schmid, S.M. & Fabbri, O. accepted: Interactions between thin- and thick-skinned tectonics at the northwestern front of the Jura fold-and-thrust belt (Eastern France). Tectonics.

MBN AG, 1998: Zur Stratigraphie des jüngeren Pleistozäns im Gebiet des Zusammenflusses von Aare, Surb, Rhein und Wutach. Bericht G819B z. Hd. Landeshydrologie und -geologie, Bern.

Meyer, B., Lacassin, R., Brulhet, J. & Mouroux, B. 1994: The Basel 1356 earthquake: which fault produced it? Terra Nova 6, 54-63.

Müller, W.H., Naef, H. & Graf, H.R. 2002: Geologische Entwicklung der Nordschweiz, Neotektonik und Langzeitszenarien Zürcher Weinland. Nagra Technischer Bericht 99-08, 226.

Nivière, B., Bruestle, A., Bertrand, G., Carretier, S., Behrmann, J.H. & Gourry, J.-C. 2008: Active tectonics of the southeastern Upper Rhine Graben, Freiburg area (Germany). Quaternary Science Reviews 27, 541-555.

Penck, A. & Brückner, E. 1909: Die Alpen im Eiszeitalter. Leipzig, Tauchnitz.

Peters, G. & Van Balen, R.T. 2007: Pleistocene tectonics inferred from fluvial terraces of the northern Upper Rhine Graben, Germany. Tectonophysics 430, 41-65.

Pflug, R. 1982: Bau und Entwicklung des Oberrheingrabens.

Philippe, Y., Colletta, B., Deville, E. & Mascle, A. 1996: The Jura fold-and-thrust belt: a kinematic model based on map-balancing. Peri-Tethys Memoir 2: Structure and prospects of Alpine basins and forelands. Ziegler, P. A. & Horváth, E. Paris. 170: 235-261.

Plenefisch, T. & Bonjer, K.-P. 1997: The stress field in the Rhine Graben area inferred from earthquake focal mechanisms and estimation of frictional parameters. Tectonophysics 275, 71-97.

Preusser, F., Blei, A., Graf, H.R. & Schlüchter, C. 2007: Luminescence dating of Würmian (Weichselian) proglacial sediments from Switzerland: methodological aspects and stratigraphical conclusions. Boreas 36, 1-13.

Rentzel, P., Preusser, F., Pümpin, C. & Wolf, J.-J. submitted: Loess, Cover Sediments and Palaeosols on the High Terrace at Sierentz, France, and Implications for the Chronology of Terrace Formation in the Southern Upper Rhine Graben. Swiss j. geosci.

Rózsa, S., Heck, B., Mayer, M., Seitz, K., Westerhaus, M. & Zippelt, K. 2005: Determination of displacements in the upper Rhine graben Area from GPS and leveling data. International Journal of Earth Sciences 94, 538-549.

Schlatter, A., Schneider, D., Geiger, A. & Kahle, H.-G. 2005: Recent vertical movements from precise levelling in the vicinity of the city of Basel, Switzerland. International Journal of Earth Sciences 94, 507-514.

Schlüchter, C. 1989: A non-classical summary of the Quaternary stratigraphy in the northern alpine foreland of Switzerland. Bull. Soc. neuchât. Géogr. 32-33, 1-157.

Schumacher, M.E. 2002: Upper Rhine Graben: Role of preexisting structures during rift evolution. Tectonics 21, 6-1 - 6-17.

Schumm, S.A. 1993: River response to baselevel change: Implications for Seqence Stratigraphy. Journal of Geology 101, 279-294.

Seeber, L. & Gornitz, V. 1983: River profiles along the Himalayan arc as indicators of active tectonics. Tectonophysics 92, 335-367.

Snyder, N.P., Whipple, K.X., Tucker, G.E. & Merritts, D.J. 2000: Landscape response to tectonic forcing: Digital elevation model analysis of stream profiles in the Mendocino triple junction region, northern California. GSA Bulletin 112, 1250-1263.

Theobald, N., Vogt, H. & Wittman, O. 1977: Néotectonique de la partie méridionale du bloc rhénan. Bull. B.R.G.M. (2ème sér.), sect. IV 2, 121-140.

Ustaszewski, K. & Schmid, S.M. 2007: Latest Pliocene to recent thick-skinned tectonics at the Upper Rhine Graben - Jura Mountains junction. Swiss j. geosci. 100, 293-312.

Ustaszewski, K. & Schmid, S.M. 2006: Control of preexisting faults on geometry and kinematics in the northernmost part of the Jura fold-and-thrust belt. Tectonics 25, TC5003.

Ustaszewski, K., Schumacher, M.E., Schmid, S.M. & Nieuwland, D. 2005: Fault reactivation in brittle-viscous wrench systems - dynamically scaled analogue models and application to the Rhine-Bresse transfer zone. Quaternary Science Reviews 24, 365-382.

van Husen, D. 2004: Quaternary glaciations in Austria. Quaternary Glaciations—Extent and Chronology. Ehlers, J. & Gibbard, P. L. Amsterdam, Elsevier: 1-13.

Verderber, R. 2003: Quartärgeologie im Hochrheingebiet zwischen Schaffhausen und Basel. Zeitschrift der Deutschen Geologischen Gesellschaft 154, 369-406.

Villinger, E. 1998: Zur Flussgeschichte von Rhein und Donau in Südwestdeutschland. Jber. Mitt. oberrheinische geologische Ver. 80, 361-398.

Villinger, E. 2003: Zur Paläogeographie von Alpenrhein und oberer Donau. Zeitschrift der Deutschen Geologischen Gesellschaft 154, 193-253.

Wang, N. & Grapes, R. 2008: Infrared-stimulated luminescence dating of late Quaternary aggradation surfaces and their deformation along an active fault, southern North Island of New Zealand. Geomorphology 96, 86-104.

Wirsing, G., Luz, A., Engesser, W. & Koch, A. 2007: Hochauflösende Refelktionsseismik auf dem Rhein und dem Rheinseitenkanal zwischen Mannheim und Rheinfelden. LGRB-Fachbericht 1/07, 60.

Wittmann, O. 1961: Die Niederterrassenfelder im Umkreis von Basel und ihre kartographische Darstellung. Basler Beiträge zur Geographie und Ethnologie 3, 46.

Ziegler, P.A. 1990: Geological Atlas of Western and Central Europe. The Hague, Shell Internationale Petroleum Maatschappij B.V.

Ziegler, P.A. 1992: European Cenozoic rift system. Tectonophysics 208, 91-111.

Ziegler, P.A. 1994: Cenozoic rift system of the western and central Europe: an overview. Geol. en Mijnb. 73, 99-127.

Ziegler, P.A. & Dèzes, P. 2007: Cenozoic uplift of Variscan Massifs in the Alpine foreland: Timing and controlling mechanisms. Global and Planetary Change 58, 237-269.

Ziegler, P.A. & Fraefel, M. submitted: Response of drainage systems to Neogene evolution of the Jura fold-thrust belt and Upper Rhine Graben. Swiss j. geosci.

Zippelt, K. & Dierks, O. 2007: Auswertung von wiederholten Präzisionsnivellements im südlichen Schwarzwald, Bodenseeraum sowie in angrenzenden schweizerischen Landesteilen. Nagra Arbeitsbericht 07-27.

Summary

Summary

It is important to gain knowledge about neotectonic activity in the area of Basel, and this was the starting point of this study. However, a correct interpretation of geomorphological landforms requires a good understanding of their genesis, and the quantification of movement rates requires age controls. Hence, a significant part of this study was dedicated to datings and sedimentological analysis.

Dating Pleistocene gravel deposits has been hitherto possible only in very limited cases. This study has investigated the possibility of using carbonate crusts that formed within the gravel for uranium-series disequilibrium dating. Such an approach is theoretically possible, but it appears that uranium content and bacterial activity play a key role in the precision and reproducibility of the method. Indeed, the low uranium content of the samples forced to make several measures per sample, and to average these. The averaging highlighted an important scatter of the measures, which could be partly attributed to bacterial activity and colloidal transport of Thorium. Most samples yielded Holocene ages, although the gravel deposition is expected to be of Late Pleistocene age. This is coherent with stable isotope data, which indicates that the carbonate has precipitated under temperate climate and implies presence of soil. This provides only a minimal age to the gravel formation.

The gravel of the Lower Terrace system was usually accepted as being deposited during the Late Pleistocene, although chronologic ages are generally missing. Based on luminescence, radiocarbon and uranium-series disequilibrium dating, we propose a precise chronology for the aggradation and terrace formation of the Lower Terrace in the area of Basel and the Hochrhein. Aggradation started after the Late Pleniglacial interstadial, between 30 and 27 ka, and reached maximum elevation (accumulation level) during the Younger Dryas (about 11 ka). The base level dropped quickly afterward, and the first terrace surfaces were formed in the same climatic period. More terrace surfaces were formed throughout the Holocene. Field observation and remote sensing show that the flood events are important factors in both accumulation and erosion processes, and that the climate, although important, is not the sole controlling factor of river regime.

Geomorphologic analysis in the Hochrhein area indicates subsidence in the Southern Upper Rhine Graben, and incision upstream of it during Pleistocene. During the same time, the Main Border Fault zone in the area of Basel, striking NNE-SSW, may have undergone tectonic activity with a normal fault component, although the exact movement cannot be determined. Field data show

that also NW-SE striking normal faults have been active during Pleistocene. Activity on both fault orientation, also known in the area of Freiburg-in-Breisgau, suggests that the general orientation of extension stress in the Southern Upper Rhine Graben is close to ENE-WSW.
The potential of high precision digital elevation model for assessing neotectonic is tested on the Late Pleistocene Lower Terrace levels. The high precision enables detection of previously unnoticed attitudes of the terrace surface, but also results in much “noise” of sedimentary origin that should be recognized prior to neotectonic interpretation.

Outlook

Contrary to the Lower Terrace, the age of the High Terrace, Lower and Higher Deckenschotter are still very poorly constrained. The Deckenschotter are probably too old for OSL dating, but this method would theoretically be suitable for the High Terrace. During field work, two outcrops of the High terrace gravel were found, with potential, uncemented sand lenses for OSL sampling: the active Holcim gravel pit in Wallbach (634100/267360) and the East side of the abandoned “Hörndlibuck” pit, East of Koblenz (661380/273660).
U/Th dating of crusts within gravel of the Lower Terrace has shown potential and limitations. The same crusts can also be found in the High Terrace, and even if they give only a minimal age, a well constrained age would be most welcome for the High Terrace.
It has been noted that the river regime in the Southern URG is not only controlled by climatic conditions, but probably also by the regional slope. A geomorphologic study of the Rhine could help constraining the tilting of the area.
It has been shown that definite tectonic structures exist in Pleistocene sediments, but are accessible almost only by trenching. Developing trenching on key sites and monitoring construction sites would probably yield valuable data for the timing and quantification of neotectonic movements.
The longitudinal profile of the Lower Terrace was built using the high precision DEM of the cantons Aargau and Basel-Land, which unfortunately are limited to the Swiss border. The longitudinal profile of Early and Middle Pleistocene showed interesting features NW of the city of Basel, and a prolongation of the Lower Terrace profile into France or Germany would be most interesting. However, corresponding high precision DEM are at the moment not available.

Curriculum Vitae of Stéphane Kock

Date of Birth:	January 7th, 1978
Place of Birth:	Geneva, Switzerland
Nationality:	Swiss, French

Education

December 2003 - June 2008	PhD student, University of Basel, Switzerland. PhD title: “Pleistocene terraces in the Upper Rhine area – formation, age constraints and neotectonic implications”. Supervisor: Prof. A. Wetzel.
October 1997 - March 2003	Msc student, University of Lausanne, Switzerland. Msc title: “Nouvelles données stratigraphiques, métamorphiques et géochimiques sur la série autochtone des Talea Ori (Crète centrale)”. Supervisor: Prof. G.M. Stampfli.
March 1997	Matura in Lausanne, Switzerland.

Experience

December 2003 - December 2007	Teaching assistant in several field courses and practical exercises in Sedimentology and stratigraphy at the University of Basel.
July 2003:	Teaching assistant on a mapping course, University of Lausanne.
April 2003 - June 2003	Work experience in the Swiss Institute for speleology and Karst Studies, La-Chaux-de-Fonds, Switzerland.

Languages

French (mother tongue), English (good), German (good), Italian (good bases).